

PUMP DISPLACEMENT CONTROL IN
STEERING ON-HIGHWAY COMMERCIAL VEHICLES

A Dissertation

Submitted to the Faculty

of

Purdue University

by

Amine Nhila

In Partial Fulfillment of the

Requirements for the Degree

of

Doctor of Philosophy

December 2018

Purdue University

West Lafayette, Indiana

**THE PURDUE UNIVERSITY GRADUATE SCHOOL
STATEMENT OF DISSERTATION APPROVAL**

Dr. Monika Ivantysynova, Co-Chair

School of Mechanical Engineering

Dr. Andrea Vacca, Co-Chair

School of Mechanical Engineering

Dr. Dan E. Williams

ZF Friedrichshafen AG

Dr. Greg Shaver

School of Mechanical Engineering

Dr. Jose M. Garcia

School of Engineering Technology

Approved by:

Dr. Anil K. Bajaj

Head of the School of Mechanical Engineering

I dedicate this work to my parents, Ahmed Nhila and Aicha Rahmoune, who have sacrificed a lot for me to be able to reach this point in my life. I am grateful to them for their love and support that made this achievement possible. I also dedicate this work to my sister Fatine, brother Nassif, and girlfriend Lusine for their persistent encouragement that made this long journey tolerable.

ACKNOWLEDGMENTS

I thank my advisor, Professor Monika Ivantysynova, for her guidance and extremely valuable feedback which helped improve my research and dissertation. I feel very lucky to have crossed paths with her and having had the chance to work with her. I will always remember her enthusiasm and excitement inside and outside the lab. May she rest in peace!

I also thank my supervisor and mentor, Dr. Dan E. Williams, for his continued support and encouragement. I also thank him for taking the time to read my dissertation and provide valuable feedback.

I also acknowledge the rest of my PhD advisory committee members: Prof. Andrea Vacca, Prof. Greg Shaver, and Prof. Jose Garcia. I appreciate their feedback and support, particularly, after the passing of professor Ivantysynova.

I also thank ZF Friedrichshafen AG for their continued support throughout my PhD program and for giving me the flexibility to pursue it while working at ZF.

I also thank James Arihood, Anthony Gillam, David Tyner, Ken Sherwin, and Todd Proctor for taking the time to help me with the experimental work for this project. I very much appreciated all their help and advice.

TABLE OF CONTENTS

| | Page |
|---|-------|
| LIST OF TABLES | viii |
| LIST OF FIGURES | ix |
| SYMBOLS | xv |
| ABBREVIATIONS | xviii |
| ABSTRACT | xix |
| 1. EVOLUTION OF STEERING SYSTEMS IN ON-HIGHWAY COMMERCIAL VEHICLES | 1 |
| 1.1 Background | 1 |
| 1.2 Motivation | 2 |
| 1.3 Manual Steering | 3 |
| 1.4 Power Cylinder with a Linear Link Valve | 4 |
| 1.5 Semi-Integral Steering Systems | 6 |
| 1.6 Integral Steering Gear | 7 |
| 1.7 Pumping Elements | 13 |
| 1.7.1 Fixed-Displacement Pumps | 13 |
| 1.7.2 Variable Displacement Pumps | 15 |
| 1.7.3 Fixed Displacement Pump with Variable Speed Electric Motor: | 16 |
| 1.8 Research Aims: | 18 |
| 1.9 Original Contributions: | 18 |
| 1.10 Dissertation Organization: | 20 |
| 2. STATE OF THE ART LITERATURE REVIEW | 21 |
| 2.1 Pump Displacement Control: | 21 |
| 2.1.1 Pump Displacement in Closed Circuit Configurations: | 22 |
| 2.1.2 Pump Displacement in Open Circuit Configurations: | 22 |
| 2.2 Active Steering Systems: | 23 |
| 2.2.1 Electro-Hydraulic Steering: | 23 |
| 2.2.2 Steer-by-Wire Systems: | 29 |
| 2.3 Active Safety Using Steering | 32 |
| 3. INVESTIGATION OF DISPLACEMENT CONTROL IN STEER-BY-WIRE FOR ON-HIGHWAY APPLICATIONS | 35 |
| 3.1 Advantages of DC Steer-by-Wire | 35 |
| 3.2 Possible Configurations: | 36 |

| | Page |
|--|------|
| 3.2.1 Mechanical Configurations: | 36 |
| 3.2.2 Hydraulic Circuit Configurations: | 38 |
| 3.3 Investigation of the DC Pump in Closed-Circuit with Single Rack Cylinder Configuration: | 44 |
| 3.3.1 System Description | 44 |
| 4. SYSTEM MODELING AND SIMULATION | 46 |
| 4.1 Hydraulic Subsystem Model: | 47 |
| 4.1.1 Pump Loss Model | 47 |
| 4.1.2 Pressure Build-up Model | 49 |
| 4.1.3 Pump Displacement Control Model | 51 |
| 4.2 Mechanical Subsystem Model: | 53 |
| 4.2.1 Steering Actuator Mechanical Model: | 54 |
| 4.2.2 External Load Torque Modeling: | 55 |
| 4.2.3 Vehicle Model: | 61 |
| 4.3 Model Validation: | 65 |
| 4.3.1 Vehicle Model Validation: | 65 |
| 4.3.2 External Load Model Validation: | 69 |
| 5. STEER-BY-WIRE CONTROL SYSTEM DESIGN AND ANALYSIS | 70 |
| 5.1 Simplified System Model | 70 |
| 5.1.1 Derivation of the Simplified Model | 71 |
| 5.1.2 Validation of Simplified Model: | 73 |
| 5.2 Adaptive Robust Control Strategy I: | 76 |
| 5.2.1 Controller Synthesis: | 76 |
| 5.2.2 Simulation Results: | 83 |
| 5.2.3 Control Limitations and Challenges: | 84 |
| 5.3 An Even Simpler System Model: | 85 |
| 5.4 Adaptive Robust Control Strategy II: | 87 |
| 5.4.1 Controller Synthesis: | 87 |
| 5.4.2 Simulation Results | 90 |
| 5.4.3 Laboratory Experimental Results | 92 |
| 5.4.4 Vehicle Experimental Results | 98 |
| 5.5 Performance of the Adaptive Robust Control System | 101 |
| 6. STEER-BY-WIRE FAIL SAFE MECHANISM | 104 |
| 6.1 Fail-Safe Using a Clutch Mechanism: | 104 |
| 6.2 Fail-Safe Using Redundant Independent Steering Systems: | 105 |
| 6.2.1 Implementation of Rear Axle Steering As Fail-Safe Mechanism: | 109 |
| 6.2.2 Experimental Results: | 116 |
| 6.3 Fail-Safe Using Differential Braking for Steering: | 127 |
| 7. INSTRUMENTATION AND EXPERIMENTAL SETUP | 129 |
| 7.1 Laboratory Setup | 129 |

| | Page |
|--|------|
| 7.1.1 Single Rack Steering Actuator | 133 |
| 7.1.2 Linear Steering Actuator | 134 |
| 7.1.3 Position Sensor for Linear Steering Actuator | 134 |
| 7.1.4 Position Sensor for Single Rack Steering Actuator | 135 |
| 7.1.5 Steering Pump | 137 |
| 7.1.6 Swash Plate Control System | 138 |
| 7.1.7 Control ECU | 141 |
| 7.2 Vehicle Setup | 142 |
| 7.2.1 System Architecture: | 143 |
| 7.2.2 Wiring Schematics | 144 |
| 7.2.3 Cylinder Installation | 145 |
| 7.2.4 Pump Installation | 148 |
| 7.2.5 External Gasoline Engine | 148 |
| 7.2.6 Driver Torque Feedback System | 149 |
| 7.2.7 Voltage Inverter | 150 |
| 7.3 Fail-Safe Mechanisms Implementation Into Vehicle | 151 |
| 7.3.1 Fail-Safe Mechanism Using a Clutch | 151 |
| 7.3.2 Fail-Safe Mechanism Using Rear Axle Steering System | 154 |
| 8. ACTIVE CONTROL OF STEERING EFFORT USING DISPLACEMENT CONTROLLED PUMPS | 158 |
| 8.1 The Concept of Active Control of Steering Effort | 158 |
| 8.2 Advantages of Active Control of Steering Effort | 159 |
| 8.3 Active Control of Steering Effort Using DC Pumps | 161 |
| 8.4 Other Possible Implementations: | 162 |
| 8.4.1 Variable Displacement Pump in a Open-Circuit Configuration: | 162 |
| 8.4.2 Fixed Displacement Pump in a Open-Circuit Configuration with a Variable Speed Electric Motor: | 162 |
| 9. CONCLUSIONS AND FUTURE WORK | 166 |
| 9.1 Conclusions | 166 |
| 9.2 Future Work | 167 |
| REFERENCES | 170 |
| A. STEER-BY-WIRE SYSTEM SIZING METHODOLOGY | 174 |
| A.1 System Sizing Methodology: | 174 |
| A.1.1 Cylinder Sizing | 174 |
| A.1.2 DC Pump Sizing | 175 |
| A.1.3 DC Swash Plate Control System Sizing | 176 |
| A.2 Charge Pump Sizing | 176 |
| A.2.1 Sizing Exercise: | 177 |

LIST OF TABLES

| Table | Page |
|---|------|
| 7.1 Linear Position Sensor Specifications | 135 |
| 7.2 Rotary Position Sensor Specifications | 136 |
| 7.3 DC Pump Specifications | 137 |
| 7.4 Control Valve Specifications | 139 |
| 7.5 Charge Pump Specifications | 140 |
| 7.6 External Engine Specifications | 149 |

LIST OF FIGURES

| Figure | Page |
|--|------|
| 1.1 Illustration of Manual Steering System. | 3 |
| 1.2 Manual Steering System with Add-On Power Cylinder and Control Valve | 5 |
| 1.3 Operation of Linear Link Valve [3] | 6 |
| 1.4 Integral Gear with Spool Valve on Cam and Lever Gear [3] | 7 |
| 1.5 Rotary Control Valve Operation: On-Center and Off-Center | 7 |
| 1.6 Integral Steering Gear Section Cut | 8 |
| 1.7 Illustration of an Open-Center Steering System | 9 |
| 1.8 Illustration of an example of Closed-Center Steering System | 10 |
| 1.9 Illustration of an example of a Modified Closed-Center Steering System . | 12 |
| 1.10 Flow Control Circuit of Conventional Steering System Pump. | 13 |
| 1.11 Dual Displacement Pump Flow Control Concept | 15 |
| 1.12 Variable Displacement Pump with Conventional Steering System | 16 |
| 1.13 Fixed Displacement Pump with Variable Speed Electric Motor with Con- ventional Steering System | 17 |
| 2.1 Column-Mounted and Gear-Mounted Electric Torque Overlay Systems . . | 24 |
| 2.2 Steering with Active Pressure Control [23] | 28 |
| 2.3 Active Pressure Control in an Integral Steering Gear Configuration | 28 |
| 3.1 Single Rack Configuration | 37 |
| 3.2 Linear Double Acting Cylinder Configuration | 37 |
| 3.3 Linear Single Acting Cylinder Configuration | 37 |
| 3.4 DC Pump in Closed Circuit with Rotary Cylinder | 38 |
| 3.5 DC Pump in Closed Circuit with Linear Double Acting Cylinder | 39 |
| 3.6 DC Pump in Closed Circuit with Linear Single-Acting Cylinder | 39 |
| 3.7 DC Pump in Open Circuit with Rotary Cylinder | 40 |

| Figure | Page |
|---|------|
| 3.8 DC Pump in Open Circuit with Double Acting Cylinder | 40 |
| 3.9 DC Pump in Open Circuit with Single Acting Cylinder | 41 |
| 3.10 DC Pump in Closed Circuit with Rotary Cylinder | 41 |
| 3.11 Variable Speed Motor with Fixed Displacement Pump in Open Circuit with Double Acting Cylinder | 41 |
| 3.12 Variable Speed Motor with Fixed Displacement Pump in Open Circuit with Single Acting Cylinder | 42 |
| 3.13 Displacement Control Steer-by-Wire System. | 43 |
| 3.14 Swash Plate Control System. | 45 |
| 4.1 Overall Model Architecture. | 46 |
| 4.2 Pump Volumetric Losses at Full Displacement [2] | 48 |
| 4.3 Pump Torque Losses at Full Displacement [2]. | 49 |
| 4.4 illustration of Pressure Build-up in Cylinder | 50 |
| 4.5 Swash Plate Control System. | 51 |
| 4.6 DC Steer-by-Wire Mechanical Subsystem. | 53 |
| 4.7 Steering Actuator Model. | 55 |
| 4.8 External Loads on DC Steer-by-Wire System. | 56 |
| 4.9 Road Wheel Rotation Geometry. | 57 |
| 4.10 Kingpin Moment due to Lateral Tire Forces | 58 |
| 4.11 Tire Force Distribution | 59 |
| 4.12 Kingpin Moment due to Longitudinal Tire Forces | 60 |
| 4.13 Development Vehicle | 60 |
| 4.14 Vehicle FBD with Lateral Forces Only | 62 |
| 4.15 Generalized Three-Axle Bicycle Model | 63 |
| 4.16 Overall DC Steer-by-Wire System Model | 64 |
| 4.17 Vehicle Model in Simulink | 65 |
| 4.18 Inputs Used for Model Validation: (a) Double Lane Change Maneuver, (b) Figure 8 Maneuver. | 66 |

| Figure | Page |
|--|------|
| 4.19 Vehicle Dynamics Validation: (a) Double Lane Change Maneuver, (b) Figure 8 Maneuver. | 67 |
| 4.20 Tire Side Forces Validation: (a) Double Lane Change Maneuver, (b) Figure 8 Maneuver. | 68 |
| 4.21 Kingpin Moment Validation: (a) Double Lane Change Maneuver, (b) Figure 8 Maneuver. | 69 |
| 5.1 Bode plot of T_M and T_Q | 72 |
| 5.2 Simplified Model Validation Diagram | 74 |
| 5.3 Simplified Model Validation: (a) Steering Rate Response, (b) Steering Position Response. | 75 |
| 5.4 Simulation Results for a Sinusoidal Desired Steering Rate. | 83 |
| 5.5 Simulation Results for a Square Desired Steering Rate. | 84 |
| 5.6 Bode Plot Comparison of the Two Simplified Models. | 86 |
| 5.7 Simpler Model Validation. | 87 |
| 5.8 Simulation Results for a Sinusoidal Desired Steering Position | 91 |
| 5.9 Simulation Results for a Square Desired Steering Position | 91 |
| 5.10 Schematics of Experimental Laboratory Setup using Single Rack Cylinder | 92 |
| 5.11 Single Rack Experimental Results for a Sinusoidal Wave Desired Steering Position | 93 |
| 5.12 Single Rack Experimental Results for a Square Wave Desired Steering Position | 94 |
| 5.13 Schematics of Experimental Laboratory Setup using Linear Cylinder | 95 |
| 5.14 Experimental Results for a Sinusoidal Wave Desired Steering Position. | 96 |
| 5.15 Experimental Results for a Filtered Step Desired Steering Position | 97 |
| 5.16 Experimental Vehicle Setup Schematics | 98 |
| 5.17 Experimental Results for a Low Speed Double Lane Change Maneuver | 99 |
| 5.18 Experimental Results for a Static Steering Maneuver (Dry Park) | 100 |
| 5.19 Performance of the ARC System | 103 |
| 6.1 Fail-Safe Mechanism using Clutch with Modified Steering Gear. | 106 |
| 6.2 Fail-Safe Mechanism using Clutch with Linear Acting Cylinder | 107 |

| Figure | Page |
|---|------|
| 6.3 Fail-Safe Mechanism using Redundant Steering on the Same Axle | 108 |
| 6.4 Fail-Safe Mechanism using Redundant Steering on the Rear Axle | 108 |
| 6.5 Vehicle Yaw Rate Simulation Response when Rear Wheels Steered and Front Wheels Locked in Straight-Ahead Position | 113 |
| 6.6 Vehicle Yaw Rate Response when Rear Wheels Steered and Castered Front Wheels | 115 |
| 6.7 Test Vehicle Equipped with Rear Axle Steering System | 116 |
| 6.8 Model Validation Results with Front and Rear Steered Sequentially . . . | 118 |
| 6.9 Model Validation Results with Front and Rear Steered Simultaneously . | 119 |
| 6.10 Experimental Validation Results for Fail-Safe Using Steering: Typical Steering Maneuvers | 120 |
| 6.11 Experimental Validation Results for Fail-Safe Using Steering: Large Steer- ing Maneuvers | 121 |
| 6.12 Experimental Validation Results for Fail-Safe Using Steering with Feed- back Term | 123 |
| 6.13 Experimental Validation Results for Fail-Safe Using Steering Equation 6.27 With Castered Front Axle | 125 |
| 6.14 Experimental Validation Results for Fail-Safe Using Steering Equation 6.26 With Castered Front Axle | 126 |
| 7.1 Schematics of Experimental Laboratory Setup using Single Rack Cylinder | 130 |
| 7.2 Experimental Laboratory Setup using Single Rack Cylinder | 131 |
| 7.3 Schematics of Experimental Laboratory Setup using Linear Cylinder . . | 132 |
| 7.4 Experimental Laboratory Setup using a Linear Cylinder | 132 |
| 7.5 Single Rack Steering Actuator | 133 |
| 7.6 Linear Steering Actuator | 134 |
| 7.7 Linear Position Transducer | 135 |
| 7.8 Tilt Sensor for Measuring Pitman Arm Position | 136 |
| 7.9 DC Steering Variable Displacement Pump | 137 |
| 7.10 Swash Plate Control System. | 138 |
| 7.11 Proportional Directional Control Valve | 139 |

| Figure | Page |
|--|------|
| 7.12 ZF TRW EPHS Pump | 140 |
| 7.13 Swash Plate Angle Position Sensor | 141 |
| 7.14 dSPACE MicroAutobox | 142 |
| 7.15 Test Vehicle: Freightliner FL60 | 142 |
| 7.16 Experimental Vehicle Setup Schematics | 143 |
| 7.17 Vehicle Setup Wiring Schematics of DC Steer-by-Wire | 145 |
| 7.18 Cylinder Installation on Vehicle | 146 |
| 7.19 Cylinder Installation on Vehicle Close-Up | 146 |
| 7.20 Engine-Pump Installation on Vehicle: Top View | 147 |
| 7.21 Engine-Pump Installation on Vehicle: Side View | 147 |
| 7.22 Honda GX270 External Gasoline Engine | 148 |
| 7.23 ZF ReAX Torque Overlay Steering System Used as Torque Feedback Device | 150 |
| 7.24 Xantrex PROwatt Voltage Inverter | 151 |
| 7.25 Vehicle Fail-Safe Mechanism Using a Pneumatic Clutch | 152 |
| 7.26 Fail-Safe Mechanism Using a Clutch: Inside Cab. | 153 |
| 7.27 Fail-Safe Mechanism Using a Clutch: Engine Compartment. | 153 |
| 7.28 Rear Axle Steering System on Test Vehicle | 155 |
| 7.29 Rear Axle Steering System on Test Vehicle : Top View. | 156 |
| 7.30 Rear Axle Steering System on Test Vehicle : Bottom View. | 156 |
| 7.31 System Architecture of Fail-Safe Using Rear Axle Steering | 157 |
| 8.1 Proposed Torque Control Block Diagram | 159 |
| 8.2 Hand Wheel Torque Response with and without an Active Steering Effort Control system | 160 |
| 8.3 Active Steering Effort Control Using Displacement Controlled Pump in Closed-Circuit Configuration | 163 |
| 8.4 Active Steering Effort Control Using Displacement Controlled Pump in Open-Circuit Configuration | 164 |
| 8.5 Active Steering Effort Control Using Fixed Displacement Pump with Variable Speed Motor in Open-Circuit Configuration | 165 |

A.1 Single Rack Cylinder used in Steer-by-Wire System 175

SYMBOLS

| | |
|------------|--|
| A_A | area of side A of cylinder piston |
| A_B | area of side B of cylinder piston |
| $C_{H,A}$ | hydraulic capacitance term of side A of cylinder |
| $C_{H,B}$ | hydraulic capacitance term of side B of cylinder |
| C_i | tire cornering stiffness at the i^{th} axle |
| D_{sv} | proportional directional valve's DC gain |
| F_c | Coulomb friction on steering cylinder |
| $F_{y,i}$ | side force on the tires of the i^{th} axle |
| $F_{z,R}$ | vertical load on right wheel |
| $F_{z,L}$ | vertical load on left wheel |
| H | linear stroke of cylinder |
| $I_{v,z}$ | vehicle moment of inertia about the z-axis |
| K | fluid bulk modulus |
| M_L | load moment on steering actuator |
| $M_{kp,R}$ | moment at the right kingpin |
| $M_{kp,L}$ | moment at the left kingpin |
| R_{link} | steering linkage ratio |
| Q_A | flow across side A of cylinder |
| Q_B | flow across side B or cylinder |
| Q_i | ideal flow output of the pump |
| Q_e | effective flow output of the pump |
| Q_s | pump flow losses |
| $Q_{s,i}$ | internal leakage across cylinder |
| Q_r | flow across relief valve |
| T_e | effective torque on pump shaft |

| | |
|------------|--|
| T_s | pump torque losses |
| V_A | volume of side A of cylinder |
| V_B | volume of side B of cylinder |
| $V_{L,A}$ | volume of hydraulic line A |
| $V_{L,B}$ | volume of hydraulic line B |
| V_d | pump displacement |
| V_{sv} | voltage input to control valve |
| b | damping coefficient of steering cylinder |
| d | kingpin offset |
| l_{mech} | steering system mechanical trail |
| l_{pt} | tire pneumatic trail |
| m_{eq} | steering system equivalent mass |
| m_v | vehicle mass |
| n_e | engine speed |
| p_A | pressure inside side A of cylinder |
| p_B | pressure inside side B of cylinder |
| p_L | load pressure across control valve |
| r | pitch radius of of single rack steering cylinder |
| r_{tire} | tire radius |
| v_y | vehicle lateral velocity |
| v_x | vehicle longitudinal velocity |
| x | piston position |
| x_i | distance between vehicle's center of gravity and the i^{th} axle |
| y_{sv} | position of servo control spool |
| Δp | pressure differential |
| α | ratio of cylinder piston areas |
| α_i | tire side slip angle at the i^{th} axle |
| β | normalized swash plate angle of the pump |
| δ_i | steering angle at the i^{th} axle |

| | |
|---------------|--|
| δ_w | road wheel steering angle |
| λ | kingpin inclination angle |
| ν | wheel caster angle |
| ω_{sv} | natural frequency of control valve |
| θ | angle at the output shaft of the steering actuator |
| $\dot{\psi}$ | vehicle's yaw rate |
| ζ_{sv} | damping ratio of control valve |

ABBREVIATIONS

| | |
|------|---|
| ARC | Adaptive Robust Controller |
| AFS | Articulated Frame Steering |
| COG | Center Of Gravity |
| DC | Displacement Controlled |
| ECU | Electronic Control Unit |
| EPS | Electric Power Steering |
| EPHS | Electrically Powered Hydraulic Steering |

ABSTRACT

Nhila, Amine Ph.D., Purdue University, December 2018. Pump Displacement Control in Steering On-Highway Commercial Vehicles. Major Professor: Monika Ivantysynova, School of Mechanical Engineering.

Due to recent advances in sensor technology and the exponential increase in computation power of electronic control units (ECUs) along with their increasing affordability, active safety and vehicle automation have become major trends in the commercial vehicle industry. New regulations for increased safety are also a major driver behind the industry's increased interest in that topic. As a result, being a crucial part of vehicle automation, steering systems had to be adapted to enable Active Steering. Consequently, commercial vehicle steering designers introduced the concept of torque and angle overlay using an electric motor in series with the conventional hydraulic steering system. However, despite the fact that these systems are becoming more prevalent in the market, they still suffer from inefficiencies intrinsic to the conventional hydraulic steering system still being used. These inefficiencies are a result of flow metering losses due to the use of control valves to regulate the pump flow output, as well as inside the steering gear with the use control valves to build assistance pressure.

In this research project, we investigate the potential use of the proven pump Displacement Control (DC) technology in steering on-highway commercial vehicles. DC pumps have been shown to significantly improve system efficiency as they allow the removal of control valves typically used to regulate flow [1]. Instead, the displacement of the pump can be directly controlled to vary the pump's flow rate and direction, and thus eliminating throttling losses. The DC technology has been successfully used in a steer-by-wire configuration for an articulated frame steering vehicle and has

been shown to significantly improve efficiency and productivity, as well as result in a reduction in fuel consumption [2].

In this work, we propose a steer-by-wire system, using DC pump technology, for on-highway commercial vehicles, and present the different possible configurations in which it can be implemented. Moreover, the benefits and drawbacks of the steer-by-wire system are researched and identified. Subsequently, the system is designed and validated in simulation, on laboratory test setup, as well as on a test vehicle to prove its feasibility.

Chief among the drawbacks of the steer-by-wire system is potential failures that can lead to the complete loss of the steering function of the vehicle. As a result, different possible fail-safe mechanisms are researched from which the most suitable ones are proposed to allow the steer-by-wire system to fail safely. Moreover, two of the proposed fail-safe mechanism are implemented onto the test vehicle to prove and validate their feasibility.

Furthermore, an alternative way of using displacement controlled pumps for active steering is be proposed. For this concept, we investigate the possibility of actively controlling the driver's steering effort by varying the pump displacement while maintaining the mechanical link between the steering wheel and the road wheels. If successful, this method will allow for a more efficient way of providing steering assistance as it does away with the conventional control valves used to build pressure and regulate pump flow, and thus eliminating throttling losses. This method has also the advantage of having an intrinsic fail-safe mechanism with manual steering being always possible should the hydraulic or electric systems fail.

1. EVOLUTION OF STEERING SYSTEMS IN ON-HIGHWAY COMMERCIAL VEHICLES

1.1 Background

As commercial vehicles grew in size to keep up with society's needs, hydraulic power steering with their higher power density became an integral part of modern heavy vehicles. Starting as add-on systems in parallel with the manual steering system, hydraulic power steering has undergone a long evolution that resulted in more compact and sophisticated systems that are relatively more efficient. Nonetheless, the power steering systems currently available in the market still suffer from inefficiencies mainly stemming from flow metering that is still being used to adjust pump flow output with engine speed, and to build the required assistance pressure. Furthermore, due to the ever increasing demand for safety systems and vehicle automation systems such as Lane Keeping Assistance, Automated Docking, and Highway Autopilot Systems, steering designers had to come up with ways to allow steering systems to be actively controlled by external systems. As a result, different system designs have been proposed in the recent decades, particularly, in the passenger car industry which could afford to transition to fully electric steering systems by taking advantage of their lower front axle weight which can be steered with reasonably sized 12 Volt motors. Consequently, using electric motors, solutions such as the torque and angle overlay systems were proposed in which the motor torque or position is overlaid on top of the driver's input to help improve steering comfort but also enhance safety using systems such as stability control and lane keeping assistance. Moreover, some passenger manufacturers introduced electric steer-by-wire systems using electric motors to drive the road wheels based on vehicle dynamics and measured inputs at the hand-wheel. However, up to now, these electric solutions have not been viable in com-

mercial vehicles due to their significantly higher weight and the relatively low power density of electric motors operating at the currently available voltage ranges (12-24 Volts). As a result, with the goal of implementing active steering into commercial vehicles, steering system suppliers introduced the concept of torque and angle overlay into heavy vehicles by using an electric motor in series with the already existing hydraulic steering system, and thus leveraging the high power density of hydraulics along with the electronic controllability of motors. Nevertheless, while this concept enables active steering in commercial vehicles, the inefficiencies of the unchanged hydraulic steering system remain, i.e. flow throttling losses as will be shown in the rest of this chapter.

Most recently, however, a more efficient electro-hydraulic steer-by-wire system was proposed for off-road articulated frame steering vehicles where a Displacement Controlled (DC) pump was used to control the motion of the actuating cylinder [2]. Using the proven DC pump technology [1], the rate and direction of the flow to the actuator can be controlled directly from the pump by actively varying its displacement instead of using metering valves, and thus, improving efficiency significantly. This system also helped improve productivity by controlling steering effort and varying steering ratio based on operating conditions.

1.2 Motivation

The motivation behind this research project is to investigate the possibility of using DC pump technology in steering systems for on-highway commercial vehicles in order to enable active steering while improving efficiency. Doing so will be a major improvement on the currently available systems which still suffer from inefficiencies as a result of valve throttling losses. Efficiency, Active Safety, and Vehicle Automation are all global mega-trends in the commercial vehicle industry and steering using pump Displacement Control technology can be the key to achieving all three simultaneously.

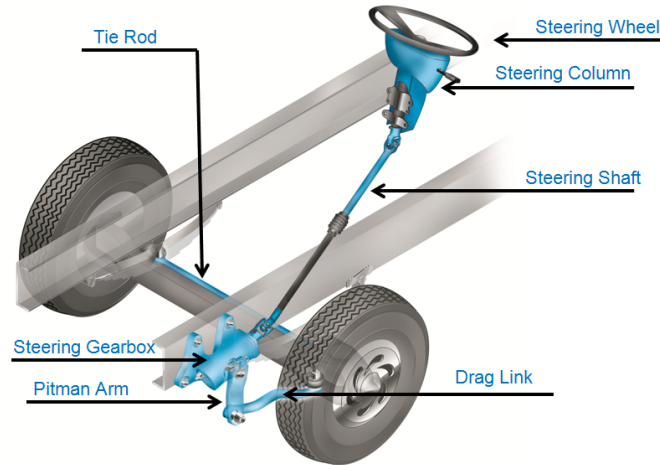


Figure 1.1. Illustration of Manual Steering System.

1.3 Manual Steering

The purpose of steering systems on commercial vehicles is to convert the steering wheel displacement into a displacement of the road wheels. The transfer of energy from hand-wheel to road wheel is achieved through a series of mechanical links (Figure 1.1). Turning the steering wheel, turns the intermediate shaft which in turn results in turning the input of the steering gear. As a result, the output of the steering gear rotates and with it the pitman arm which moves the drag link that pulls or pushes the steering arm resulting in the rotation of the driver side road wheel. A tie rod between the road wheels causes the right wheel to move with the left wheel. Additionally, a manual steering system aims to decrease the driver's required effort to steer the vehicle through torque amplification at the steering gear box. Typically, a manual steering gear box on a commercial vehicle will have a ratio up to 32:1. While the higher the gear ratio the easier it will be for the operator to steer the vehicle, it will also take more hand-wheel rotation to achieve the same displacement at the road wheels which becomes undesirable if too high [3].

As commercial vehicles grew in size to keep up with society's needs, so did their weight. With increased weight, trucks became harder to steer and manual steering no

longer offered a satisfying solution. While mechanical steering provided good steering feel, it failed to provide the necessary steering efforts for heavier vehicles which led to the gradual emergence of hydraulic power steering systems. Hydraulic power steering uses a pressurized fluid inside a cylinder with one or both ends connected to steering system linkage to provide additional steering force to help the driver. All production hydraulic power steering systems use this principle to provide steering assistance and they only differ from each other in (1) the mechanism used to provide flow, i.e. types of pumps, (2) the mechanism used to pressurize the fluid, i.e. types of control valve, and (3) the way hydraulic energy is converted into mechanical energy, e.g. external power cylinder or cylinder integrated into the steering gear.

1.4 Power Cylinder with a Linear Link Valve

Initially, hydraulic power steering in commercial vehicles was a niche market and its rate of installation was relatively low [3]. Consequently, the first systems were designed to be add-on systems that would be implemented into already existing manual steering systems. The goal of these systems was reduce efforts while maintaining some type of steering feel. In such designs, a hydraulic cylinder is attached to the steering system linkage to provide additional assistance to steer the vehicle. An engine driven pump is used to supply fluid to the power cylinder and a control valve is used to direct the flow to the proper chamber of the cylinder depending on the direction of steering. Among the early control valve used was a linear valve manufactured into the drag link with its body attached to the steering arm and the spool connected to the pitman arm (Figure 1.2). When the valve is in the neutral on-center position, the flow from the pump circulates through the valve and returns to the reservoir. The valve is held in the center position using centering springs in addition to the hydraulic reaction force; The pressure used to assist the driver is also communicated to the ends of the valve through the holes in the spool (Figure 1.3) resulting in additional resistance on its motion which leads to improved steering feel for the driver.

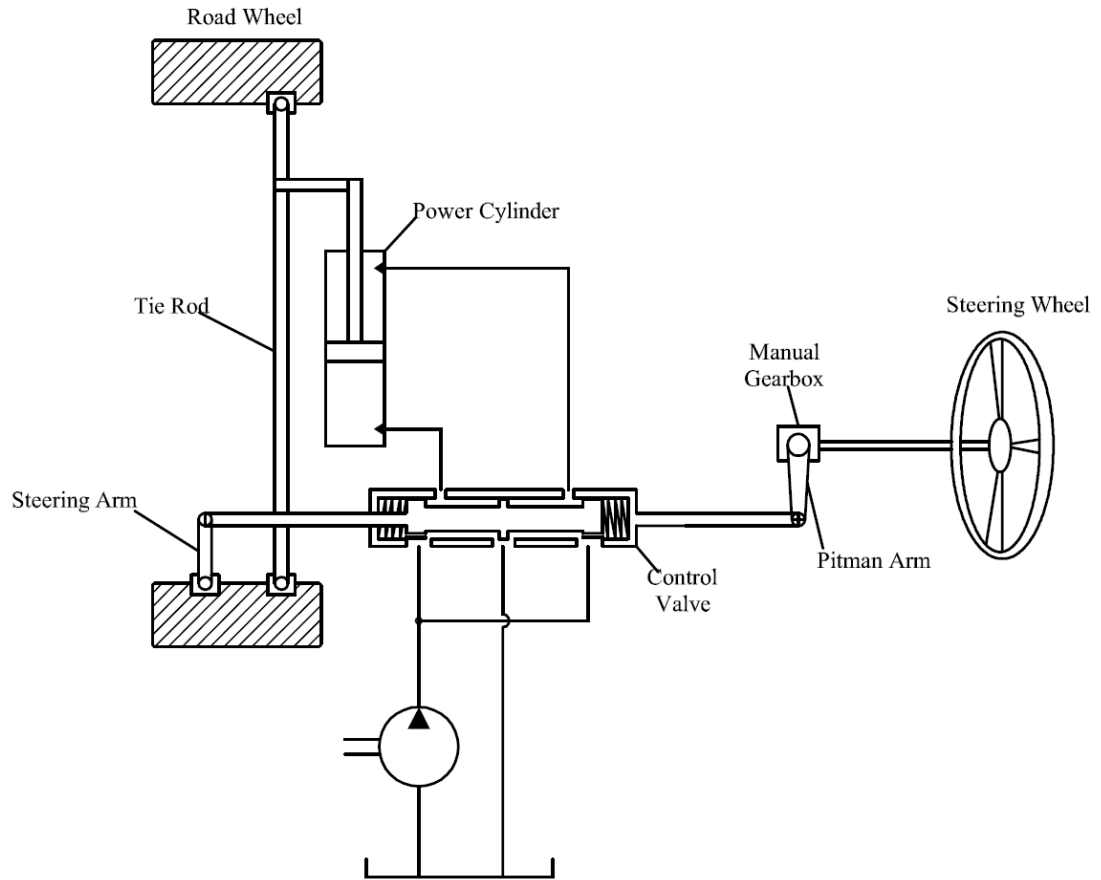


Figure 1.2. Manual Steering System with Add-On Power Cylinder and Control Valve

In addition to providing centering force, the centering springs also provide road feel to the driver during on-center driving by mechanically transmitting some of the road forces to the steering wheel, i.e. "steering on the spring". When the force in the link required to steer the vehicle becomes greater than the spring centering force and the hydraulic reaction force, the spool is displaced allowing the pressurized fluid to flow into one side of the power cylinder while simultaneously connecting the other side to the reservoir port on the valve. As the efforts to steer the vehicle increase, the valve opening increases providing incremental assistance to the driver. Moreover, in addition to providing steering feedback to the driver, the centering springs and

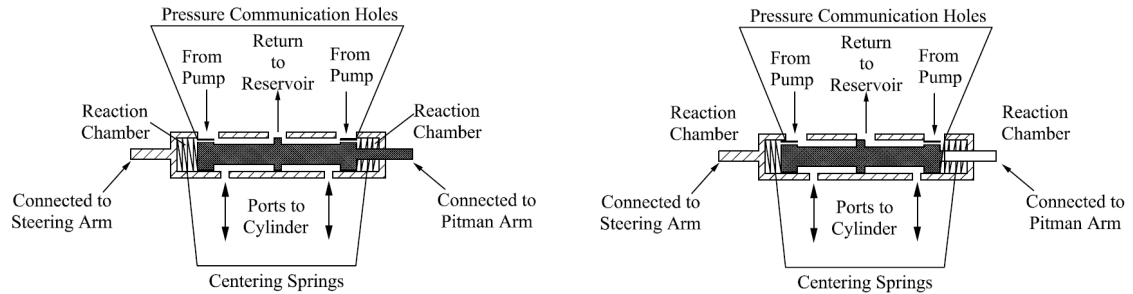


Figure 1.3. Operation of Linear Link Valve [3]

the hydraulic reaction force also determine the reversibility of the steering system. Having low reversing forces that are not enough to overcome the friction and inertia of the steering system will cause the control valve to stay open and the pressure to be communicated to the power cylinder preventing the steering system from reversing. Conversely, having high reversing forces through stiffer centering springs will result in higher steering effort from the driver and a rough transition between "steering on the springs" and power assist regions. As a result, the design engineer has to properly choose the right components that will realize the desired reversibility without compromising steering feel [3].

1.5 Semi-Integral Steering Systems

As the demand for power steering started to increase, more compact designs were introduced in which the control valve was integrated with the power cylinder or the steering gear (Figure 1.4). These designs simplified installations and reduced leakage points by eliminating hydraulic lines between the control valve and power cylinder. Putting the valve at the input of the steering gear also allowed for softer centering springs since the required reversing forces are reduced by a factor equivalent to the steering gear ratio. This also makes for a more compact package. Moreover, with the semi-integral recirculating ball steering gear, a rotary control valve was used in which a torsion bar connects the input shaft of the steering gear to the valve spool.

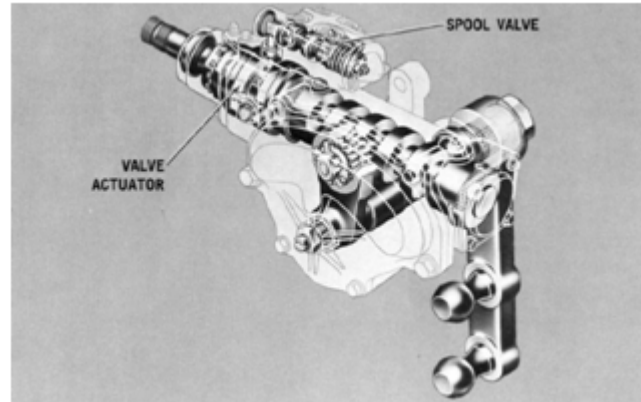


Figure 1.4. Integral Gear with Spool Valve on Cam and Lever Gear [3]

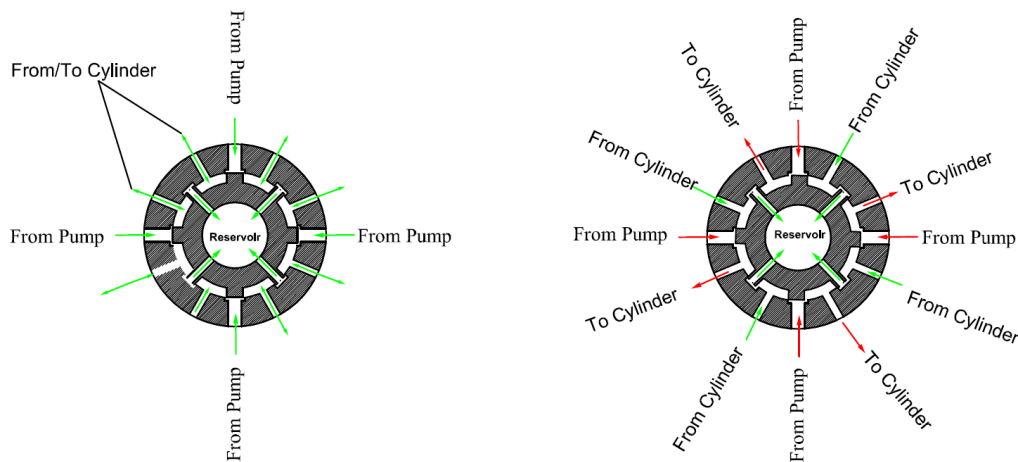


Figure 1.5. Rotary Control Valve Operation: On-Center and Off-Center

As the hand-wheel is displaced by the driver, the torsion bar twists providing valve operation and proportional road feel (Figure 1.5) [3]

1.6 Integral Steering Gear

The most current and widely used design combines the valve, the steering gear, and the power assist system into one compact unit (Figure 1.6). In addition to the compactness of the package, this design also offers other advantages such as reduced

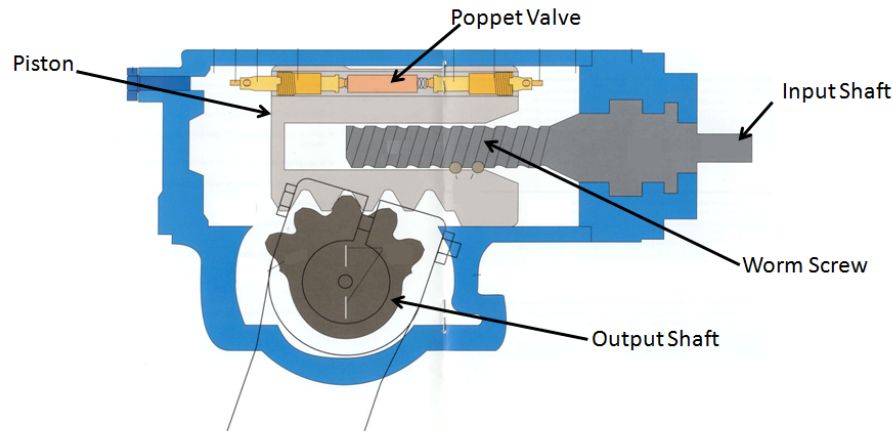


Figure 1.6. Integral Steering Gear Section Cut

re-centering force requirements. With the valve mounted at the input of the gear rather than at the output, all the friction forces below the steering gear have a reduced effect at its input requiring smaller torsion bar or centering springs to force the valve to close and help with the reversibility. This compact packages also leads to fewer external hydraulic lines which frees up space in the engine compartment and reduces the number of leak points.

Depending on the type of valve used inside the steering gear, power steering systems are classified into two categories; open-center steering systems and closed-center steering system:

Open-Center Steering

The open-center valve (Figure 1.7) which as its name suggests is open in the on-center or neutral position allowing the fluid supplied by the pump to circulate through the valve and back to the reservoir with minimal pressure drop. As the driver applies torque on the hand-wheel, the valve starts to close creating a restriction on the flow which causes the pressure of the fluid to rise. The more torque the driver applies, the bigger the restriction on the fluid, and thus, the higher the pressure of

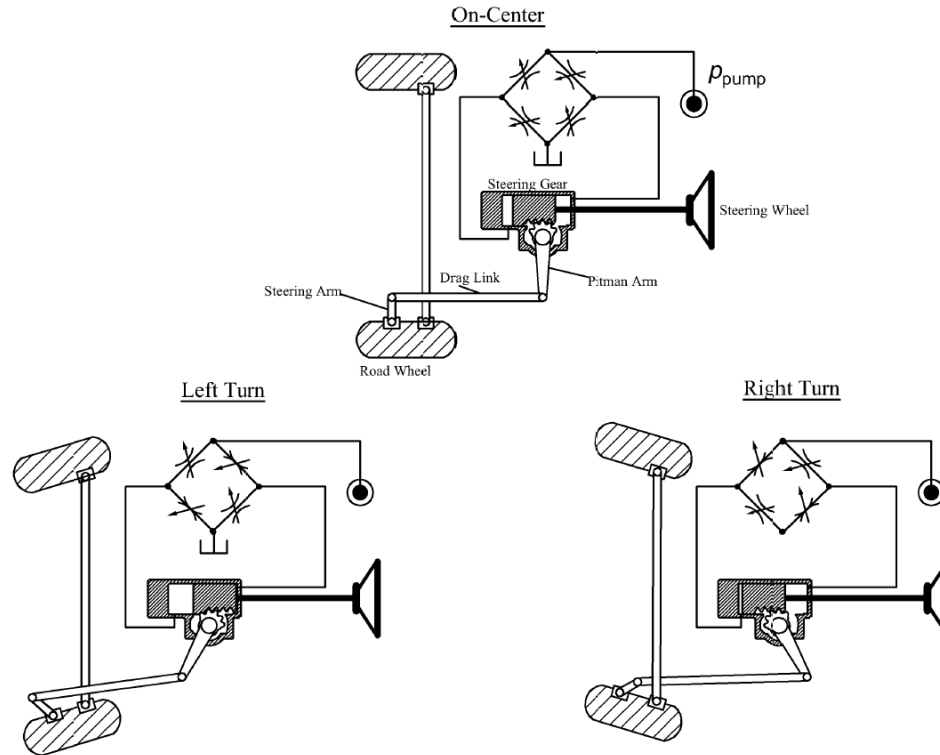


Figure 1.7. Illustration of an Open-Center Steering System

the fluid becomes, providing assistance to the driver. Additionally, the direction of displacement of the valve determines the chamber of the steering gear to which the pressurized fluid will flow, providing torque assistance in the appropriate direction.

Despite the valve being open in the neutral position, the fluid still experiences some resistance causing a small pressure drop across the valve. This is what is referred to as a parasitic loss which start to become significant for vehicles that spend the majority of their time on-center such as on-highway commercial vehicles. These parasitic losses manifest as heat in the steering fluid which can become costly for vehicle manufacturers when having to add cooling devices and for steering system suppliers when paying warranty claims. Moreover, with the open-center system, during high speed on-center driving such as in a highway lane keeping situation, even small path corrections will cause the hydraulic system to provide some assistance,

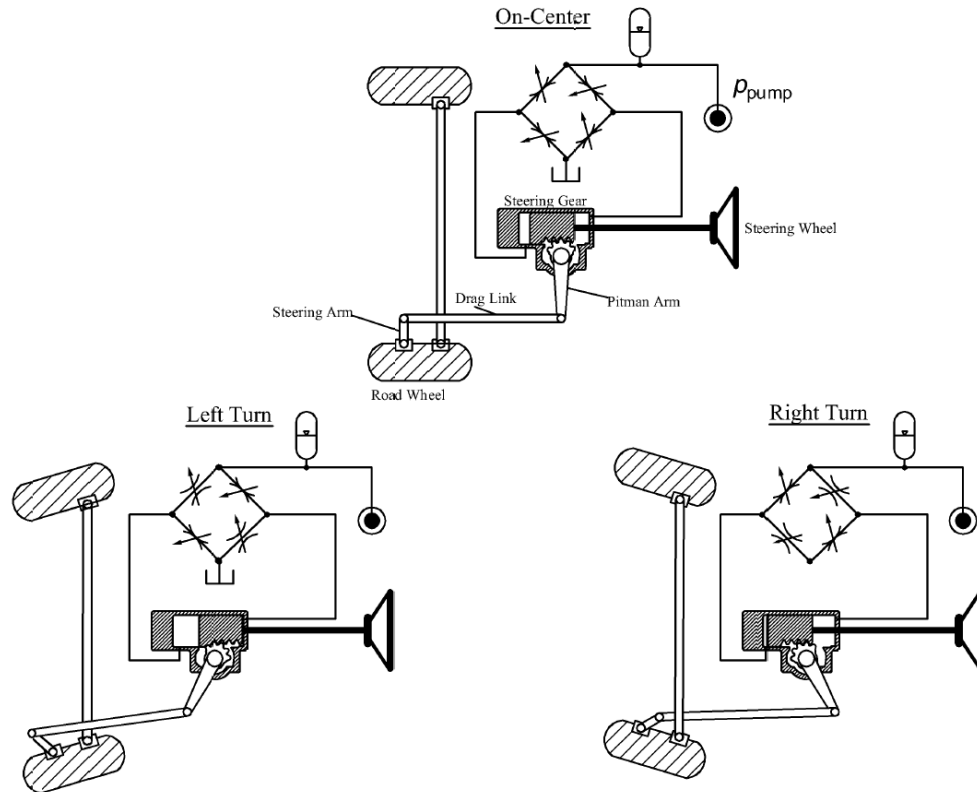


Figure 1.8. Illustration of an example of Closed-Center Steering System

though small, and may decrease the stability of the system. In fact, in these on-center driving situations a manual steering feel is preferred but is not possible with open-center control valves.

Closed-Center Steering

With parasitic losses and on-center steering feel in mind, steering system designers came up with the closed-center steering concept (Figure 1.9). As the name suggests, this system employs a valve that is closed in the on-center position preventing the fluid from flowing through it. This eliminates the pressure drop across the valves and provides a manual steering feel on-center resulting in a better road feel. As more torque is applied by the driver on the steering wheel, the closed-center valve starts

opening and supplying pressurized fluid to the appropriate chamber of the steering gear depending on the direction of displacement.

Different closed-center systems exist with different ways of generating pressure in the fluid. One of the most common ways of building pressure is through the use of an accumulator. Typically, a pump supplies fluid to the accumulator which holds the pressurized fluid until it is needed by the steering system. The pump is either a fixed displacement pump driven by an electric motor, or a variable displacement pump that is controlled by a control system that monitors the pressure level in the accumulator. Once the pressure drops below a certain threshold, fluid will be supplied to the accumulator from the pump until its pressure is restored. When the closed-center valve starts opening, the pressurized fluid is directed to the designated chamber of the steering gear and the amount of hydraulic assistance will be proportional to the valve opening area as the flow is metered from the accumulator into the steering gear. Furthermore, in order to increase the region of manual steering feel on-center, closed-center valves feature an overlap area that has to be overcome before pressurized fluid will start flowing into the steering gear.

Other closed-center systems build fluid pressure using an open-center valve in parallel with the closed-center valve as shown in Figure 1.9 [4]. When in neutral position, the closed-center valve prevents the fluid from going into the steering gear chambers, while the open-center valve is fully open and allows fluid to circulate back to the reservoir. As the steering wheel starts displacing away from center, the open-center valve starts closing and thus building fluid pressure. At the same time, the closed-center valve starts opening and directing the pressurized fluid to the appropriate chamber of the steering gear. With the use of an open-center valve in parallel with a closed-center valve, the parasitic losses still remain an issue. However, this system does provide the desired manual steering feel on-center with use of an overlapped closed-center valve.

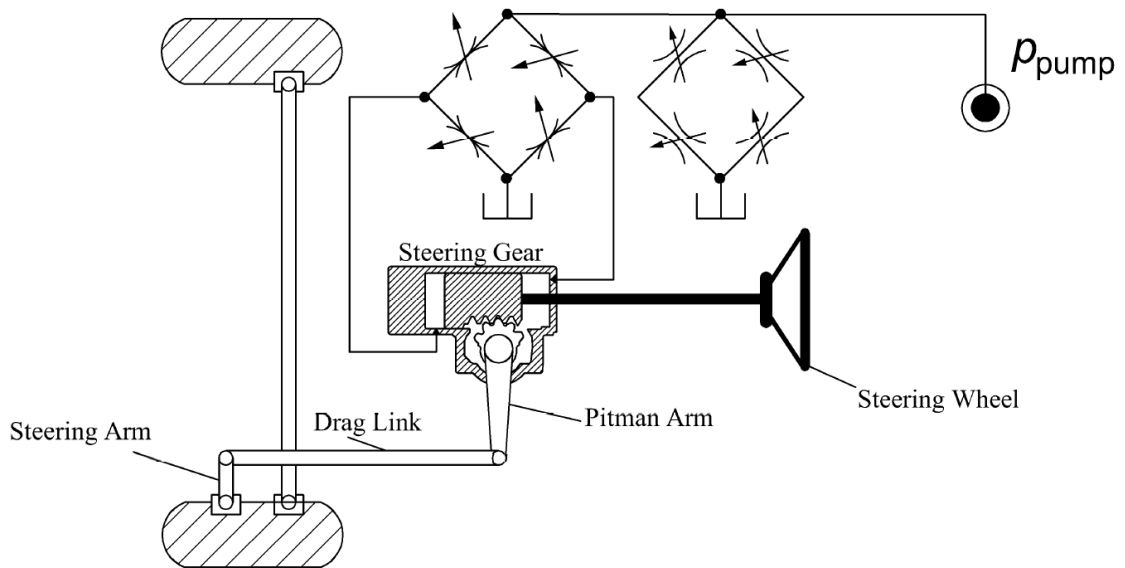


Figure 1.9. Illustration of an example of a Modified Closed-Center Steering System

result, engine-driven fixed-displacement pumps used in steering feature some form of flow control that regulates the flow output as a function of engine speed. The basic function of the flow control is to bypass the excess flow away from the steering gear and back to the reservoir (Figure 1.10). Typically, a fixed orifice placed right after the pump is used as an indirect measure of engine speed as the faster the pump rotates, the higher its flow output, resulting in a higher pressure drop across the orifice which is then used to displace the spool of the flow control valve as shown in Figure 1.10. However, bypassing the flow by throttling the flow increases the steering system parasitic losses. These losses not only affect the energy consumption of the system but also increase the fluid temperature which shortens the life of the seals, increasing the chance of leak occurrences and affecting performance. To mitigate this issue some systems use cooling devices to reduce fluid temperature. However, these additional components increase system cost and use more of the already limited space in the engine compartment.

In order to reduce the parasitic losses with the use of fixed-displacement pumps, steering system manufacturer ZF has introduced the dual displacement concept in their ActivMode pump ([5], [6]) (Figure 1.11). This pump is based on the typical vane pump design but has an asymmetrical cam profile that allows for two different displacements from the two pumping chambers. These chambers are designed such that at engine idle; the flow from both chambers is combined and supplied to the steering gear. However, at engine cruising speeds, the flow from the smaller chamber is enough to provide hydraulic assistance at the steering gear, and therefore, the flow from the bigger chamber is completely circulated back to the reservoir with minimal parasitic pressure drop. The dependency of the pump's flow output on engine speed is established using a fixed orifice at the output of the pump across which the pressure drop increases as flow, and thus engine speed increases. That pressure drop is then used to actuate the spool of the flow control valve. As a result, the ActivMode pump significantly decreases parasitic losses; however, some losses still persist when bypassing the excess fluid through a fixed size port. Another issue that arises with

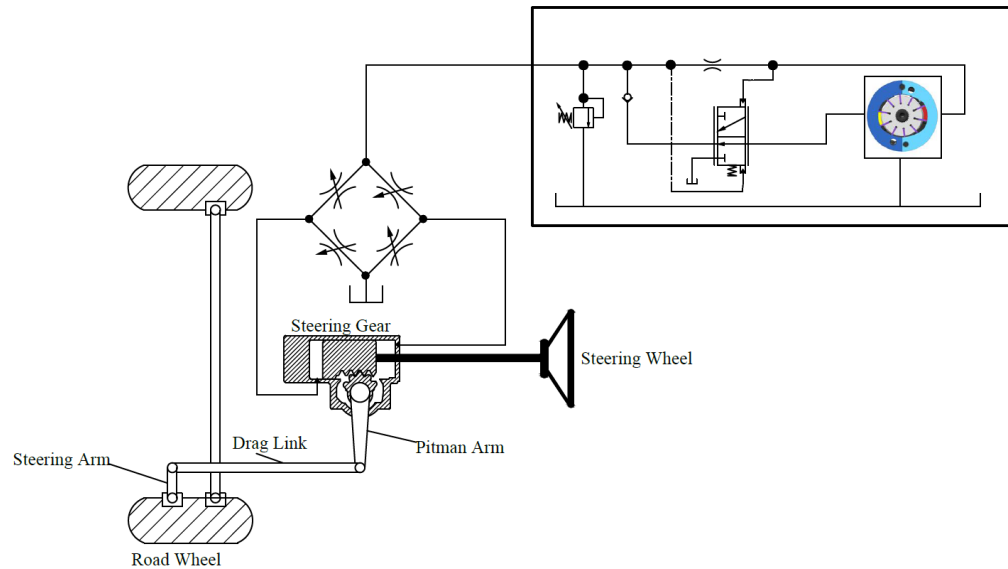


Figure 1.11. Dual Displacement Pump Flow Control Concept

this type of pump is the unbalanced loads on the pumps drive shaft, as a result of the asymmetrical cam profile, which has to be accounted for in the design. However, such asymmetry in loading is minimal as it only occurs at low pressure when the vehicle is traveling at higher speeds during which it does not require much assistance from the hydraulic steering system. Consequently, this pump is still an attractive option for original equipment manufacturers (OEMs) due to its simple design which allows for a small package, and energy savings that are comparable to the variable displacements pumps currently available in the market.

1.7.2 Variable Displacement Pumps

With the aim of reducing parasitic losses in steering systems, some steering system suppliers have introduced variable displacement pumps to directly regulate the flow output of the pump as a function of engine speed (Figure 1.12). However, in order to keep the system simple and affordable, these pumps are passively controlled using hydraulic force feedback. For example, the Varioserv pump by Bosch, uses pressure

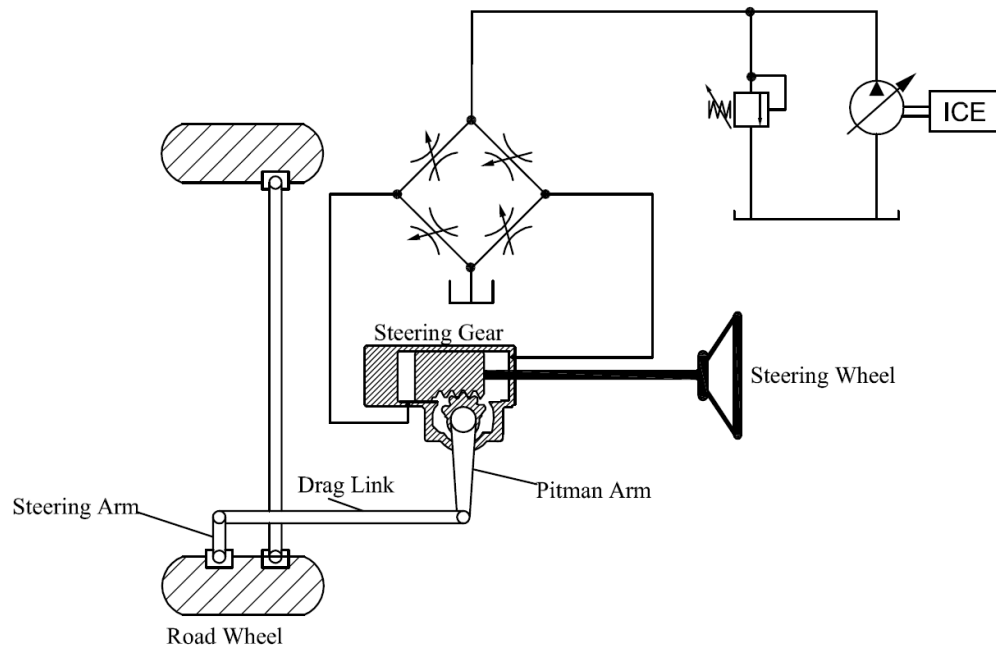


Figure 1.12. Variable Displacement Pump with Conventional Steering System

of the fluid around an eccentrically supported cam ring to shift it and change the geometrical displacement of the pump, ultimately regulating its the flow output as a function of engine speed.

Electronically controlled variable pumps can also be used in steering systems and have the potential to solve many of the issues from which steering systems suffer, i.e. parasitic losses and on-center stability. Nonetheless, these pumps have not gained traction in the commercial vehicle industry yet, but as the technology becomes more affordable it may prove to be the new state of the art.

1.7.3 Fixed Displacement Pump with Variable Speed Electric Motor:

Another option that was proposed by the industry is the use of a fixed displacement pump driven by a variable speed electric motor. With this system, the speed of the motor can be varied based on different vehicle dynamics parameters such as vehicle speed and steering rate. As a result, when at stand still, the pump provides maximum

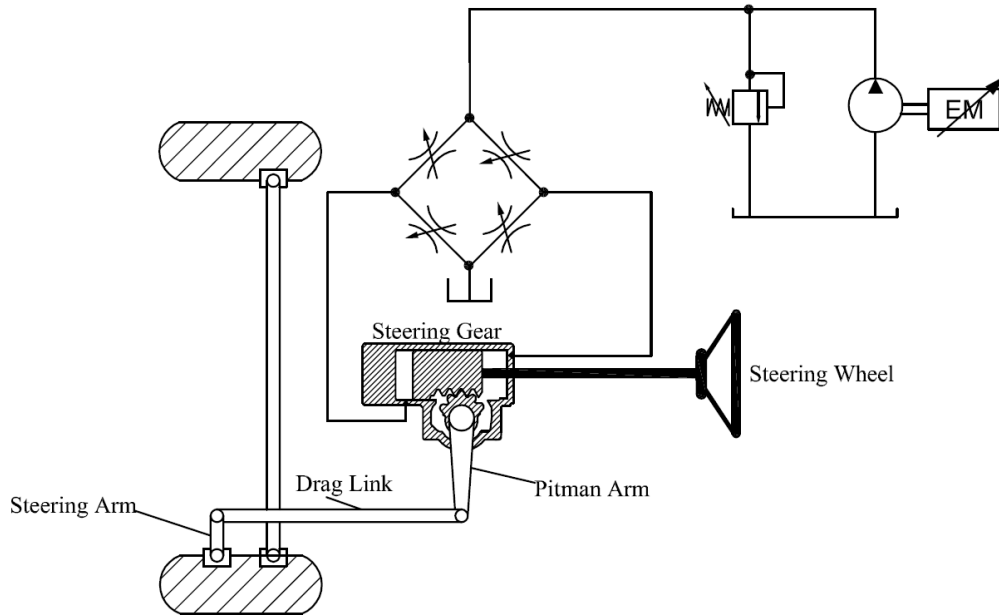


Figure 1.13. Fixed Displacement Pump with Variable Speed Electric Motor with Conventional Steering System

flow for static steering maneuvers, whereas at highway speeds, the motor speed is decreased to a minimum as low efforts are required for on-center driving. However, the motor is not stopped at highway speed because for heavy commercial vehicles a small flow rate from the pump is still required to reject the road disturbances by making use of the low compliance of the hydraulic system [7]. Moreover, in situations where fast steering maneuvers are required, such as in an obstacle avoidance scenario, the motor is sped up when a high steering rate is detected.

While this system helps reduce power losses by varying the flow output of the pump depending on the driving conditions, it does have a few drawbacks that prevents it from becoming a more prevalent solution. Typically, this system comes in one package combining the pump, electric motor, and electronics which makes it challenging to fit inside the engine compartment. Moreover, being an electronically controlled system, it does require a control system, and thus production software, making it more complex and costly. Furthermore, in order to implement it in heavier

vehicles, more power is required that the conventional 12 V electrical system may not be able to provide. Also, more power will also require bigger electric motor which leads back to the packaging issue.

1.8 Research Aims:

The aim of this project is to research new ways displacement controlled pumps can be used in steering on-highway commercial vehicles with the goal of improving system efficiency and enabling active steering. Once the candidate solutions are identified, they are first designed and analyzed in simulation in order to validate the concept, after which the experimental implementation will be performed.

First, a steer-by-wire solution will be examined by researching and studying its feasibility, overall potential benefits and drawbacks, as well as the different possible ways of implementation into a commercial vehicle. Furthermore, different possible fail-safe mechanisms will be researched and solutions will be proposed to mitigate any potential failures in the steer-by-wire system.

Next, the possibility of using displacement control to actively control driver steering effort without the use of the conventional throttling control valve in the steering gear will be studied. If successful, such solution will offer a novel and efficient way of achieving active steering while maintaining the mechanical link between the steering wheel and road wheels, and thus avoiding the safety concerns imposed by the steer-by-wire system.

1.9 Original Contributions:

In this research project, several original contributions were made as will be presented in more details this dissertation. A brief list of the different contributions is listed below:

- Researched, designed, and validated the first throttle-less electro-hydraulic steer-by-wire system for on-highway commercial vehicles.

- Proposed different mechanical and hydraulic configurations for how to implement the new steer-by-wire system on commercial vehicles using Displacement Controlled Pumps.
- Built a complete mathematical model of the proposed steer-by-wire system with all the relevant dynamics of the vehicle that affects it.
- Validated all models through a combination of high fidelity commercial software and vehicle experiments.
- Designed and validated in simulation two different Adaptive Robust Control (ARC) systems to control the steer-by-wire system. Both control systems were based on two simplified models that closely match the performance of the complete model in the range of operation of interest.
- Validated the chosen ARC system experimentally in a laboratory setup as well as on the test vehicle.
- Experimentally validated two of the proposed configurations of steer-by-wire system on a laboratory setup. One configuration used a linear cylinder as the steering actuator, while the other used a single rack cylinder.
- Successfully implemented one of the proposed steer-by-wire system configurations on a test vehicle.
- Researched, proposed, and designed different fail-safe mechanisms for the steer-by-wire system.
- Successfully implemented two of the proposed fail-safe mechanisms on the test vehicle.
- Proposed the concept of throttle-less active driver steering effort control using pump displacement control while maintaining the mechanical link between hand-wheel and road wheels.

1.10 Dissertation Organization:

The remaining of this dissertation is organized as follows; A summary of the state-of-the-art of displacement control, active steering systems, and active safety using steering is presented in chapter 2. In chapter 3, the possibility of using pump displacement control in a steer-by-wire system for on-highway commercial vehicles is investigated and different potential system configurations are proposed. In chapter 4, a complete mathematical model for the proposed steer-by-wire system is presented and validated. In chapter 5, the derived system model is simplified and validated against the complete model, and then used to design and analyze the control system for the proposed steer-by-wire system. An Adaptive Robust Control (ARC) system is presented and shown to track the desired steering rate both in simulation and experimentally despite parametric and nonlinear uncertainties. In that same chapter, an even simpler system model and ARC system are proposed. Simulation and experimental results show the second proposed ARC to closely track the desired steering position in the presence of system uncertainties. Furthermore, different fail-safe mechanisms for the steer-by-wire system are proposed in chapter 6 to mitigate potential failures in the steer-by-wire system. Two of the proposed fail-safe mechanisms are implemented into the test vehicle and shown to behave as expected. In chapter 7, the experimental setup and instrumentation of the laboratory test rig and the vehicle are presented with all the relevant details of the system architecture and its components. In chapter 8, we present the concept of active driver steering effort using displacement control while maintaining the mechanical link between the steering wheel and the road wheels. And finally, chapter 9 summarizes the work performed in this research project, and discusses the future work to further develop and validate the DC steer-by-wire system and investigate the concept of actively controlling driver steering effort using pump displacement control when the mechanical link between hand-wheel and road wheels is preserved.

2. STATE OF THE ART LITERATURE REVIEW

The aim of this project is to investigate the use of pump displacement control to enable the active control of steering systems in commercial vehicles which in turn allows for steering to be used to enhance their safety with systems such as lane keeping assistance and stability control, as well as automating the driver's task with autonomous driving. As such, this review first presents the state of the art of pump displacement control technology which is a crucial part of the proposed system. Secondly, an overview of the state of the art of active steering systems is given, and lastly, the state of the art of different active safety systems that use steering is presented to highlight the importance of active steering in safety and the motivation for this project.

2.1 Pump Displacement Control:

Varying pump flow output for the purpose of direct actuation of hydro-mechanical systems has been used in several applications for some time now. Doing so, as opposed to throttling the flow with valves, can significantly reduce the power losses of the system. Moreover, doing away with the resistive control associated with the use of metering valves helps keep the temperature of the fluid, and thus the system, low, resulting in improved performance and prolonged life. Examples of systems that use pump displacement control include motion control applications such as the actuation of an excavator's boom, bucket, or swing, where the pump flow output is regulated to directly control the motion of a linear cylinder or a motor. Pump displacement control has also been used in hydrostatic transmissions in which an engine driven pump drives a hydraulic motor that is coupled with the vehicle's wheels. As a result, varying the pump's displacement effectively changes the drive ratio of the hydrostatic transmission.

In this section, we give a brief summary of the different technologies that have been proposed to solve some of the problems encountered when using displacement control.

2.1.1 Pump Displacement in Closed Circuit Configurations:

In its first closed circuit applications, pump displacement control was used in systems in which the actuators had chambers with equal volumes such as double acting cylinders and motors in hydrostatic transmissions. However, when used with single acting cylinders which have chambers with different volumes, new strategies had to be devised to handle the difference in volume. Many of the initial proposed solutions were complex circuits designs that made use of servo-valves as proposed in [8] and [9], or using a tandem unit hydraulic transformer [10]. Complex designs of single-acting cylinders with equal chamber volumes have also been proposed [11] , [12]. A simpler approach by [1] proposed using two pilot-operated check valves to connect the low pressure side of the cylinder to a low pressure flow supply system which provides or absorbs the volume difference between the cylinder chambers depending on the mode operation.

2.1.2 Pump Displacement in Open Circuit Configurations:

Another approach for displacement control is to use it in an open-circuit configuration as in [13] in which one or more valves are used to direct flow to the appropriate chamber of the actuator, as opposed to doing it directly with the pump as in the closed circuit configuration. With this method, the difference in volume between the actuator chambers is irrelevant. Moreover, in some cases this approach can allow for the use of smaller displacement pumps by making use of flow recirculation from one side of the actuator to the other to boost the pump flow and bypassing the pump in conditions such as load aiding, e.g. lowering of a boom. On the other hand, to im-

plement these functionalities more valves are required which makes the system more complex [14].

A similar approach to displacement control is Electro-Hydrostatic Actuation (EHA) in which an electric motor is used to drive a fixed displacement pump and its flow output is controlled by varying the speed of the electric motor. Such approach can be advantageous in large systems, i.e. aircrafts, that would otherwise require long hydraulic lines to transport fluid from a central power supply ([15], [16]), resulting in added weight and significant losses. Nonetheless, EHA has its limitation, particularly, its relatively low bandwidth compared to other systems such displacement control due to the higher inertia of the pump and electric motor combination. Moreover, using an electric motor, would require more electronic components and advanced control strategies to control it, particularly, at low speeds where friction and cogging forces become more relevant.

2.2 Active Steering Systems:

2.2.1 Electro-Hydraulic Steering:

Due to its higher power density, hydraulic power steering has remained the main solution for steering heavy vehicles. While the passenger car industry has made an almost complete transition to electric steering, a similar transition in commercial vehicles has not yet taken place. Due to their significantly higher weight, heavy vehicles require more power to steer and using electric power to do so would require large motors which would take up a lot of space, or higher voltage which would require electric converters, increasing the system cost and package size [17].

On the other hand, using electric motors in steering opens the door to new applications that are not possible with the conventional hydraulic steering system. Electric steering allows other systems on the vehicle or even miles away from it to have access to its steering system. As a result, applications such as active lane keeping assistance, autonomous driving, automated parking, and much more become possible. Conse-

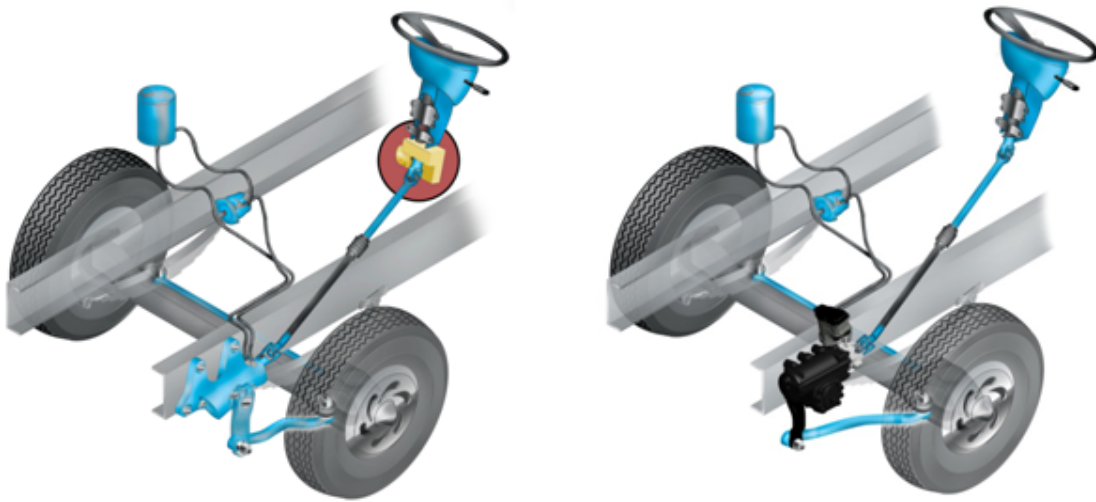


Figure 2.1. Column-Mounted and Gear-Mounted Electric Torque Overlay Systems

quently, in order to combine the benefits of electric steering with the power density benefits of hydraulics, steering system suppliers have introduced the so-called torque and position overlay systems in which an electric motor is overlaid on top of the hydraulic steering system (Figure 2.1). The electric motor is typically mounted on the upper steering column or at the input of the steering gear, allowing the steering system to be actively controlled.

Torque Overlay:

Torque overlay is currently the most widely used type of active steering system in both passenger and commercial vehicles. In commercial vehicles, the torque from the electric motor is combined with the torque supplied by the driver and applied at the input of the steering gear to actuate the hydraulic valve. Typically, a motor torque of 10-20 Nm is all that is needed to actuate the steering gear which then generates the hydraulic assistance to steer the vehicle. Depending on the driving situation, the motor torque is either added or subtracted from the driver's torque. For instance,

in a parking on dry pavement situation, low efforts are desired at the hand wheel, and therefore, the motor torque is added to the driver's torque to help him steer the vehicle. However, when driving at high speed on the highway, a stiffer torque feel is desired. As a result, the motor torque might have to be subtracted from the driver's torque in order to maintain a stiff and stable steering feel. Consequently, in addition to the safety and automation benefits of active steering, torque overlay can also be used to improve the steering feel and stability of the system by directly controlling the driver's input torque, decreasing his or her workload and providing ergonomic benefits.

Two main approaches for implementing torque overlay have been proposed. First, the open-loop method is where the input torque of the driver is measured and a corresponding motor torque is computed and applied at the input side of the steering gear. This method essentially mimics the boost curve of the hydraulic valve in a conventional steering system where each twist angle of the valve's torsion bar corresponds to a fluid pressure, and thus, an assistance torque. The drawback of this method, as its name suggests, is that it is open loop which means that the steering system will perform differently under different external conditions which may affect its stability. As a result, the driver's steering feel will change depending on operating condition e.g. driving surface conditions, vehicle load, component variability, etc.

A second approach for doing torque overlay is what's commonly known as the closed-loop torque overlay ([18], [19], [20], [21]). In this method, the measured input torque from the driver is compared to a desired torque that is computed based on the current state of the vehicle, e.g. vehicle speed, hand wheel position, lateral acceleration, etc. A control algorithm then minimizes the error between the measured and desired torque and insures that the measured torque tracks the desired torque. As a result the driver feels the computed desired torque at the hand wheel regardless of the external disturbances to which the vehicle is subjected. Nonetheless, it is worth noting that the difference between these two torque-overlay approaches is mainly in

the software. The same hardware can be used for either approach but system suppliers will typically have a preference of one over the other.

Different torque overlay solutions for commercial vehicles exist in the market. ZF's ReAX was first introduced in 2005 as part of the steering column, and then a steering gear-mounted configuration was recently introduced. In both systems, the electric motor is placed in series with the hydraulic steering system which provides the main steering assistance. The motor torque is superimposed on the driver's hand wheel torque using the closed-loop torque control approach, and thus, closely controlling the driver's steering feel based on driving conditions. Moreover, the Servotwin is a similar system provided by Bosch in which an electric motor is directly placed at the input of the steering gear to provide additional torque to the driver. However, similar to ZF's ReAX system, most of the steering assistance is provided by the hydraulic steering gear. Volvo has also recently introduced a similar system called the Volvo Dynamic Steering.

Angle Overlay

With position overlay, the steering angle from the driver is superimposed on the steering angle provided by an electric motor through some type of gearbox which combines the two angles and applies them at the input of the steering or pinion gear [23]. The Lexus Variable Gear Ratio Steering (VGRS) system uses angle overlay in the form of a gearbox which changes ratio between input and output using strain wave gearing with the help of an electric motor. Audi's Dynamic Steering uses a similar mechanism to achieve angle overlay while Bosch and BMW introduced an angle overlay system that uses a planetary gear to combine the driver's hand wheel position with the position of an electric motor to rotate the input of the pinion gear. On the commercial vehicle side, some OEMs such as Scania have also proposed angle overlay [22].

Regardless of the mechanism used, angle overlay aims to change the effective steering gear ratio between the hand wheel and the road wheels depending on the driving conditions [23]. At low speeds, the steering ratio is decreased (fewer turns lock-to-lock) by having the electric motor provide most of the steering angle, and thus, decreasing the driver's steering effort. This also increases the agility and handling of the vehicle at medium speeds. On the other hand, at high speeds, the steering ratio is increased in order to prevent over-corrections from the driver and improve the vehicle's stability. Moreover, angle overlay has a fundamental advantage when used with active safety systems that use steering. Steering angle corrections provided by these systems can be added or subtracted from the driver's steering input without interfering with him. This provides a continuous steering experience without any interruptions even during emergency situations. This is not the case in torque overlay systems in which any torque input from the active safety system will directly affect the driver's input.

Torque Overlay and Angle Overlay systems have generated a lot of interest in the commercial vehicle industry due to their many potential applications, particularly, in Advanced Driver Assistance Systems (ADAS), and Autonomous Driving. Nevertheless, the existing active steering systems do not solve the aforementioned inefficiency issues of the hydraulic system, namely the parasitic losses inside the pump and steering gear.

Active Pressure Control:

To avoid the complexities of using electric motors in series with the hydraulic steering system, other studies such as [23] have proposed directly controlling the pressure inside the steering gear in order to actively control the steering system (Figure 2.2). The pressure of the fluid is controlled through the use of pressure control valves on both side of the cylinder. Dell'Amico's approach was applied to a rack-and-pinion steering system but it can also be applied to a system with an integral steering gear (Figure 2.3). While this solution allows for the steering system to become active, it,

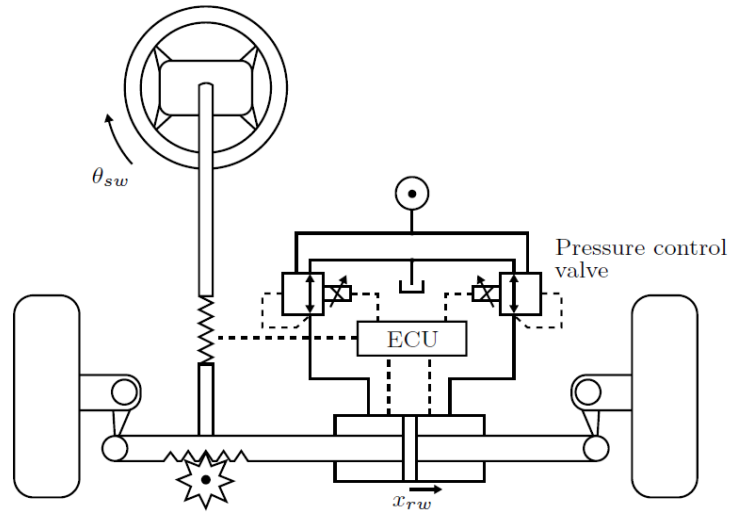


Figure 2.2. Steering with Active Pressure Control [23]

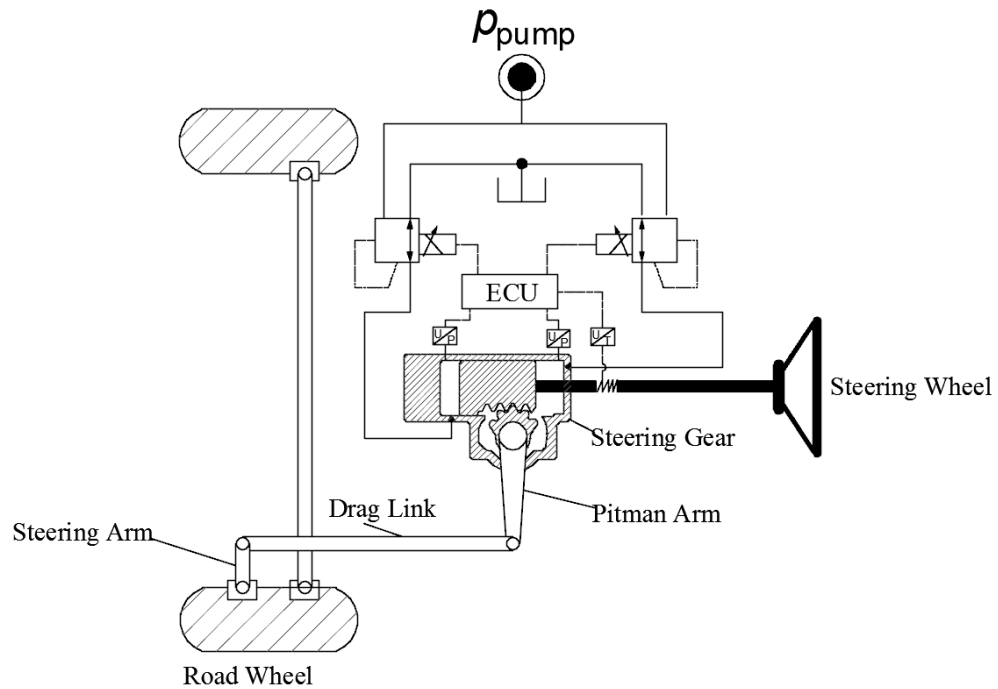


Figure 2.3. Active Pressure Control in an Integral Steering Gear Configuration

too, does not solve the inefficiency issues due its use of throttling valves to control the pressure of the system.

2.2.2 Steer-by-Wire Systems:

X-by-Wire refers to technologies that rely on electric signals through wires to receive information on the state of the vehicle and driver intent from different sensors, and send commands to actuators to achieve a particular task. Typically, these technologies replace a mechanical or hydraulic connection between the machine operator and the component to be actuated. For example, most current commercial and military aircraft are equipped with fly-by-wire systems in which the pilot's commands are relayed to different actuators through electric signals. The fly-by-wire technology not only simplifies the aircraft design and improves space utilization, but more importantly has led to the improvement of performance and maneuverability of the aircraft and allowed intrinsically unstable ones to be flown safely with the aid of sophisticated control systems. X-by-wire technology has also existed on ground vehicles for some time now. Many vehicles are currently equipped with brake-by-wire and throttle-by-wire systems in which a sensor measure the position of the pedals to which a controller reacts by sending the appropriate command to the brake system or engine. Furthermore, rear-axle steering systems can also be considered an x-by-wire technology in which the front axle steering angle is measured and sent to a controller that then commands a corresponding angular displacement at the rear axle. These systems can dramatically decrease tire wear and increase vehicle maneuverability at low speeds, as well as improve stability at high speeds.

In a steer-by-wire system, there is no mechanical link between the hand wheel and road wheel. Typically, the steering column and shaft are removed and the displacement of the steering wheel is relayed to the road wheels through an electric or hydraulic actuator that achieves the desired displacement. A steering angle sensor sends the position or velocity of the steering wheel to a controller which then based on the current state of the vehicle sends the appropriate command to the actuator which in turn achieves the desired steering response. In the conventional steering system, steering feel and road feedback are directly transferred to the driver through the steer-

ing linkages. However, that is no longer possible in the steer-by-wire system due to the absence of that mechanical link between the driver and the road. Consequently, a tactile feedback device is typically attached to the steering wheel and is used to send an artificial steering feel to the driver depending on the vehicle's operating conditions and dynamics. For example, in a parking situation, the tactile feedback device can be commanded to generate a low steering feel at the driver's hands so that he or she can achieve the task with low efforts, but highway speeds a stiffer feel at the hand wheel is usually desired for improved stability and performance.

There are many advantages to decoupling the hand wheel from the road wheel. The most direct one is the possibility to have more efficient space utilization. Without the steering column and shaft, vehicle manufacturers have more flexibility and space in designing the layout of the engine compartment. Moreover, in steer-by-wire systems, steering feel is no longer dictated by the road forces coming up through the steering systems, particularly, the tires' self-aligning moment and road noise. With the use of a tactile feedback device, disturbances can be completely eliminated and steering feel is artificially generated depending on the driving situation or even the driver's choice of driving mode, e.g. sport settings for a more aggressive feel that is highly dependent on the vehicle dynamics, or comfort settings for a more relaxed comfortable feel only slightly dependent on the vehicle's dynamics. Furthermore, unlike conventional steering, with a steer-by-wire system, the steering performance of the vehicle can be made consistent despite the external conditions to which it is subjected. Additionally, with steer-by-wire, the steering system ratio can be varied electronically based on vehicle operating conditions. For instance, when parking the vehicle, the steering ratio can be decreased (fewer turns lock-to-lock), and thus decreasing the driver's workload. Conversely, at high speeds, the steering ratio can be increased to enhance the stability of the vehicle and prevent over-corrections by the driver. This is not possible with conventional steering systems.

By design steer-by-wire is an active steering system. Such a system allows steering to be used in advanced applications such as active safety and autonomous driving.

Moreover, unlike other active steering systems, when doing active safety with a steer-by-wire system, the safety control system does not interfere with the driver when correcting his or her steering input. When the safety system intervenes, it only affects the road wheels' displacement and not the steering wheel, thus, giving the driver a continuous steering experience. This is not always the case with other active steering systems, e.g. torque overlay, for which any correction by the active safety system will directly affect the steering wheel and interrupt the steering experience. However, in emergency situations such interventions are considered acceptable as the safety of the driver and passengers are more important than their comfort or steering experience.

Steer-by-wire systems have been the subject of academic research for a few decades already. [24] proposed a fault-tolerant electro-hydraulic steer-by-wire system on a wheel loader articulated vehicle. This system is fitted with two power steering circuits and two redundant electronic controllers in which a steering control module performs the vehicle steering task while a failure detection system monitors the overall health of the system and handles existing faults based on a Finite State Machine concept. In [25], a passenger car with hydraulic power assist was converted into an electric steer-by-wire vehicle using an electric motor. The steering control strategy of this system emphasizes on the use feed-forward controller to deal with known disturbances, specifically, the self aligning torque. In this same study, the author proposes using full vehicle estimated state feedback to augment the driver's steering input which he claims allows the driver to change the vehicle's fundamental dynamic characteristics and responsiveness. In [26], a steer-by-wire for commercial vehicles proposed using an electric motor to actuate the input of a conventional hydraulic steering gear. The motor would receive driver steering commands electronically based on the position of the steering wheel. More recently, [2] proposed an electro-hydraulic steer-by-wire system for a wheel loader using pump displacement controlled actuation which improves the system's efficiency by eliminating flow throttling, and increases productivity. To perform the steering task, the author proposed two different control strategies. The first one is based on feedback control combined with a feed-forward

strategy realized by inverting the system's transfer function. The second strategy makes use of a self-tuning regulator to estimate the coefficients of the system's equivalent transfer function, and uses minimum degree pole placement to track a desired hand wheel steering rate. Recently, [27] proposed an electro-hydraulic steer-by-wire system that uses four independent meter-in and meter-out valves to actuate the steering cylinder. With this approach, it is claimed that a full redundant steering system is not necessary for on-highway vehicle as single valve failures can be compensated for with appropriate valve control strategies. Moreover, steer-by-wire systems have also caught the interest of the passenger car, commercial vehicle, and agricultural vehicle industries alike. Different systems have been proposed and published, and some systems were even put into production such as Nissan's Infiniti Q50 model which was introduced as the market's first steer-by-wire passenger car in 2014.

2.3 Active Safety Using Steering

Active safety is one of the most discussed and pursued topics among the members of the commercial vehicle industry nowadays. While passive safety systems have existed for some time now, e.g. airbags and seatbelts, active safety systems are just now emerging in commercial vehicles. As different technologies become more available and affordable, the case for active safety is becoming stronger. Moreover, active safety is viewed as the next stepping stone towards full vehicle autonomy which is of major interest to the industry.

In active safety systems, a control module is constantly monitoring one or more states of the vehicle such as roll rate, yaw rate, and lateral acceleration in a stability controller, or lane position in a lane keeping assistance system, and intervening whenever the vehicle enters a dangerous situation to prevent events such as rollovers and lane departures that may ultimately lead to accidents. Such interventions can be achieved either by steering or braking the vehicle, or actuating the engine throttle as in the case of cruise control.

Using active steering in safety systems for commercial vehicles has been researched extensively in the past decades and many systems have been proposed to prevent different kinds of potentially dangerous situations. Different lane keeping assistance and lane departure avoidance systems have been proposed to either warn the driver or intervene when the vehicle attempts to make an unintentional lane departure. Other systems are constantly working in parallel with the driver to help keep the vehicle at the center of the lane [28]. These systems use different types of sensor technologies to determine the vehicle's position in the lane. Vision based sensors are currently the most widely used and rely on fast image processing to determine the distance between the camera and the lane markers. GPS based systems have also been proposed, however, these systems still suffer from accuracy issues but are nonetheless improving. Moreover, magnetic nails along lane markers have been used to determine the position of a vehicle in the lane, [29], but these require changing infrastructure. However, unlike the vision based systems, this technology works in all weather and visibility conditions.

Active steering can also be used in stability control systems. These systems are inherently better and faster at handling dangerous situations than human drivers due to their fast reaction capability and more accurate awareness of the state of vehicle. It has been shown by [30] that a stability control system that uses active steering in combination with braking is more efficient than a system that employs braking only. The authors state that steering has an immediate effect on the vehicle's roll response while the braking response is more delayed. Moreover, steering requires only a fraction of the front tire force compared to braking, leaving more tire force for the driver to operate the vehicle. Another study by [31] has also shown that active steering alone or in combination with braking can be used to effectively avoid vehicle rollovers in emergency situations.

Many control algorithms have been proposed in the literature to perform stability control by attenuating yaw disturbances and keeping the vehicle in the stable region. Yaw disturbances can be due to different factors such as cross-wind, asymmetric

braking by the brake controller, or split- μ situations where different tires are on surfaces with different friction coefficients, e.g. icy patches of road. In [32], a robust control strategy that decouples the lateral dynamics from the yaw dynamics of the vehicle was proposed which was then combined in [33] with a yaw attenuating strategy that actively keeps the yaw dynamics in the stable region, leaving the driver with the simple task of path following without needing to worry about the yaw stabilization task. Many other stability control algorithms have followed such as [34] and [35] to name a few.

Other studies have investigated the possibility of using active steering of axles other than the front axle for stability control. This technique allows for a stabilizing controller that does not interfere with the driver who's steering the front axle for path following while the other axles are steered to achieve yaw stabilization. [36] proposed a model predictive controller based on a linear model capable of controlling the roll dynamics of the vehicle with small steering commands at the rear axle, and thus preserving the validity of the linear system model. More recently, [37] showed that by steering only the third axle of a vehicle, it can be controlled in a way such that it exhibits the same yaw response as a front axle steered vehicle in a lane keeping mode. This approach allows the actively steered third axle to be a source of redundancy in case of failure of the front axle steering system, e.g. steer-by-wire system failure.

3. INVESTIGATION OF DISPLACEMENT CONTROL IN STEER-BY-WIRE FOR ON-HIGHWAY APPLICATIONS

Displacement Control (DC) technology was first introduced by (Rahmfeld & Ivantysynova, 1998). Steer-by-wire using DC technology was first investigated by (Daher, 2014) who introduced the world's first throttle-less electro-hydraulic steer-by-wire system for Articulated Frame Steering (AFS) vehicles. This work, on the other hand, investigates the application of DC steer-by-wire technology in on-highway commercial vehicles which have different steering architecture and duty cycle.

3.1 Advantages of DC Steer-by-Wire

The displacement control technology allows for the actuation of different systems such as cylinders and motors by controlling flow rate without throttling, resulting in significant energy savings. When implemented into a wheel loader by (Rahmfeld & Ivantysynova, 2004), fuel savings up to 15% were demonstrated. Another 15-20% fuel savings were achieved in a skid steer loader by (Williamson & Ivantysynova, 2007), and as much as 40% in an excavator system implemented by (Zimmerman, 2008). Consequently, when it comes to steering systems DC technology is an attractive solution to remedy the energy inefficiency issues discussed in the previous chapters, namely, inefficiencies due to throttling the flow inside the pump and steering gear. In fact, a DC steer-by-wire system has been proposed and implemented into a wheel loader by (Daher, 2014) and resulted in 14.5% reduction in fuel consumption and an overall fuel efficiency improvement of 43.5%. Moreover, Daher's systems has also helped improve machine productivity by 22.6% by doing more steering work in less amount of time while reducing driver workload.

In addition to energy and fuel savings, DC steering offers many other advantages. When used in a steer-by-wire system, all the previously mentioned advantages of steer-by-wire can be achieved. Space in the engine compartment can be more efficiently used with the absence of the steering column and shaft, the driver's steering effort can be directly controlled based on driving conditions, and steering efforts can be decreased and productivity increased by actively varying the steering system ratio based on operating conditions. Moreover, by design, the DC steer-by-wire system is an active steering system, and thus has many potential applications, particularly, in active safety systems that employ steering such as yaw and roll stability control, and lane keeping assistance. DC steer-by-wire can also be used to enable lateral control of autonomous vehicles.

3.2 Possible Configurations:

3.2.1 Mechanical Configurations:

Three different possible mechanical configurations are proposed as a solution for a steer-by-wire system for commercial vehicles. These configurations mainly differ from each other in the type of actuator used, i.e. a single rack cylinder, a single acting linear cylinder, or a double acting cylinder. Choosing one configuration over the other is highly dependent on the application and available space around the steered axle. Nevertheless, the single rack cylinder has the advantage of making use of the already existing steering system architecture. The intermediate shaft can be removed and the steering gear replaced by the new single rack cylinder (Figure 3.1). When a linear cylinder is the preferred configuration, two options are possible depending on the available space. A double-acting cylinder might make more sense where each end of the cylinder can be directly attached to a wheel's steering arm while the cylinder itself is attached to the frame of the vehicle (Figure 3.2). Alternatively, a single acting cylinder can be used where one end is connected to the vehicle frame and the other end is attached to the steering arm of one of the wheels with a tie rod connecting

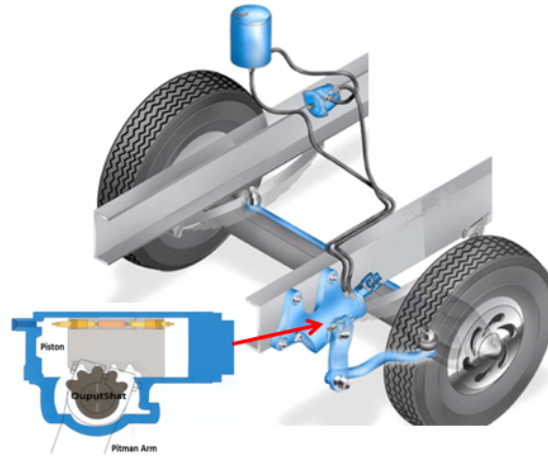


Figure 3.1. Single Rack Configuration

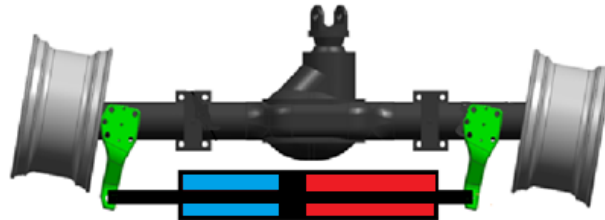


Figure 3.2. Linear Double Acting Cylinder Configuration

the two wheels as shown in Figure 3.3. This configuration offers more flexibility in placing the cylinder to use the space around the axle more efficiently.

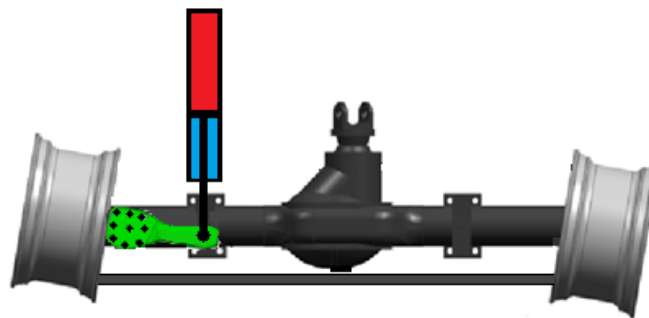


Figure 3.3. Linear Single Acting Cylinder Configuration

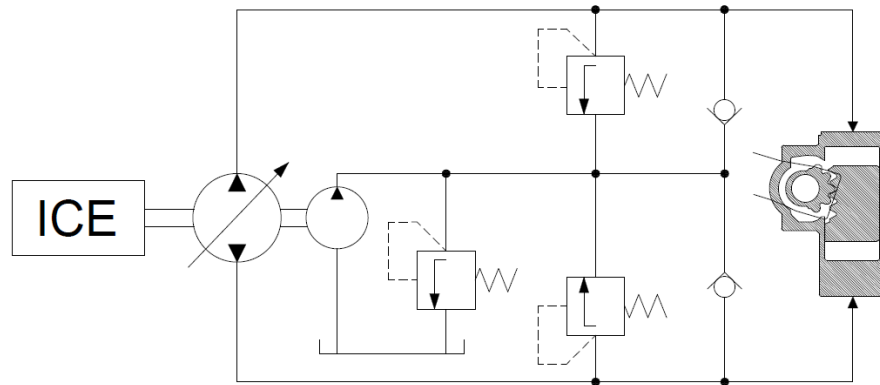


Figure 3.4. DC Pump in Closed Circuit with Rotary Cylinder

3.2.2 Hydraulic Circuit Configurations:

The proposed hydraulic circuit configurations are classified based on the actuator used and whether the circuit is open or closed. All three proposed mechanical configurations can be used in either open or closed hydraulic circuit configurations.

Variable Displacement Pump in Closed-Circuit Configuration:

In the closed circuit configuration (Figures 3.4, 3.5, and 3.6), the direction of the flow, and thus steering, can be directly controlled by a variable displacement pump without the use of control valves. The main pump actuates the cylinder by supplying flow to the appropriate side, and a charge pump is used to compensate for the system losses and provide flow for the main pump displacement control system. The circuit is separated into a high and low pressure systems using check valves and pressure relief valves. The charge pump remains in the low pressure system at all times while the check valves connect the low pressure side of the cylinder to the low pressure system depending on operating conditions. When the single acting cylinder is the preferred configuration, the check valves are replaced by pilot-operated check valves due to the unequal surface areas of the cylinder piston (Figure 3.6).

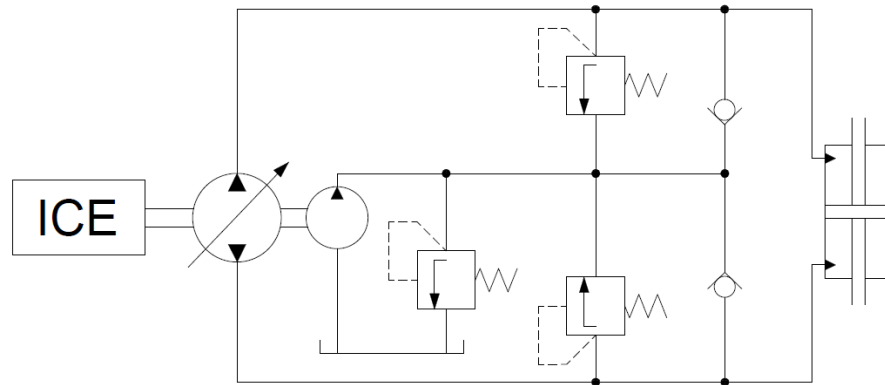


Figure 3.5. DC Pump in Closed Circuit with Linear Double Acting Cylinder

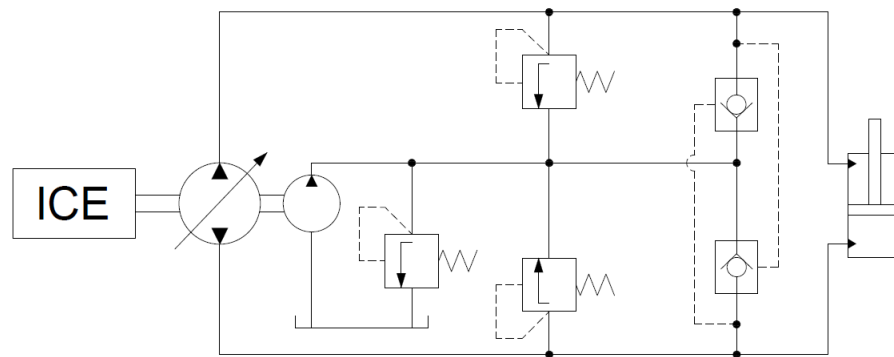


Figure 3.6. DC Pump in Closed Circuit with Linear Single-Acting Cylinder

Variable Displacement Pump in Open-Circuit Configuration:

Alternatively, the steer-by-wire system can be implemented using open hydraulic circuits (Figures 3.7, 3.8, and 3.9). In this configuration, a control valve is needed to direct the flow to the appropriate side of the cylinder depending on the mode of operation. As opposed to the closed circuit configuration, the open circuit system does not depend on the type of actuator used.

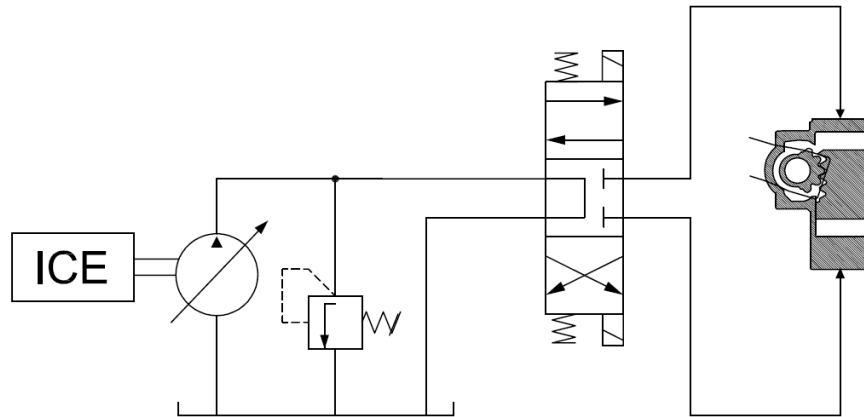


Figure 3.7. DC Pump in Open Circuit with Rotary Cylinder

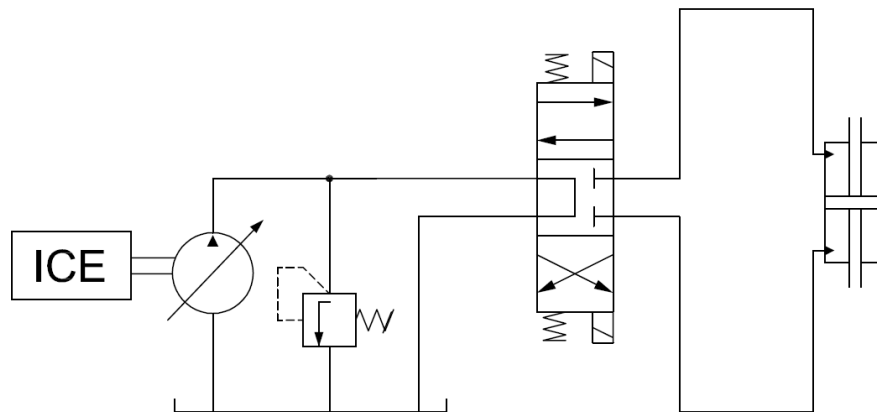


Figure 3.8. DC Pump in Open Circuit with Double Acting Cylinder

Fixed Displacement Pump with Variable Motor Speed:

An alternative approach to implementing a hydraulic steer-by-wire system is through the use of a fixed displacement pump driven by a variable speed electric motor (Figure 3.10, 3.11, and 3.12). However, this system is limited by its relatively lower bandwidth due to the higher inertia of the motor compared to the inertia of the swash plate of the pump for example.

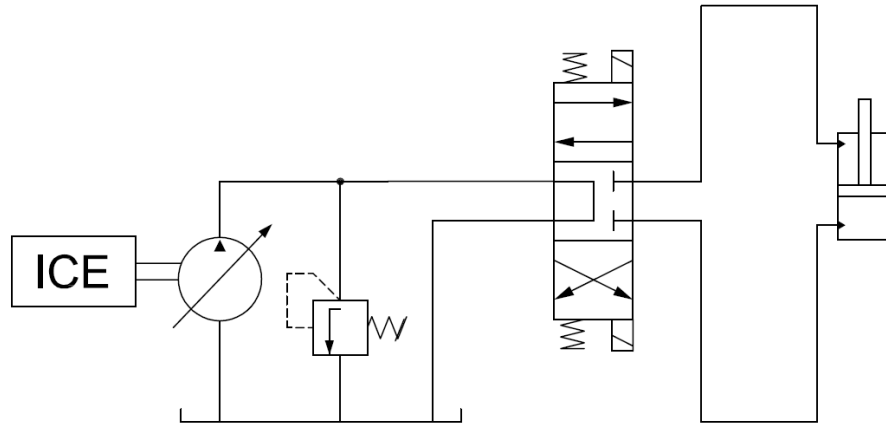


Figure 3.9. DC Pump in Open Circuit with Single Acting Cylinder

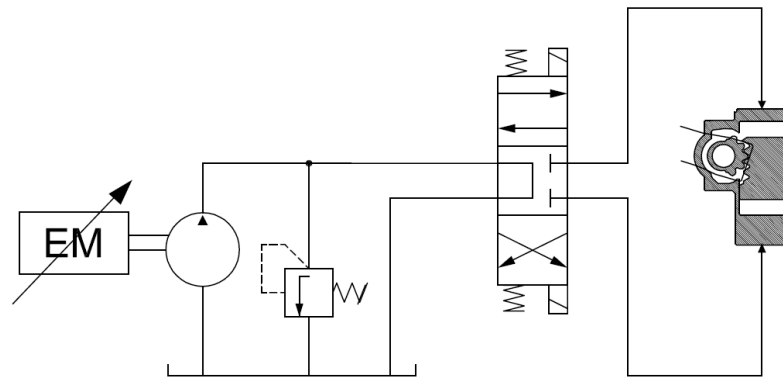


Figure 3.10. DC Pump in Closed Circuit with Rotary Cylinder

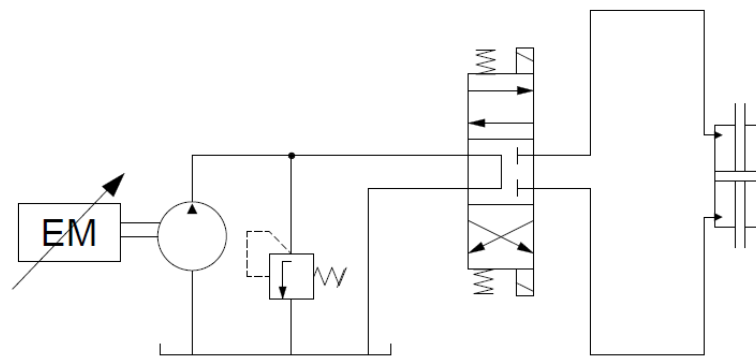


Figure 3.11. Variable Speed Motor with Fixed Displacement Pump in Open Circuit with Double Acting Cylinder

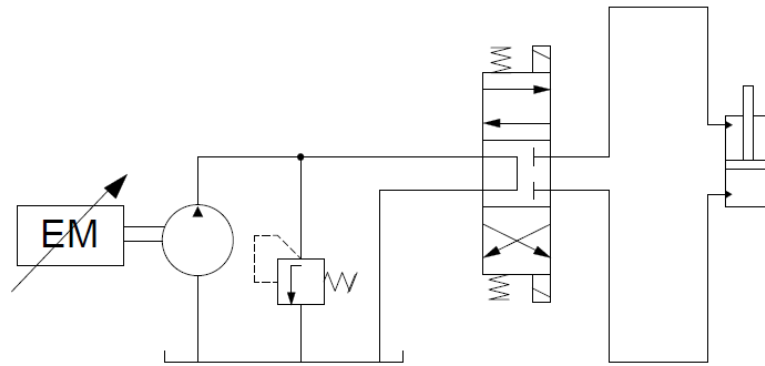


Figure 3.12. Variable Speed Motor with Fixed Displacement Pump in Open Circuit with Single Acting Cylinder

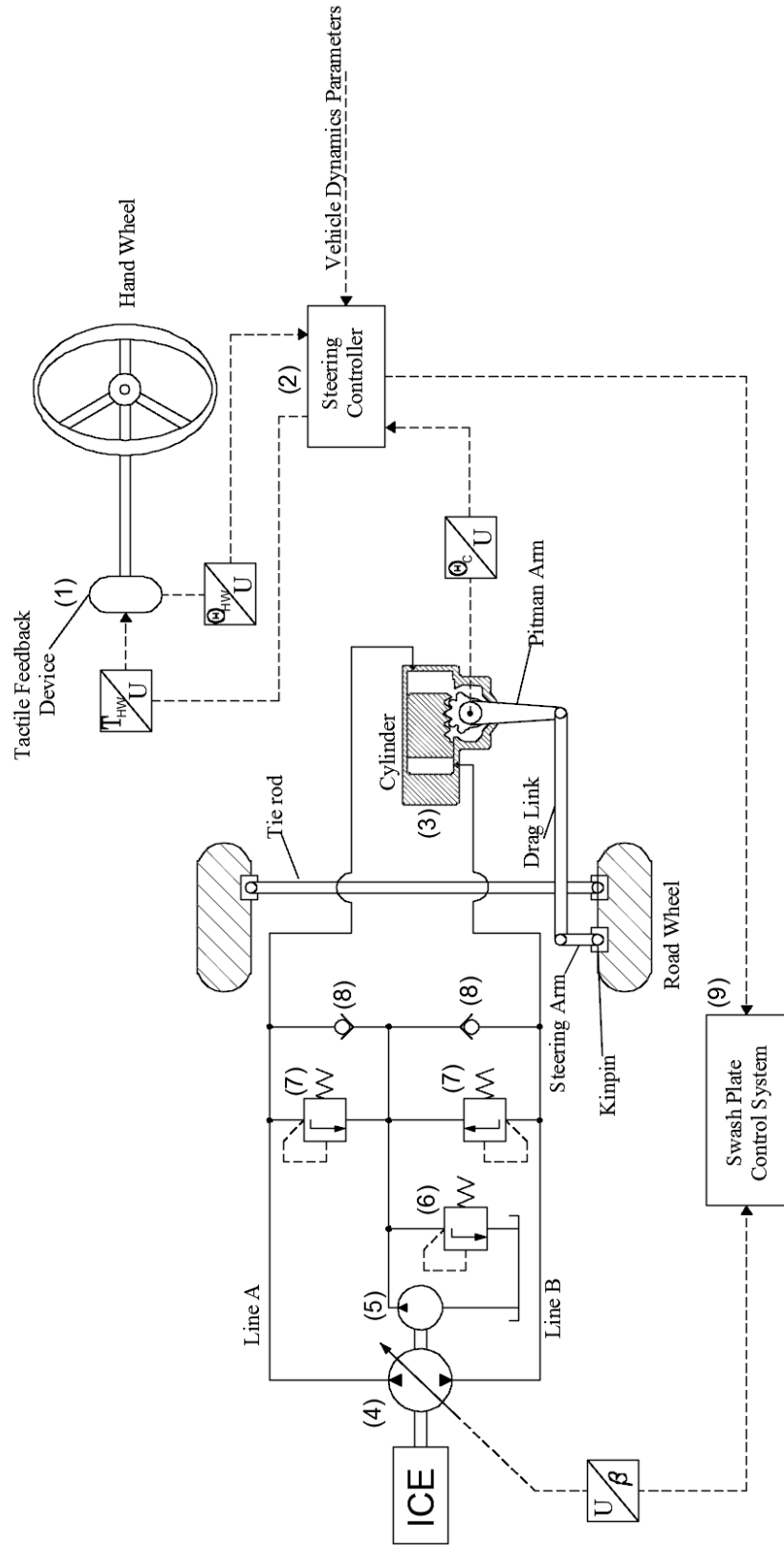


Figure 3.13. Displacement Control Steer-by-Wire System.

3.3 Investigation of the DC Pump in Closed-Circuit with Single Rack Cylinder Configuration:

3.3.1 System Description

To demonstrate the functionality of the DC steer-by-wire technology on a commercial vehicle, the mechanical configuration with the single rack cylinder is chosen because it's the easiest to implement as it makes use of the already existing steering system architecture. Moreover, the closed-circuit hydraulic configuration is chosen as the hardware is already available in the laboratory. In the proposed steer-by-wire system (Figure 3.13), the steering wheel displacement is measured by a position sensor that is part of the tactile feedback device (1), and relayed to the steering system controller (2) that controls the motion of the cylinder (3) which is rigidly connected to the road wheels through a series of linkages, i.e. pitman arm, drag link, steering arms, and tie rod. Whether it's in steering position or steering rate control mode, the steering system is controlled by minimizing the error signal between a computed desired steering position or rate, and the actual measured position or rate of the cylinder output shaft, θ_C . The desired steering position and rate are computed based on the motion of the steering wheel, θ_{HW} , and other vehicle dynamics parameters such as vehicle speed. The cylinder is then actuated by sending the appropriate flow rate to the to the appropriate cylinder chamber from a variable displacement over-center axial piston pump (4). The rate and direction of the of the flow is varied by changing the pump's swash plate angle which is controlled by the swash plate control system (9). Because the DC circuit is a closed system, a charge pump (5) is used to compensate for any hydraulic losses, as well as provide flow to the swash plate control system. The charge pump is connected to the low pressure side of the cylinder at all times through the use of check valves (8). Moreover, the pressure of the low-pressure system is set by the relief valve (6), while the high pressure system is limited by the relief valves (7).

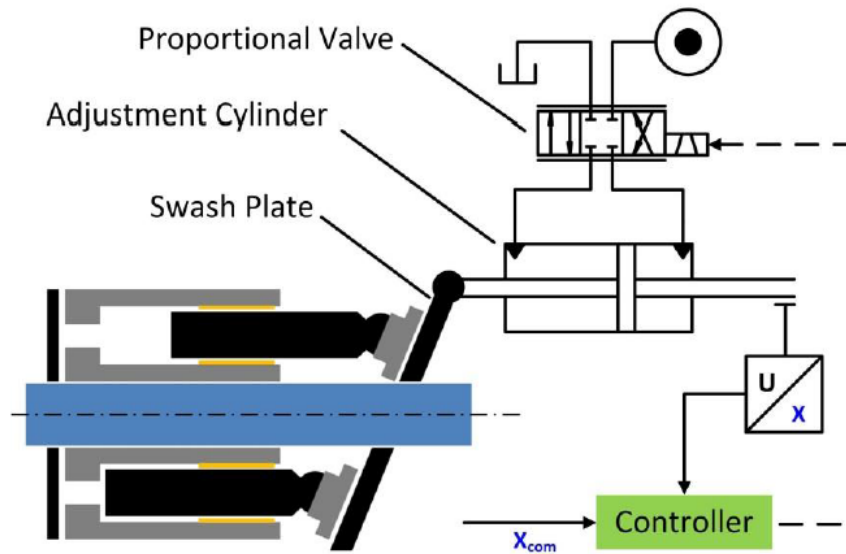


Figure 3.14. Swash Plate Control System.

To actively vary the displacement of the pump, a double acting cylinder (Figure 3.14) is mechanically connected to the swash plate and actuated by metering flow provided by the charge pump through a proportional valve. The linear displacement of the double acting cylinder corresponds to an angular displacement of the swash plate which determines the effective volumetric displacement of the pump. Consequently, the displacement of the pump is controlled by actuating the double acting cylinder. As a result, based on the measured displacements at the hand wheel and the steering cylinder output shaft, as well as the current operating conditions of the vehicle (e.g. vehicle speed), the steer-by-wire control system commands the appropriate swash plate angle to the pump to ultimately control the displacement of the road wheels and steer the vehicle.

4. SYSTEM MODELING AND SIMULATION

A mathematical model of the system provides invaluable information that allows for a deeper understanding of it. The model also allows studying the feasibility of the project through simulation, particularly when designing its control system, before building the actual system, saving time and resources. The DC steer-by-wire system model can be broken down into two different subsystems (Figure 4.1); the hydraulic subsystem driven by flow from the pump which results in the motion of the actuator, i.e. cylinder. The pressure build-up inside the cylinder is a direct result of the load acting on it which the mechanical subsystem is responsible for computing based on the steering system geometry and vehicle dynamics. The subsequent sections present a detailed description of the hydraulic and mechanical subsystem mathematical models.

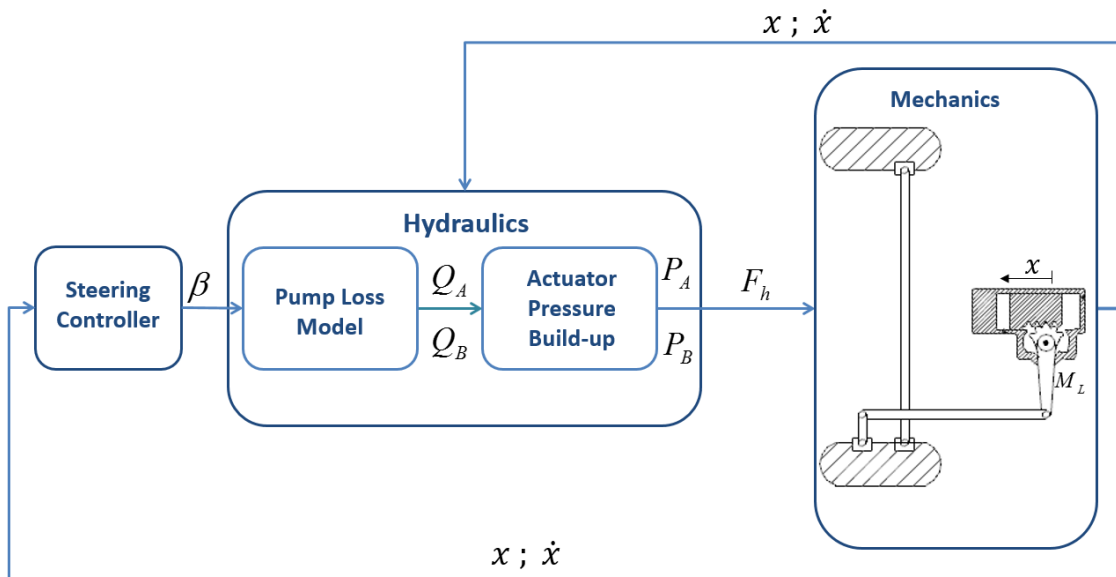


Figure 4.1. Overall Model Architecture.

4.1 Hydraulic Subsystem Model:

The hydraulic subsystem is itself composed of different components whose behavior can be described mathematically. These include the pump loss model with its volumetric and torque loss models, the swash plate control system model, and the pressure build-up model which describes the dynamics of the steering fluid's pressure based on the loads exerted on the system.

4.1.1 Pump Loss Model

Effective outlet flow depends on two main parameters; The pump displacement, V_d , and the speed of rotation of the pump, n_e . Consequently, the theoretical flow of the pump, Q_i , is expressed as:

$$Q_i = \beta V_d n_e \quad (4.1)$$

Where β represents the normalized swash plate angle of the pump as determined by the displacement control system.

However, due to leakage, the actual pump displacement slightly differs from the theoretical one. As a result, the actual displacement of the pump is computed empirically using the Toet Method based on steady state measurements at constant temperature, inlet pressure and speed, and for multiple load pressures. The Toet Method is conducted in two steps. First, the flow output of the pump is plotted against different rotation speeds, and then fitted into a line equation of a particular slope. This is repeated for different load pressures and the slope values of the fitting lines are plotted against the load pressures and fitted into another line equation. The y-intersect of that line, i.e. at $\Delta p = 0$, represents the actual pump displacement which can be expressed mathematically by Eq. (4.2):

$$V_d = \frac{1}{n} \frac{\sum_{j=1}^k Q_{ej} \sum_{j=1}^k \Delta p_j^2 - \sum_{j=1}^k \Delta p_j \sum_{j=1}^k \Delta p_j Q_{ej}}{k \sum_{j=1}^k \Delta p_j^2 - (\sum_{j=1}^k \Delta p_j)^2} \quad (4.2)$$

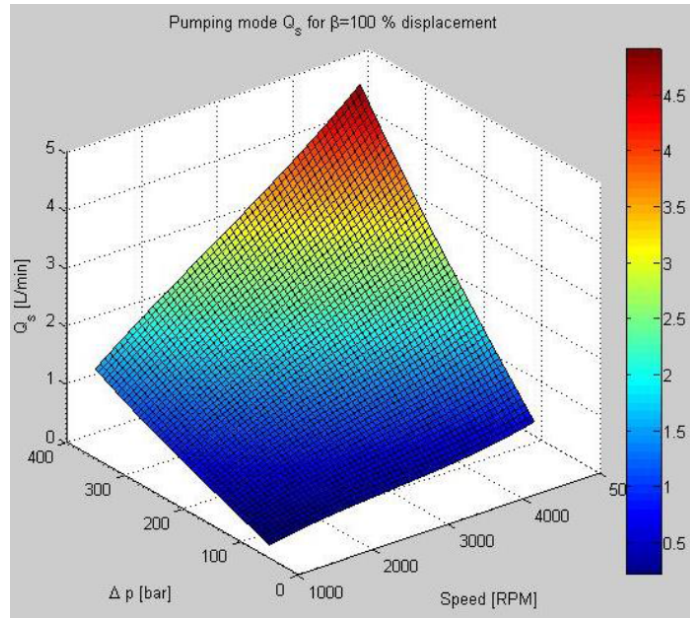


Figure 4.2. Pump Volumetric Losses at Full Displacement [2]

Where Q_{ej} is the effective flow rate of the j^{th} port for a pump with a total number of k ports, and Δp_j is the pressure difference across the j^{th} port.

Moreover, as with all hydraulic machines, perfect sealing is not possible. As a result, leakage flows develop as pressure differentials between the different moving parts of the pump arise. Consequently, a volumetric loss term, Q_s , is included in the pump model to account for these flow losses:

$$Q_e = \beta V_d n - Q_s \quad (4.3)$$

Q_s is described by an empirical loss model with coefficients that are determined by fitting steady state measurements into 3rd or 4th degree polynomials. These measurements are taken at constant inlet temperature, and various load pressures, speeds, and swash plate angles. The flow loss model is then given by:

$$Q_s(V_d, n, \Delta p)_{T=cst} = \sum_{i_1=0}^{I_1} \sum_{i_2=0}^{I_2} \sum_{i_3=0}^{I_3} K_Q(i_1, i_2, i_3) V_d^{i_1} n^{i_2} \Delta p^{i_3} \quad (4.4)$$

Moreover, the effective torque, T_e , necessary to drive the pump is expressed as:

$$T_e = \frac{\beta V_d \Delta p}{2\pi} - T_s \quad (4.5)$$

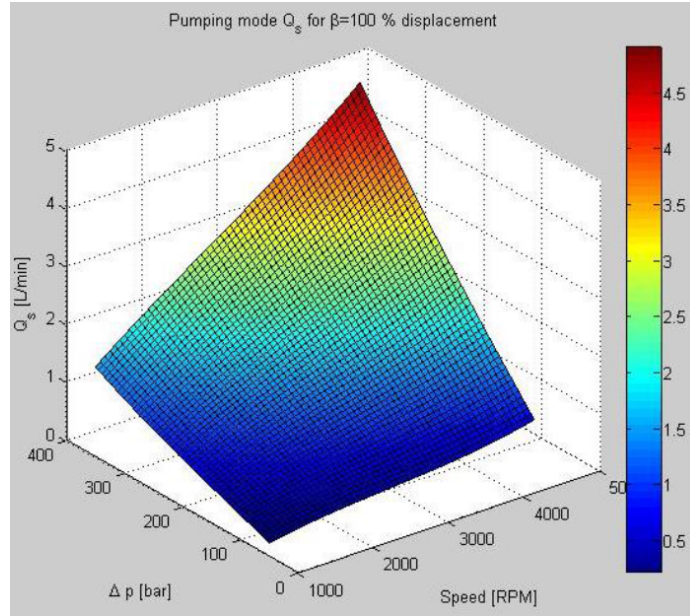


Figure 4.3. Pump Torque Losses at Full Displacement [2].

Where T_s is the torque term representing the mechanical losses, e.g. friction. It is determined in the same manner as the volumetric loss Q_s , i.e. by fitting steady state measurement data into a polynomial, and is given by Eq. (4.6):

$$T_s(V_d, n, \Delta p)_{T=cst} = \sum_{i_1=0}^{I_1} \sum_{i_2=0}^{I_2} \sum_{i_3=0}^{I_3} K_T(i_1, i_2, i_3) V_d^{i_1} n^{i_2} \Delta p^{i_3} \quad (4.6)$$

4.1.2 Pressure Build-up Model

The pressure change of the compressible fluid inside the steering cylinder (Figure 4.4) is directly related to the flow rates entering and leaving that control volume including the flow rate due to the piston motion resulting from of all the forces acting on it. This behavior can be described mathematically by combining the conservation of mass flow rate principle with the bulk modulus and continuity equations. As a result, the pressure build up in chamber A of the cylinder is expressed as:

$$\dot{p}_A = \frac{1}{C_{H,A}} (Q_A + A_A \dot{x} - Q_{s,i} - Q_r) \quad (4.7)$$

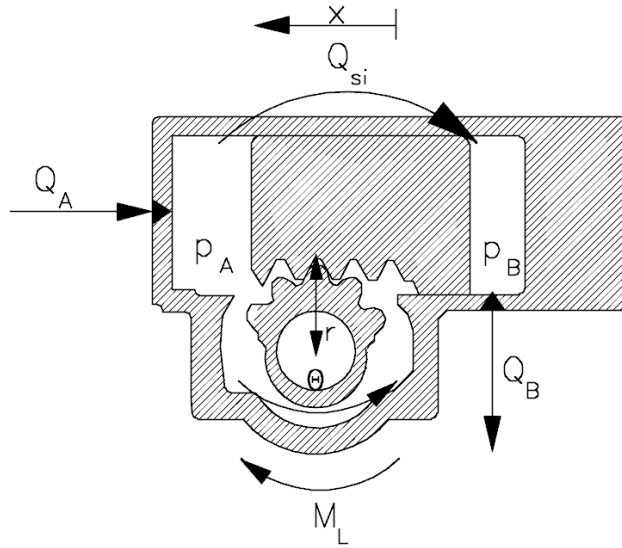


Figure 4.4. illustration of Pressure Build-up in Cylinder

Where p_A is the pressure in chamber A of the cylinder, Q_A is the net flow entering that chamber based on the operating conditions, A_A is the surface area of side A of the piston, \dot{x} is the linear velocity of the piston of the cylinder, $Q_{s,i}$ is the internal leakage across the cylinder chambers, and Q_r is the flow rate through the high pressure system relief valve.

The hydraulic capacitance term $C_{H,A}$ is based on the instantaneous volume of the cylinder chamber which changes as the piston moves, as well as volume on the hydraulic lines and any existing dead volume. Assuming the zero position of the output shaft ($x = 0$) to be at mid-stroke, the capacitance equation is given by:

$$C_{H,A} = \frac{V_A}{K} = \frac{1}{K} \left[\left(\frac{H}{2} - x \right) A_A + V_{dead} + V_{L,A} \right] \quad (4.8)$$

Where K is the fluid bulk modulus, H is the cylinder stroke, V_{dead} the dead volume, and $V_{L,A}$ is the volume of line A.

Similarly, the pressure build-up in chamber B is given by:

$$\dot{p}_B = \frac{1}{C_{H,B}} (-Q_B - A_B \dot{x} + Q_{s,i} - Q_r) \quad (4.9)$$

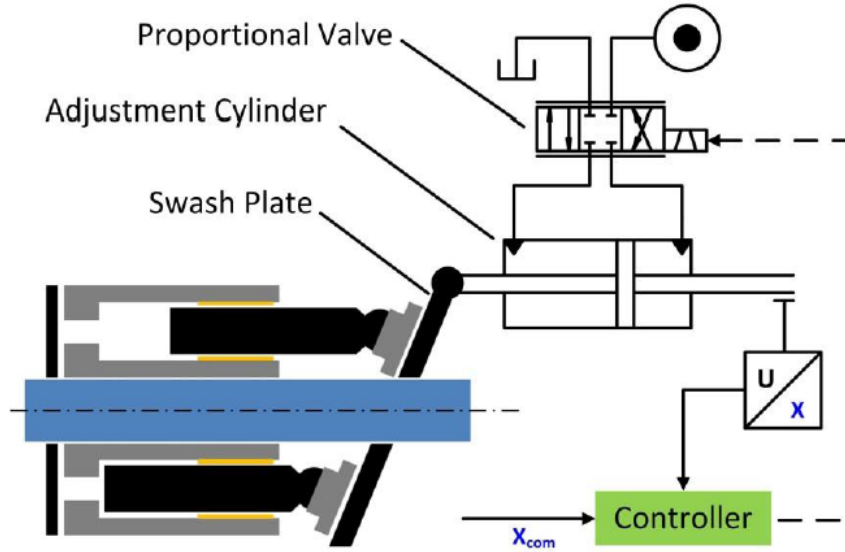


Figure 4.5. Swash Plate Control System.

Where A_B is the surface area of side B of the piston, Q_B is the net flow leaving side B, and $C_{H,B}$ its capacitance:

$$C_{H,B} = \frac{V_B}{K} = \frac{1}{K} \left[\left(\frac{H}{2} + x \right) A_B + V_{dead} + V_{L,B} \right] \quad (4.10)$$

4.1.3 Pump Displacement Control Model

In order to actuate the steer-by-wire system, the steering system controller sends the desired swash plate commands to the pump displacement control system (Figure 4.5) which then drives the swash plate to the desired position. The output of the swash plate controller is a voltage signal that controls the electronic proportional valve which in turn controls the double-acting control cylinder, and thus actuating the swash plate. The dynamics of the proportional valve can be modeled as a second order system with a transfer function that relates the input voltage, v_{sv} to the valve spool position, y_{sv} :

$$Y_{sv}(s) = \frac{D_{sv} \omega_{sv}^2}{s^2 + 2\zeta_{sv} \omega_{sv} s + \omega_{sv}^2} V_{sv}(s) \quad (4.11)$$

where D_{sv} is the valve's static gain, ω_{sv}^2 and ζ_{sv} are the valve's natural frequency and damping ratio, respectively.

As the valve spool is displaced, a corresponding flow rate will result based on the load pressure, P_L , across the control cylinder. This relationship can be approximated by the valve's linearized equation:

$$Q_{sv} = C_Q y_{sv} - C_{Q,P} P_L \quad (4.12)$$

With C_Q being the valve's flow gain, and $C_{Q,P}$ its pressure gain.

Moreover, since in this application, the dynamics of the valve used are much slower than the dynamics of the hydro-mechanical system, namely, the control cylinder and its hydraulic circuit, the normalized swash plate angle of the pump can be approximated by the following expression:

$$\beta = \frac{x_c}{H_c} = \frac{1}{H_c} \int \dot{x}_c = \frac{1}{H_c A_c} \int Q_{sv} \quad (4.13)$$

Where x_c is the displacement of the control cylinder, A_c its piston surface area, and H_c its stroke.

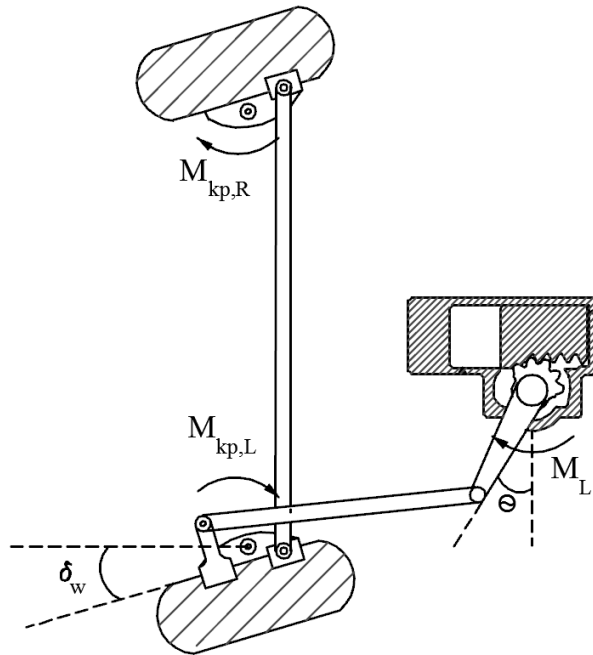


Figure 4.6. DC Steer-by-Wire Mechanical Subsystem.

4.2 Mechanical Subsystem Model:

As the pump delivers fluid to the actuator, the load moments acting on it cause the fluid pressure to build which in turn leads to a reaction torque that displaces the output shaft of the steering cylinder in the desired direction. The dynamics of such behavior are captured by the steering actuator's mechanical model (Figure 4.6) presented in the next section. The actuator is mechanically connected to the road wheels through a series of linkages that can be considered rigid and therefore with much higher natural frequency than of the steering system and vehicle dynamics. As a result, the linkage dynamics can be ignored and the position and torque at the actuator's output are assumed to be directly proportional the position and torque at the road wheels' kingpins:

$$\delta_w = \frac{\theta}{R_{link}} \quad (4.14)$$

$$M_{kp} = M_{kp,L} + M_{kp,R} = M_L R_{link} \quad (4.15)$$

Where δ_w is the angular position at the road wheel, R_{link} is the linkage ratio between the cylinder's output shaft and the road wheel kingpin, M_L is the load acting on the steering cylinder, and M_{kp} is the load torque at the kingpins.

Consequently, in order to have a complete model of the mechanical system, the load at the kingpin, M_{kp} , needs to be modeled. M_{kp} is highly dependent on the steering system geometry, as well as the lateral and longitudinal vehicle dynamics as will be shown in the subsequent sections. As such, the road wheel position, δ_w , is taken as the input to a vehicle model which is then used to compute the torque at the kingpin, M_{kp} , and the load torque on the steering cylinder, M_L , which is used as one of the inputs to the steering actuator's mechanical model.

4.2.1 Steering Actuator Mechanical Model:

Newton's second law is used to build a simple model that describes the dynamics of the actuator by balancing all the moments exerted on it:

$$m_{eq}\ddot{x} = -b\dot{x} - F_c \text{sign}(\dot{x}) - A_{APA} + A_{BPB} + \frac{M_L}{r} \quad (4.16)$$

Where m_{eq} represents the equivalent mass of the system, b its damping coefficient, F_c is the Coulomb friction term, M_L represents the external load torque applied at the output shaft of the steering cylinder, and r is the pitch radius of the output shaft of the steering cylinder.

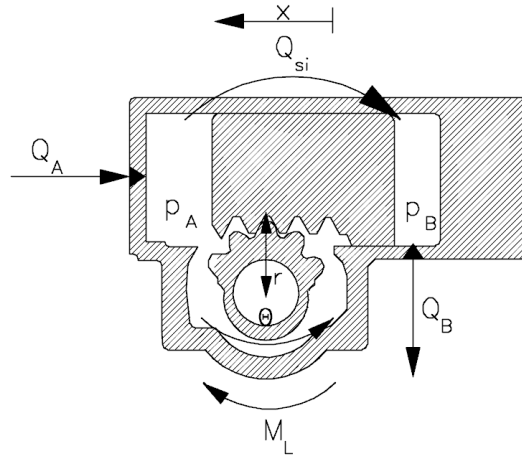


Figure 4.7. Steering Actuator Model.

4.2.2 External Load Torque Modeling:

The external load on the output shaft of the steering cylinder, M_L , is a direct result of the loads at the road wheels' kingpins (Figure 4.8). As a result, a thorough understanding of how these loads develop is essential to creating a mathematical model that describes them. Particularly, understanding the geometry of the steering system is critical to computing the moments resulting from the vertical load on the steered axle, as well as the lateral forces on the tires resulting from the vehicle's dynamic performance. Moreover, since for this prototype steer-by-wire implementation we've chosen to use the preexisting conventional steering system architecture by removing the intermediate shaft and replacing the steering gear with a single rack cylinder with a rotary output shaft, the external load on the cylinder will be the same as on the typical steering gear output shaft. As a result, our load model can be built based on a typical commercial vehicle steering system and validated by commercially available vehicle dynamics simulation software.

On a commercial vehicle steering system, the kingpin axis is usually tipped outward at the bottom resulting in a kingpin inclination angle, λ , as shown in Figure 4.9-a. It is also common to place the road wheel at an offset, d , referred to as kingpin

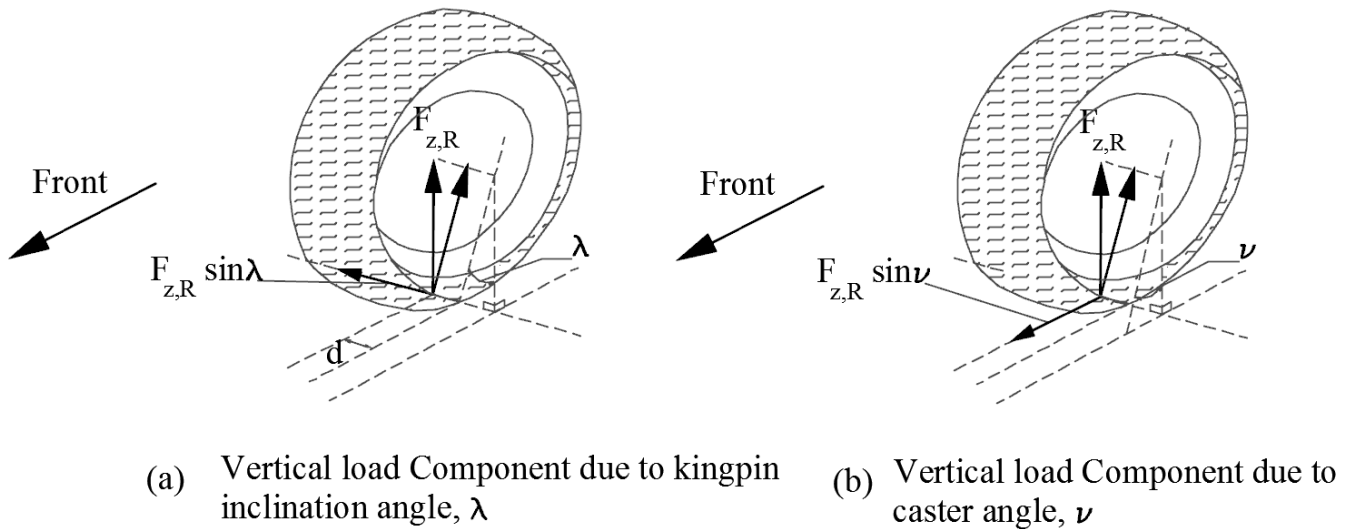


Figure 4.9. Road Wheel Rotation Geometry.

A major portion of the load on the steering system is due to vehicle's vertical load, F_z , on the steered axle. Due to the kingpin's inclination angle, λ , and caster angle, ν , the vertical load force, F_z , has a component that results in a moment, $M_{1,z}$, about the vertical z-axis. Such moment can be approximated by handling the effects of the caster and kingpin inclination angles separately and assuming them to be very small, yielding the following expression:

$$M_{1,z} = -(F_{z,L} + F_{z,R})d \sin \lambda \sin \delta_w + (F_{z,L} - F_{z,R})d \sin \nu \cos \delta_w \quad (4.17)$$

Where $F_{z,L}$ and $F_{z,R}$ are the vertical load forces on the left and right wheel of the steered axle, respectively. The first term in the equation above reflects the effect of the kingpin inclination angle, λ , which vanishes at zero steer angle, δ_w , and increases when steering the wheels, and thus providing a centering moment. The second term of equation (4.17) is a result of the caster angle, ν , and arises when there's an imbalance in the vertical load between the left and right wheels which can result in a steering pull. Vertical load imbalance can be due to different factors; As the wheels are steered,

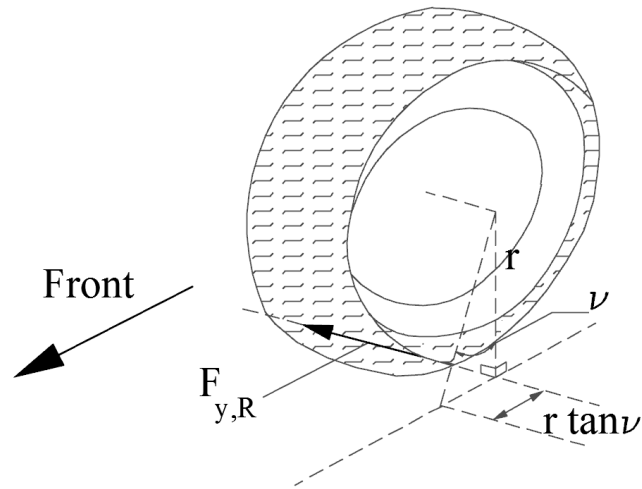


Figure 4.10. Kingpin Moment due to Lateral Tire Forces

the steering system geometry causes one side of the axle to lift and the other to drop, resulting in a difference in vertical loads that depends on the roll stiffness of the axle suspension. Moreover, when negotiating turns, the lateral acceleration on the vehicle causes load to transfer to the outside wheels, also resulting a vertical load imbalance.

Another important portion of the load that acts on the steering cylinder comes from the moment due to the lateral forces acting on the tires (Figure 4.10). As these forces generate in the tire's contact patch, their distribution is not uniform, and thus, their resulting force acts at an offset from the center of the contact patch (Figure 4.11). Such offset is known as the pneumatic trail of the tire, l_{pt} . Moreover, the caster angle, ν , creates another longitudinal offset known as the mechanical trail, l_{mech} , which can be expressed as:

$$l_{mech} = r_{tire} \tan \nu \quad (4.18)$$

With r_{tire} being the effective tire radius.

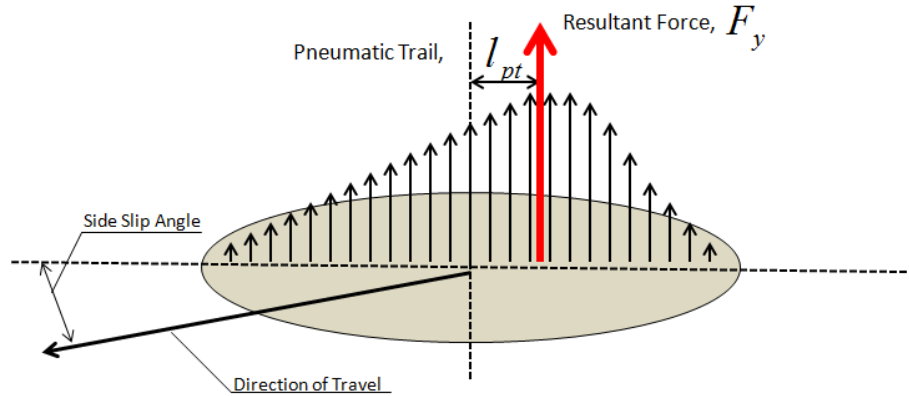


Figure 4.11. Tire Force Distribution

As a result, through the tires' pneumatic trail, l_{pt} , and the steering system's mechanical trail, l_{mech} , the lateral forces on the left and right tires, $F_{y,L}$ and $F_{y,R}$, respectively, generate a moment about the z -axis:

$$M_{2,z} = (F_{y,L} + F_{y,R})(l_{pt} + l_{mech}) \quad (4.19)$$

Where the tire's lateral forces depend on the vehicle dynamics and vertical loads as will be shown in the next section.

Additionally, traction forces can also generate moments around the kingpin through the kingpin offset, d , (Figure 4.12) but these forces are usually balanced through the tie-rod. However, in the event of a tire blowout or brake malfunction, an imbalance in the traction forces can occur leading to a steering pull and a moment about the z -axis:

$$M_{3,z} = (F_{x,L} - F_{x,R})d \quad (4.20)$$

Finally, all the aforementioned moments are summed together and their component about the kingpin axis is given by:

$$M_{kp} = (M_{1,z} + M_{2,z} + M_{3,z}) \cos(\sqrt{\lambda^2 + \nu^2}) \quad (4.21)$$

From which the load moment, M_L , acting on the steering cylinder's output shaft can be computed using equation (4.15).

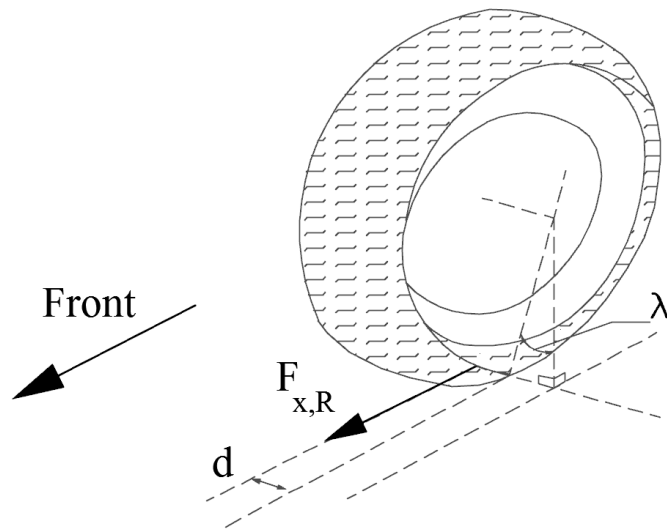


Figure 4.12. Kingpin Moment due to Longitudinal Tire Forces



Figure 4.13. Development Vehicle

$$M_L = \frac{\cos(\sqrt{\lambda^2 + \nu^2})}{R_{link}} (M_{1,z} + M_{2,z} + M_{3,z}) \quad (4.22)$$

4.2.3 Vehicle Model:

The vehicle on which the prototype steer-by-wire system will be implemented is a three-axle Freightliner FL60 (Figure 7.15). As such, the vehicle model is built to describe its dynamic response to steering inputs commanded by the DC steer-by-wire system.

The vehicle model is determined by balancing the side tire forces and resulting moments acting on the vehicle (Figure 4.14). These forces are generated as a result of the interaction of the tire with the road surface and depend on the tires' cornering stiffness, C_i , and side slip angle, α_i , at the combined tires of the i^{th} axle.

$$F_{y,i} = C_i \alpha_i \quad (4.23)$$

Different tire models have been proposed over the last few decades, chief among them Pacejka's Magic Formula. These models describe the relationship between the tire's cornering stiffness and side slip angle under different loading conditions. However, since our vehicle model will be validated by a commercial simulation software, we have used the same provided tire data relating tire's side slip angles and vertical loads to cornering stiffness which we interpolate to compute the instantaneous cornering stiffness based on the current state of the vehicle. Moreover, as most commercial vehicles have a high center of gravity, during some maneuvers lateral load transfer can occur and may affect the tire cornering forces. However, for simplicity, in our model we assume that the load transfer is minimal and therefore negligible.

The side slip angle α_i is defined as the difference between the tire's centerline and the direction of its instantaneous velocity vector. Consequently, the side force generated at the tires of the i^{th} axle (Figure 4.14) is expressed as [38]:

$$F_{y,i} = C_i \left(\delta_i - \arctan \frac{v_y + x_i \dot{\psi}}{v_x} \right) \quad (4.24)$$

Where the cornering stiffness coefficient C_i is positive, δ_i is the steering angle at the i^{th} axle, x_i is the signed position of the axle relative to the vehicle's center of gravity (COG) being positive when the axle is in front the COG, v_x and v_y are the vehicle's

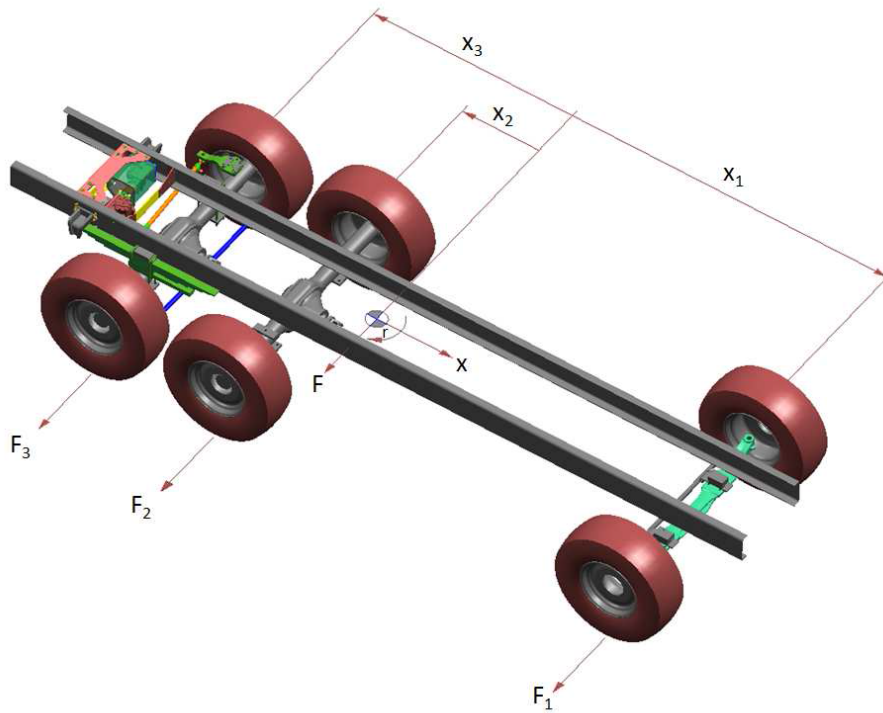


Figure 4.14. Vehicle FBD with Lateral Forces Only

longitudinal and lateral velocities, respectively, and $\dot{\psi}$ is the yaw rate of the vehicle. Elsewhere in the literature, the tire's side force is sometimes defined as:

$$F_{y,i} = C_i \left(\arctan \frac{v_y \pm x_i \dot{\psi}}{v_x} - \delta_i \right) \quad (4.25)$$

Where the cornering stiffness coefficient C_i is negative and x_i is the unsigned position of the axle relative to the vehicle's COG. However, in the rest of this dissertation, equation (4.24) is used to express the tires' side force.

To balance the tire forces and moments, the well-known bicycle model (Figure 4.15) is used which assumes negligible effect of the longitudinal and roll dynamics of the vehicle on its lateral dynamics performance. These assumptions are valid for highway on-center driving and low-speed parking lot maneuvers with no significant lateral load transfer which is typical for commercial vehicles. Moreover, the modeled vehicle is assumed to have a steerable front and back axles as indicated in Figure 4.15 by the

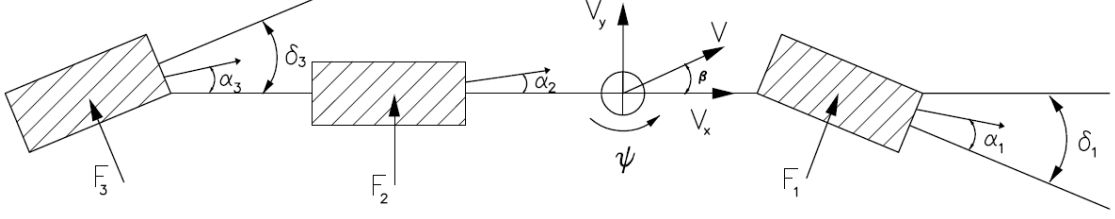


Figure 4.15. Generalized Three-Axle Bicycle Model

steer angles δ_1 and δ_3 . Steering the back axle is optional but can be used to enhance the vehicle's maneuverability and decrease tire wear. Additionally, in a steer-by-wire system, steering the back axle can be a source of redundancy to be used in case of a failure in the front axle steering system, and thus its inclusion in our model. Summing all the forces and moments acting on the vehicle yields:

$$\Sigma F_y = F_1 \cos(\delta_1) + F_2 + F_3 \cos(\delta_3) = m_v(\dot{v}_y + v_x \dot{\psi}) \quad (4.26)$$

$$\Sigma M_z = x_1 F_1 \cos(\delta_1) + x_2 F_2 + x_3 F_3 \cos(\delta_3) = I_{v,z} \ddot{\psi} \quad (4.27)$$

where m_v is the mass of the vehicle, and $I_{v,z}$ its moment of inertia about the vertical axis.

Plugging Eq. 4.24 into Eq. 4.26 and Eq. 4.27, and rearranging them leads to a state space representation of the vehicle model:

$$\begin{aligned} \dot{v}_y = \frac{1}{m_v} \{ & C_1 \cos(\delta_1) [\delta_1 - \arctan(\frac{v_y + x_1 \dot{\psi}}{v_x})] - C_2 \arctan(\frac{v_y + x_2 \dot{\psi}}{v_x}) \\ & + C_3 \cos(\delta_3) [\delta_3 - \arctan(\frac{v_y + x_3 \dot{\psi}}{v_x})] \} - v_x \dot{\psi} \quad (4.28) \end{aligned}$$

$$\begin{aligned} \ddot{\psi} = \frac{1}{I_v} \{ & x_1 C_1 \cos(\delta_1) [\delta_1 - \arctan(\frac{v_y + x_1 \dot{\psi}}{v_x})] - x_2 C_2 \arctan(\frac{v_y + x_2 \dot{\psi}}{v_x}) \\ & + x_3 C_3 \cos(\delta_3) [\delta_3 - \arctan(\frac{v_y + x_3 \dot{\psi}}{v_x})] \} \quad (4.29) \end{aligned}$$

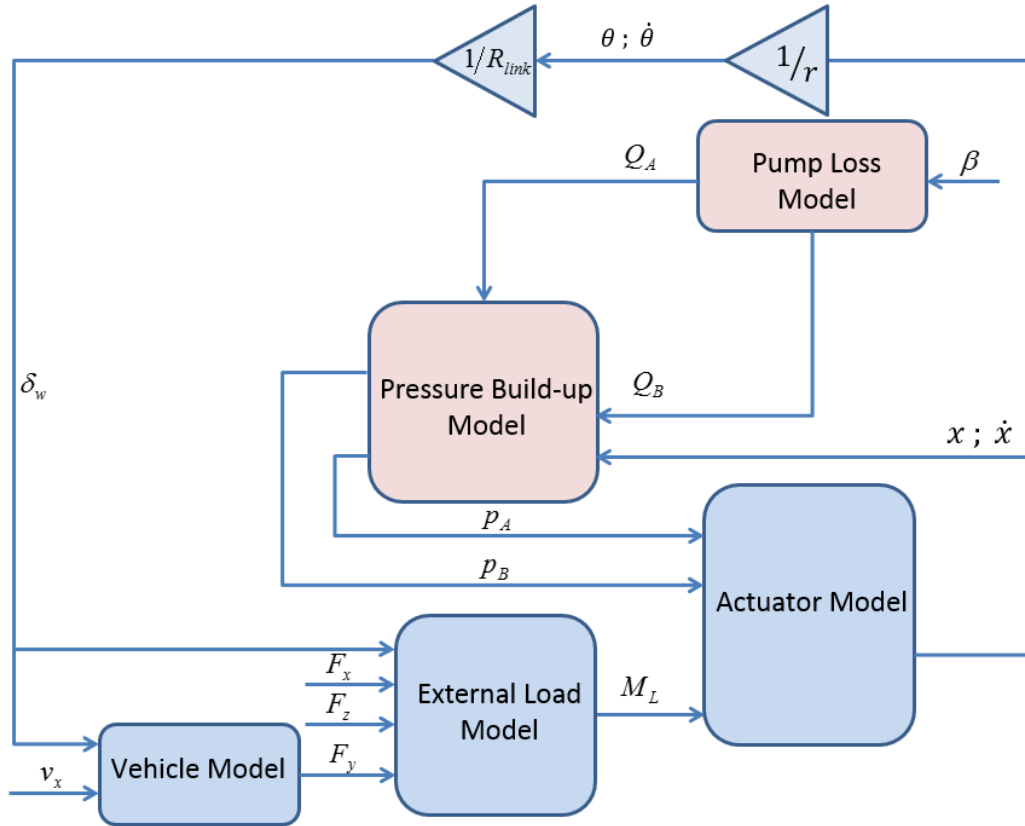


Figure 4.16. Overall DC Steer-by-Wire System Model

Equations (6.1) and (6.2) are used to simulate the vehicle performance from which the side tire forces can be computed based on the side slip angle (Eq. 4.24) which constitute part of the load torque, M_L , acting on the steering cylinder's output shaft.

$$F_{y,R} + F_{y,L} = C_1 \cos(\delta_w) [\delta_w - \arctan(\frac{v_y + x_1 \dot{\psi}}{v_x})] \quad \text{with } \delta_1 = \delta_w \quad (4.30)$$

Finally, all the derived equations of the hydraulic and mechanical mode are put together to build the DC-steer-by-wire mathematical model (Figure 4.16).

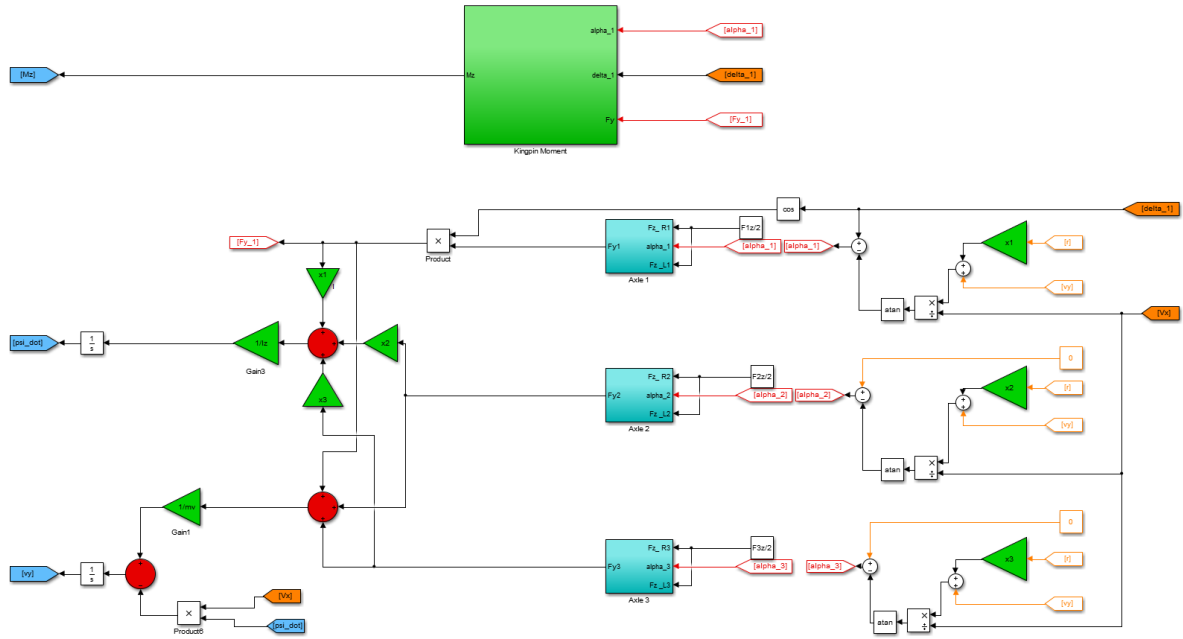
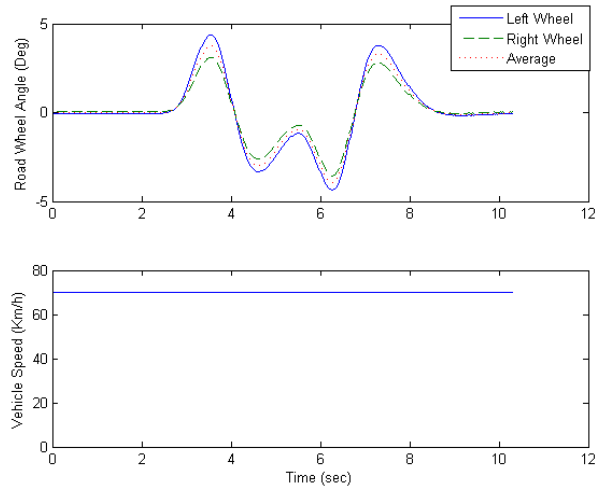


Figure 4.17. Vehicle Model in Simulink

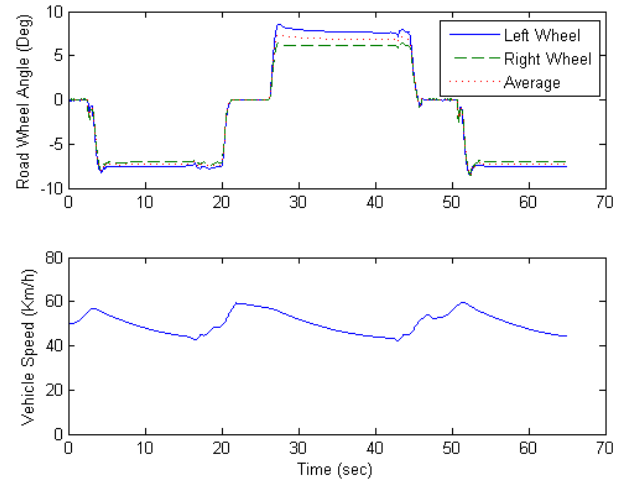
4.3 Model Validation:

4.3.1 Vehicle Model Validation:

Once the vehicle model equations are obtained, a simulation model is built in Matlab Simulink for a three-axle vehicle (Figure 4.17). Subsequently, Trucksim, a commercially available software for simulating truck dynamics, is used to validate our Simulink vehicle model with two driving scenarios; a high speed double lane change maneuver, and driving around a "figure 8" track to simulate normal driving conditions. The inputs to the model are the front wheel steering angle, δ_1 , and the vehicle's longitudinal speed, v_x , (Figure 4.18). However, since in the actual vehicle's steering system the left and right wheel steering angles are slightly different from each other due to the Ackerman geometry, we use the average of these angles as the steering input to our vehicle bicycle model.



(a)

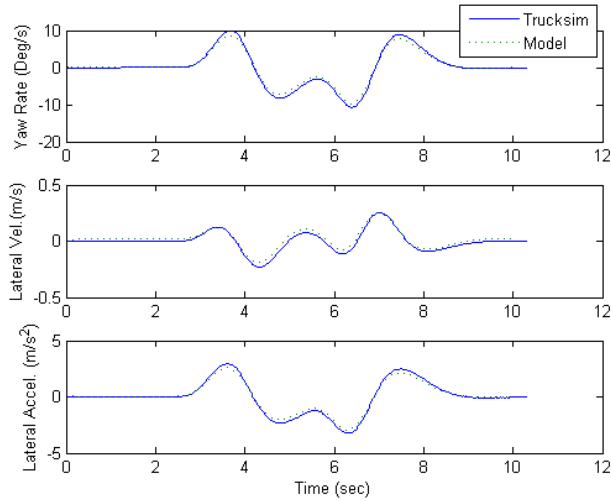


(b)

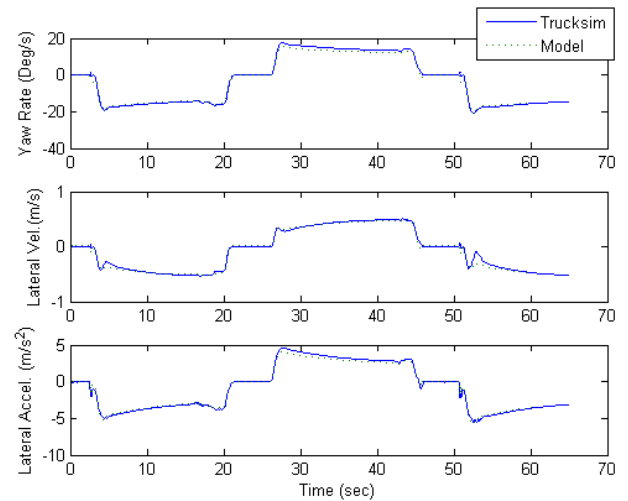
Figure 4.18. Inputs Used for Model Validation: (a) Double Lane Change Maneuver, (b) Figure 8 Maneuver.

To check the validity of the vehicle model, we compare the results of Trucksim to our model by examining the performance of the the vehicle's main lateral dynamics quantities, namely, its yaw rate, $\dot{\psi}$, lateral velocity, v_y , and lateral acceleration, a_y , for the two driving scenarios. Figure 4.19 shows a very close performance between the two models for all three dynamic parameters and for both driving maneuvers.

Next, the tires side forces are compared for both models. These forces are of interest to us, particularly, the front tire forces because of their contribution to the load experienced by the steering cylinder. Looking at the simulation results of Figure 4.20, the predicted side forces by both models are very close to each other for both the double lane change and the Figure 8 maneuver.



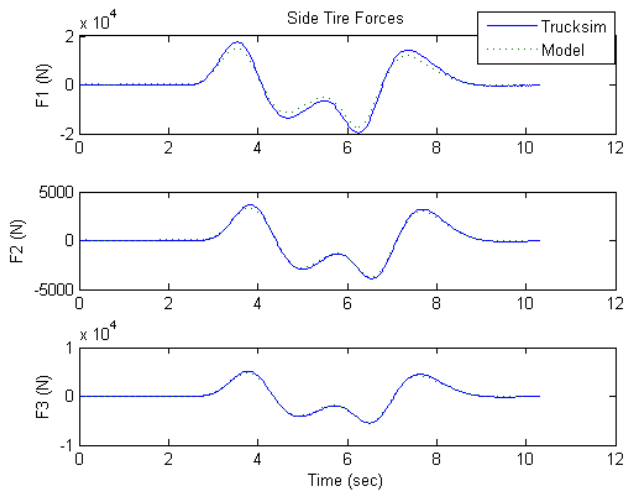
(a)



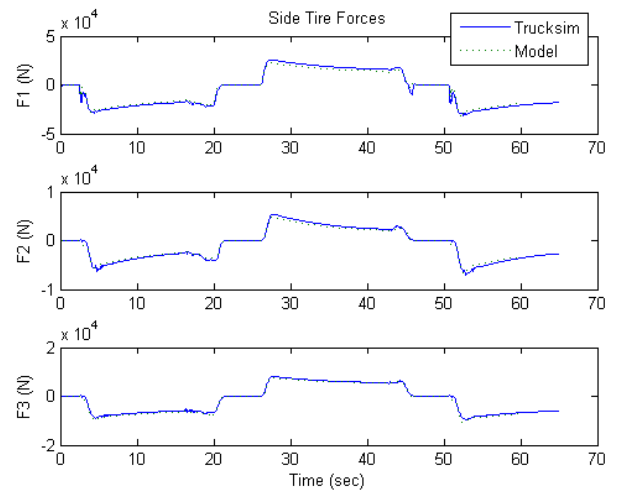
(b)

Figure 4.19. Vehicle Dynamics Validation: (a) Double Lane Change Maneuver, (b) Figure 8 Maneuver.

As a result, our vehicle model validation is achieved as it has been shown that the model can closely predict the tires' side forces. The slight differences between the simulation results can be attributed to the assumptions made in the bicycle model. Particularly, it ignores the roll and pitch dynamics of the truck and assumes no lateral load transfer as the vehicle negotiate turns. Moreover, the front steering angles being slightly different between the left and right side will result in different left and right side slip angles, and thus slightly different side forces. The trucksim model, on the other, does not make the aforementioned assumptions and takes into consideration many of the dynamics ignored in our bicycle model, e.g. roll dynamics and load transfer.



(a)



(b)

Figure 4.20. Tire Side Forces Validation: (a) Double Lane Change Maneuver, (b) Figure 8 Maneuver.

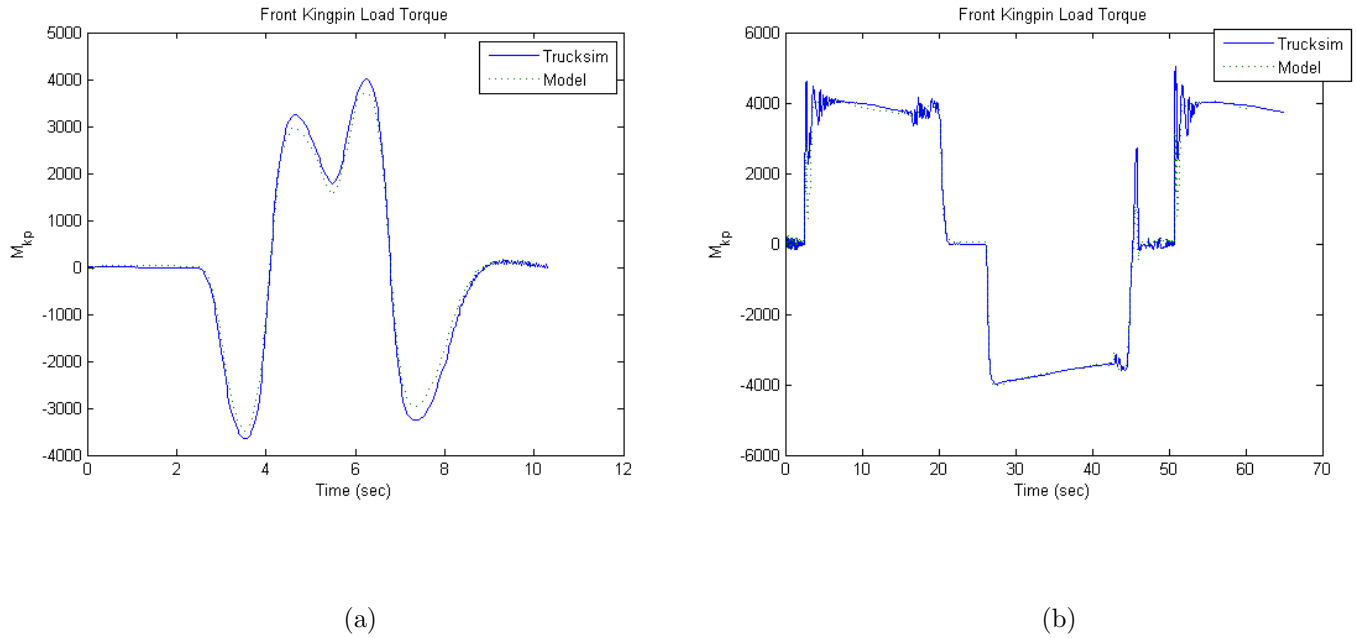


Figure 4.21. Kingpin Moment Validation: (a) Double Lane Change Maneuver, (b) Figure 8 Maneuver.

4.3.2 External Load Model Validation:

Once the front tires' side forces are computed, their contribution to the total kingpin moment can be determined through equation 4.19. Moreover, for this simulation we assume that the front right and left traction forces are equal, i.e. $F_{x,L} = F_{x,R}$, and thus by equation (4.20), $M_{3,z} = 0$.

From the obtained results in Figure 4.21, it can be seen that our model's kingpin torque prediction closely tracks the Trucksim model performance with only some minor differences. These small discrepancies results from the small differences in the tires' side forces described in the previous section which propagate to the kingpin load estimation. Nonetheless, our simplified vehicle model can, therefore, reliably predict the load torque on the steering cylinder in different driving conditions. This will, consequently, allow us to design and validate the vehicle's steering control system.

5. STEER-BY-WIRE CONTROL SYSTEM DESIGN AND ANALYSIS

Once the complete system model is derived, it is then used to validate the feasibility of the DC steer-by-wire system for on-highway commercial vehicles. Specifically, the derived model can be used to validate the steer-by-wire control systems which will be derived in this chapter. While a control system may or may not be model-based, its validation should be performed using as complete of a model as possible in order to confirm that the assumptions made during the design of the controller are valid throughout the operating range of interest. In this chapter, we simplify the derived system model after making some justified assumptions based on which we derive the control logic for the steer-by-wire system.

5.1 Simplified System Model

The complete system model derived in the previous chapter can be simplified by making certain assumptions that remain valid throughout the range of operating conditions of the system. Whether the goal is to control the position or velocity of output of the steering cylinder, the simplified model makes the design of the control system simpler. Nonetheless, the final controller will be validated using the more complete system model derived previously.

5.1.1 Derivation of the Simplified Model

Rewriting the relevant system equations derived above, namely, Equations 4.7, 4.9, and 4.16:

$$m_{eq}\ddot{x} = -b\dot{x} - F_c \text{sign}(\dot{x}) - A_A p_A + A_B p_B + \frac{M_L}{r} \quad (5.1)$$

$$\dot{p}_A = \frac{1}{C_{H,A}}(Q_A + A_A \dot{x} - Q_{s,i} - Q_r) \quad (5.2)$$

$$\dot{p}_B = \frac{1}{C_{H,B}}(-Q_B - A_B \dot{x} + Q_{s,i} - Q_r) \quad (5.3)$$

Neglecting the internal leakage of the actuator, $Q_{s,i}$ and flow across the relief valve, Q_r , and assuming the capacitance terms between side A and B to be equal, i.e. $C_{H,A} = C_{H,B} = C_H$, and then applying the Laplace transform on all three equations while defining $\mathcal{L}\{\dot{x}\} = \vartheta(s)$, yields:

$$m_{eq}s\vartheta(s) + b\vartheta(s) = -F_c \text{sign}(\vartheta(s)) - A_A p_A(s) + \alpha A_A p_B(s) + \frac{M_L}{r} \quad (5.4)$$

$$p_A(s) = \frac{1}{sC_H}(Q_A + A_A \vartheta(s)) \quad (5.5)$$

$$p_B(s) = \frac{1}{sC_H}(-Q_B - \alpha A_A \vartheta(s)) \quad (5.6)$$

Where $\alpha = \frac{A_B}{A_A}$. The response of the piston's steering velocity, $\vartheta(s)$, is found by plugging equations (5.5) and (5.6) into (5.4), and solving for $\vartheta(s)$:

$$\vartheta(s) = T_Q(s)Q_e + T_M(s)F_f \quad (5.7)$$

Where Q_e is the effective flow rate from the pump as described by equation (4.3), F_f is the combined friction and external load moments applied on the steering cylinder, and $T_Q(d)$ and $T_M(s)$ are the system's transfer functions defined as:

$$T_Q(s) = \frac{\frac{(1+\alpha)A_A}{C_H}}{m_{eq}s^2 + bs + \frac{(1+\alpha^2)A_A^2}{C_H}} \quad (5.8)$$

$$T_M(s) = \frac{s}{m_{eq}s^2 + bs + \frac{(1+\alpha^2)A_A^2}{C_H}} \quad (5.9)$$

Similarly, if our intent is to control the position, x , the following simplified model can be used:

$$\chi(s) = \frac{1}{s}\vartheta(s) = T'_Q(s)Q_e + T'_M(s)F_f \quad (5.10)$$

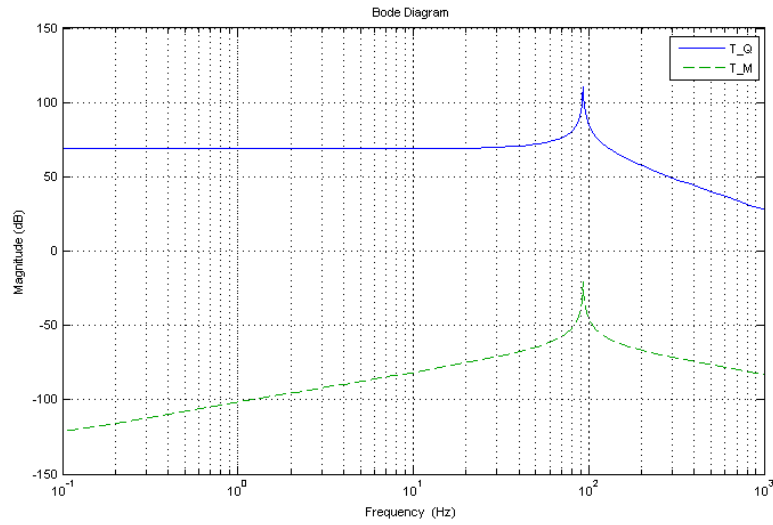


Figure 5.1. Bode plot of T_M and T_Q

With

$$T'_Q(s) = \frac{\frac{(1+\alpha)A_A}{C_H}}{m_{eq}s^3 + bs^2 + \frac{(1+\alpha^2)A_A^2}{C_H}s} \quad (5.11)$$

$$T'_M(s) = \frac{1}{m_{eq}s^2 + bs + \frac{(1+\alpha^2)A_A^2}{C_H}} \quad (5.12)$$

The transfer functions T_M and T'_M , represent the compliance of the system. Consequently, as hydraulic systems are known for their low compliance, i.e. $C_H \ll 1$, T_M and T'_M can be assumed to be negligible for a certain range of frequencies. Particularly, this assumption is valid below the cutoff frequency:

$$\omega_c = \sqrt{\frac{(1+\alpha^2)A_A^2}{m_{eq}C_H}} \quad (5.13)$$

The validity of this assumption can be visualized with the bode plot of Figure (5.1).

As a result, since the external load moment is typically of low frequency content, the simplified model for the steering velocity, $\vartheta(s)$ and position, $\chi(s)$, can be expressed as:

$$\vartheta(s) = \frac{\frac{(1+\alpha)A_A}{C_H}}{m_{eq}s^2 + bs + \frac{(1+\alpha^2)A_A^2}{C_H}} Q_e \quad (5.14)$$

$$\chi(s) = \frac{\frac{(1+\alpha)A_A}{C_H}}{m_{eq}s^3 + bs^2 + \frac{(1+\alpha^2)A_A^2}{C_H}s} Q_e \quad (5.15)$$

5.1.2 Validation of Simplified Model:

In order to validate the simplified model, its response to a changing effective flow rate is compared to the response of the complete model to the same flow input. The complete model includes the mechanical and hydraulic subsystem models of the steering system, while the simplified model is represented by equations (5.14), and (5.15). The diagram in Figure 5.2 summarizes the validation procedure, and Figure 5.3 shows the simulations results. As expected, the response of the simplified model closely matches that of the complete system model at the frequency range at which the steering system is expected to operate.

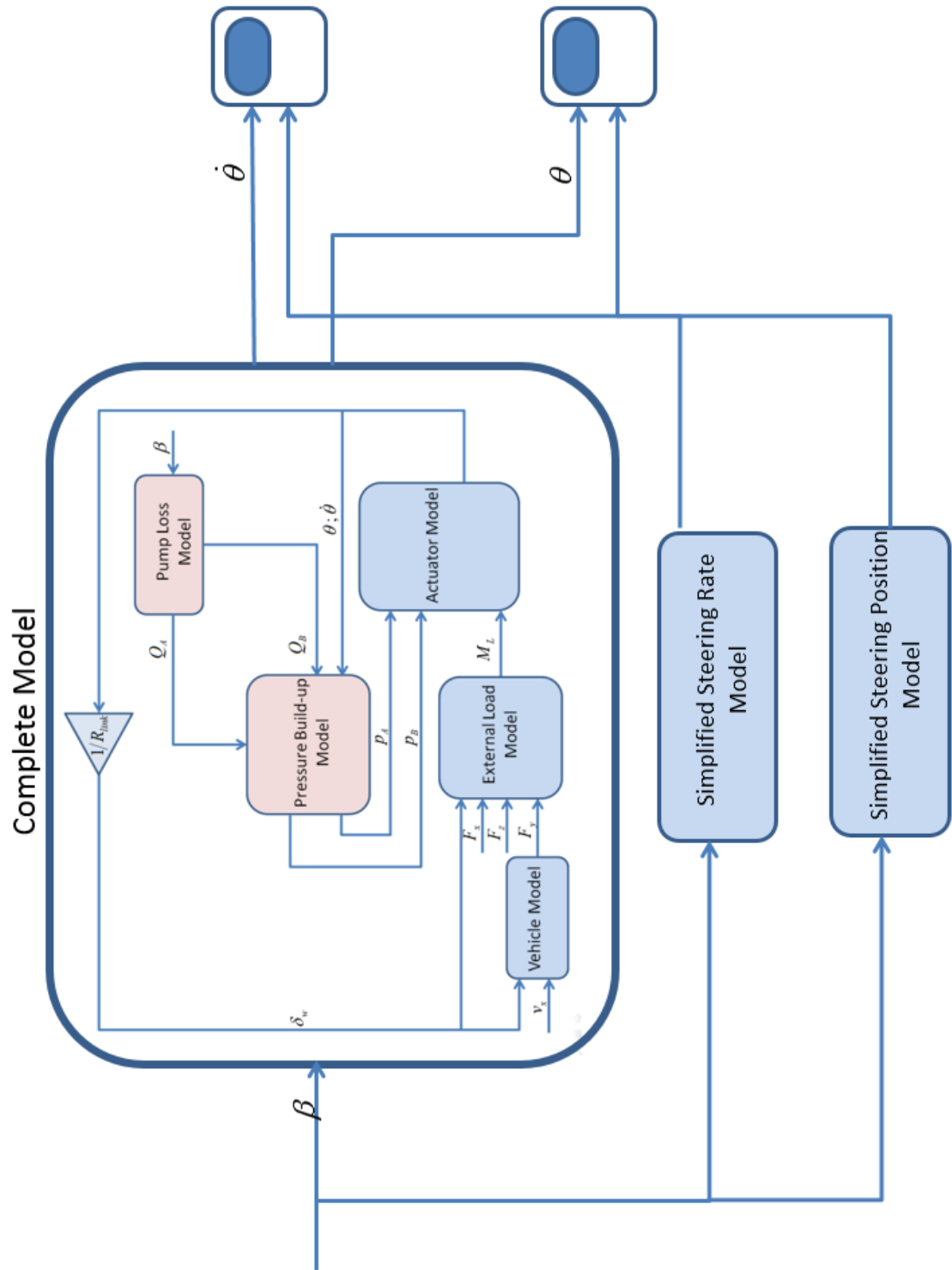
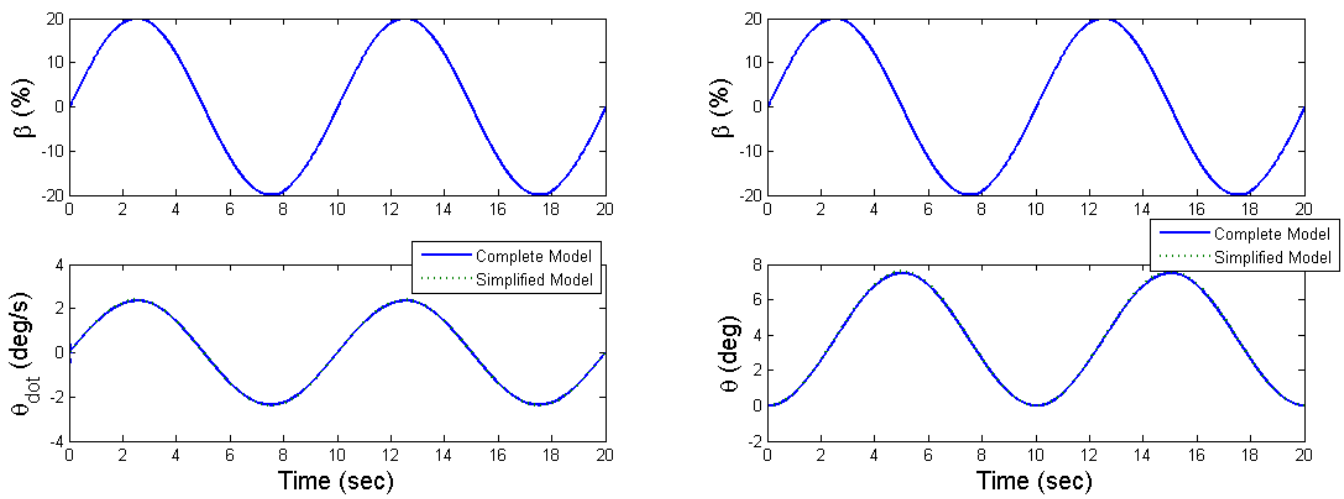


Figure 5.2. Simplified Model Validation Diagram



(a)

(b)

Figure 5.3. Simplified Model Validation: (a) Steering Rate Response, (b) Steering Position Response.

5.2 Adaptive Robust Control Strategy I:

5.2.1 Controller Synthesis:

As on-highway vehicles travel at relatively higher speeds than their off-highway counterparts, their lateral velocity response to steering inputs is also much more significant. As a result, on-highway steering systems are required to have higher control accuracy in order to allow the driver to maintain the lane while at highway speeds. With conventional steering system high control accuracy is achieved as a result of the low steering ratio between the input and output of the steering gear. As such, when driving on the highway at high speeds, typically small steering inputs, e.g. $\pm 10^\circ$ at the hand wheel, is all it takes to maintain a straight lane. Depending on the steering system, such small steering inputs translate to less than a millimeter of motion at the steering gear piston. Consequently, when designing a steer-by-wire control system for on-highway vehicles, a similar level of control accuracy of the steering cylinder piston is required to achieve an acceptable steering performance.

Furthermore, many of the steer-by-wire system parameters can be either unknown such as piston viscous damping, change under different operating conditions, e.g. fluid bulk modulus and pump losses, or simply change from one application to another such as the change in pump losses from one pump size to another or over time due wear. As a result, the steer-by-wire control system needs to be robust enough to handle the uncertainty in the system parameters, or be able to estimate them and directly compensate for their effects.

Consequently, in order to satisfy the high accuracy control requirement, the necessity for robustness to system uncertainty, and the ability to estimate and compensate for unknown parameters, an Adaptive Robust Controller (ARC) was the control system of choice as it satisfies all three of the aforementioned requirements. The ARC is designed to achieve such requirements while guaranteeing the stability and boundedness of both the transient and steady state responses. This is achieved through the use of both the adaptive and robust substructures of the controller simultaneously.

While the adaptive algorithm estimates the unknown parameters using a projection function which guarantees that the parameter estimates remain within a predefined range, the robust sub-controller guarantees the boundedness of the error signals regardless of the convergence of the parameters estimates through a robust nonlinear feedback strategy.

Starting from the derived simplified velocity response model in equation (5.14), which we repeat here for convenience::

$$\vartheta(s) = \frac{\frac{(1+\alpha)A_A}{C_H}}{m_{eq}s^2 + bs + \frac{(1+\alpha^2)A_A^2}{C_H}} Q_e \quad (5.16)$$

We first convert the model to its state space form after making the following definition, $x_1 = x$, $x_2 = \dot{x}$, and $x_3 = \ddot{x}$:

$$\dot{x}_1 = x_2 \quad (5.17)$$

$$\dot{x}_2 = x_3 \quad (5.18)$$

$$\dot{x}_3 = -\frac{b}{m_{eq}}x_3 - \frac{(1+\alpha^2)A_A^2}{m_{eq}C_H}x_2 + \frac{(1+\alpha)A_A}{m_{eq}C_H}Q_e \quad (5.19)$$

Where the effective pump flow output, Q_e , is given by:

$$Q_e = V_{sp}n_e\beta - Q_s \quad (5.20)$$

With Q_s representing the pump's flow losses.

The viscous damping parameter, b , can easily be determined empirically. However, its value may change from one steering cylinder to another depending on many factors such as the materials used, machining process, etc. Consequently, we will assume that this parameter is unknown and will attempt to estimate it using our adaptive control strategy. Similarly, the equivalent mass parameter, m_{eq} , depends on the steering system and would change with varying the front axle weight of the vehicle. As a result, it is best to assume it to be unknown and estimate it instead. Moreover, the value of the fluid's bulk modulus, K , depends on the type of fluid used, its temperature, and

pressure. Therefore, we assume that the capacitance term, $C_H = \frac{V}{K}$, to be unknown and estimate it as well. As a result, we make the following definitions:

$$\eta_1 = \frac{b}{m_{eq}} \quad (5.21)$$

$$\eta_2 = \frac{1}{m_{eq}C_H} \quad (5.22)$$

$$\eta_3 = d_o \quad (5.23)$$

$$d = \frac{-(1 + \alpha)A_A}{m_{eq}C_H}Q_s \quad (5.24)$$

$$\tilde{d} = d - d_o \quad (5.25)$$

Where d_o can be thought of as the mean value of a changing unknown parameter, d , which through equation (5.24), directly relates to the flow losses term, Q_s that may vary but is always bounded.

Combining equations (5.17) - (5.25) yields:

$$\dot{x}_1 = x_2 \quad (5.26)$$

$$\dot{x}_2 = x_3 \quad (5.27)$$

$$\dot{x}_3 = -\eta_1 x_3 + \eta_2[-(1 + \alpha^2)A_A^2 x_2 + 2A_A V_{sp} n_e \beta] + \eta_3 + \tilde{d} \quad (5.28)$$

In order to control the steering rate, x_2 , of the system, we define an error signal, $z_2 = x_2 - x_{2,d}$, where $x_{2,d}$ is the desired steering rate which the controller needs to track. Moreover, we define a second error signal, z_3 , as $z_3 = x_3 - x_{3,eq}$, where $x_{3,eq} = \dot{x}_{2,d} - k_2 z_2$. These definitions are equivalent to creating a target sliding surface, S , or in this case a line:

$$S = z_3 = \dot{z}_2 + k_2 z_2 \quad (5.29)$$

Consequently, minimizing the error signal, z_3 , is equivalent to driving the system towards the line $S_0 : \dot{z}_2 + k_2 z_2 = 0$. And, since k_2 is positive, S_0 will have a negative slope which will cause the states, \dot{z}_2 and z_2 to slide towards the origin $(\dot{z}_2, z_2) = (0, 0)$, and thus achieving the controller's goal of tracking the desired steering rate, $x_{2,d}$.

Differentiating, z_3 , and noting equation (5.28), we obtain:

$$\dot{z}_3 = -\eta_1 x_3 + \eta_2\{-(1 + \alpha^2)A_A^2 x_2 + (1 + \alpha)A_A V_{sp} n_e \beta\} + \eta_3 + \tilde{d} - \dot{x}_{3,eq} \quad (5.30)$$

Before introducing the control strategy, we first present the projection function used to estimate the unknown parameters. Letting $\hat{\eta}$ represent the online estimate of η , and $\tilde{\eta} = \hat{\eta} - \eta$ be the estimation error, we define a simple discontinuous projection function as follows([39] & [40]):

$$Proj_{\hat{\eta}}(*) = \begin{cases} 0 & \text{if } \hat{\eta}_i = \hat{\eta}_{imax} \text{ and if } * > 0 \\ 0 & \text{if } \hat{\eta}_i = \hat{\eta}_{imin} \text{ and if } * < 0 \\ * & \text{otherwise} \end{cases} \quad (5.31)$$

By using an adaptation law of the form:

$$\dot{\hat{\eta}} = Proj_{\hat{\eta}}(\Gamma\tau) \quad (5.32)$$

Where $\Gamma > 0$ is a diagonal matrix and τ is a tuning function to be determined later. Consequently, it can be shown that the projection mapping used in equation (5.31) guarantees:

$$i. \hat{\eta} \in \Omega_{\eta} \equiv \{\hat{\eta} : \eta_{min} \leq \eta \leq \eta_{max}\} \quad (5.33)$$

$$ii. \tilde{\eta}(\Gamma^{-1}Proj_{\hat{\eta}}(\Gamma\tau) - \tau) \leq 0, \forall \tau \quad (5.34)$$

We now propose the following Adaptive Robust Control strategy which minimizes the error signal, z_3 , and thus z_2 , while guaranteeing the boundedness of its transient and steady state response, and therefore guaranteeing the tracking of the desired steering rate, $x_{2,d}$:

$$\beta = \beta_s + \beta_a \quad (5.35)$$

$$\beta_s = \beta_{s,1} + \beta_{s,2} \quad (5.36)$$

$$\beta_a = \frac{1}{(1 + \alpha)A_A V_{sp} n_e \hat{\eta}_2} \{\hat{\eta}_1 x_3 - \hat{\eta}_3 + \dot{x}_{3,eq}\} + \frac{A_A}{V_{sp} n_e} x_2 \quad (5.37)$$

β_s is a robust feedback control law and β_a a feedforward control law used to directly compensate for the model uncertainties through online parameter adaptation given by (5.32) with a tuning function, $\tau = \phi_3 z_3$, where

$$\phi_3 = [-x_3 \ ; \ (1 + \alpha)A_A V_{sp} n_e \beta_a \ ; \ 1] \quad (5.38)$$

β_s consists of linear stabilizing term $\beta_{s,1}$ and a nonlinear feedback term $\beta_{s,2}$

$$\beta_s = -k_{s,3}z_3 + \beta_{s,2} \quad ; \quad k_{s,3} = \frac{k_3}{(1 + \alpha)A_A n_e V_{sp} \eta_{2min}} \quad (5.39)$$

Where $k_3 > 0$, and $\beta_{s,2}$ satisfies the following conditions:

$$i. \quad z_3 \{ (1 + \alpha)A_A V_{sp} n_e \eta_2 \beta_{s,2} - \phi_3^T \tilde{\eta} + \tilde{d} \} \leq \epsilon_3 \quad (5.40)$$

$$ii. \quad (1 + \alpha)A_A V_{sp} n_e \eta_2 z_3 \beta_{s,2} \leq 0 \quad (5.41)$$

Where ϵ_3 is a design parameter that can be made arbitrarily small. Condition (i) guarantees that $\beta_{s,2}$ will dominate the model uncertainties due to parametric uncertainties, $\tilde{\eta}$, as well as uncertain nonlinearities, \tilde{d} , while condition (ii) guarantees that $\beta_{s,2}$ is dissipating in nature, and thus, does not interfere with the adaptive control part, β_a [41]. Moreover, $\tilde{\eta}$ is defined as:

$$\tilde{\eta} = \hat{\eta} - \eta = [\tilde{\eta}_1; \tilde{\eta}_2; \tilde{\eta}_3] \quad (5.42)$$

Substituting the control law described by equations (5.35)-(5.37), and (5.39) into (5.30) yields:

$$\dot{z}_3 = -(1 + \alpha)A_A V_{sp} n_e \eta_2 k_{s,3} z_3 + (1 + \alpha)A_A V_{sp} n_e \eta_2 \beta_{s,2} - \phi_3^T \tilde{\eta} + \tilde{d} \quad (5.43)$$

Defining a semi-positive Lyapunov function, $V_3 = \frac{1}{2}(z_3)^2$, its time derivative is expressed as:

$$\dot{V}_3 = \dot{z}_3 z_3 = -(1 + \alpha)A_A V_{sp} n_e \eta_2 k_{s,3} z_3^2 + z_3 \{ (1 + \alpha)A_A V_{sp} n_e \eta_2 \beta_{s,2} - \phi_3^T \tilde{\eta} + \tilde{d} \} \quad (5.44)$$

Theorem 1: [41] *Let the parameter estimates be updated by the adaptation law (5.32) in which τ_3 is given by:*

$$\tau_3 = z_3 \phi_3 \quad (5.45)$$

A. In general, the output tracking error, z_3 , is bounded. Furthermore, V_3 is bounded above:

$$V_3(t) \leq \exp(-\lambda_{v3}t) V_3(0) + \frac{\epsilon_3}{\lambda_{v3}} [1 - \exp(-\lambda_{v3}t)] \quad ; \quad \lambda_{v3} = 2k_3 \quad (5.46)$$

B. If after a finite time t_o , $\tilde{d} = 0$, i.e., in the presence of parametric uncertainties only, then, in addition to the results in A, asymptotic output tracking is also achieved.

Proof A:

Noting the formula for $k_{s,3}$ and equations (5.40) and (5.44):

$$\dot{V}_3 = -\frac{\eta_2}{\eta_{2min}}k_3z_3^2 + z_3\{(1+\alpha)A_A V_{sp}n_e\eta_2\beta_{s,2} - \phi_3^T\tilde{\eta} + \tilde{d}\} \quad (5.47)$$

$$\leq -k_3z_3^2 + z_3\{(1+\alpha)A_A V_{sp}n_e\eta_2\beta_{s,2} - \phi_3^T\tilde{\eta} + \tilde{d}\} \quad (5.48)$$

$$\leq -k_3z_3^2 + \epsilon_3 \quad (5.49)$$

$$\leq -\lambda_v V_3 + \epsilon_3 \quad (5.50)$$

Leading to the result in (5.46) of Theorem 1 which can also be expressed in terms of the tracking error, z_3 :

$$|z_3|^2 \leq \exp(-2k_3t)|z_3(0)|^2 + \frac{\epsilon_3}{k_3}[1 - \exp(-2k_3t)] \quad (5.51)$$

As a result, the tracking error, z_3 , exponentially decays at a rate of $2k_3$ to a ball of radius, $\sqrt{\frac{\epsilon_3}{k_3}}$, which is determined by the controller parameters', ϵ_3 , and k_3 . This is an important result that sets the ARC control system apart from other control strategies. It shows that the transient performance of the system, and boundedness of the tracking error is guaranteed even before the convergence of the parameter estimation. This is not the case for other adaptive control strategies such as the Self Tuning Regulator (STR) for which the performance heavily relies on the convergence of the parameter estimation, and thus, its transient response is not guaranteed.

Proof B:

When $\tilde{d} = 0$, (5.48) becomes:

$$\dot{V}_3 \leq -k_3z_3^2 + z_3\{(1+\alpha)A_A V_{sp}n_e\eta_2\beta_{s,2} - \phi_3^T\tilde{\eta}\} \quad (5.52)$$

Recalling condition (ii) on the nonlinear feedback term, $\beta_{s,2}$, in (5.41), and the expression for the tuning function, τ_3 , of (5.45), equation (5.52) becomes:

$$\dot{V}_3 \leq -k_3z_3^2 - \tilde{\eta}^T\tau_3 \quad (5.53)$$

Selecting a positive semi-definite Lyapunov function, $V_a = V_3 + \frac{1}{2}\tilde{\eta}^T\Gamma^{-1}\tilde{\eta}$, with its time derivative:

$$\dot{V}_a = \dot{V}_3 + \tilde{\eta}^T\Gamma^{-1}\dot{\tilde{\eta}} \quad (5.54)$$

$$\leq -k_3z_3^2 + \tilde{\eta}^T(\Gamma^{-1}Proj_{\tilde{\eta}}(\Gamma\tau_3 - \tau_3)\tilde{\eta}^T\tau_3) \quad (5.55)$$

Noting the projection property (ii) mentioned in (5.34):

$$\dot{V}_a \leq -k_3z_3^2 \quad (5.56)$$

Therefore, $z_3 \in L_2$. One can also show that \dot{z}_3 is bounded, and so by Barbalat's Lemma, $z_3 \rightarrow 0$ as $t \rightarrow \infty$, which proves part B of Theorem 1.

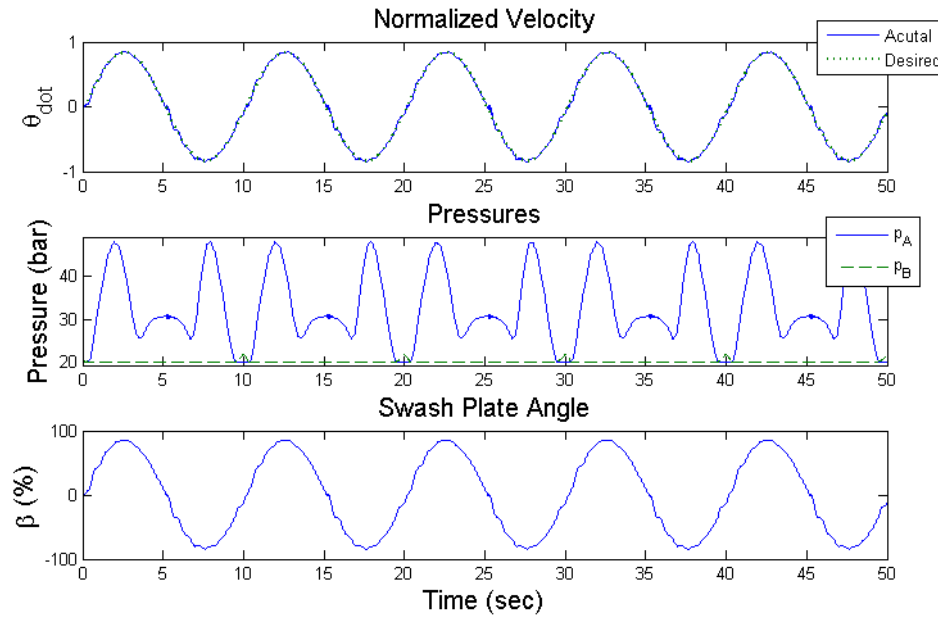


Figure 5.4. Simulation Results for a Sinusoidal Desired Steering Rate.

5.2.2 Simulation Results:

Despite the controller being designed using the simplified model, to illustrate its performance, a simulation is performed using the ARC controller with the complete system model presented in the previous chapter, i.e. steering system mechanical and hydraulic models, vehicle model, swash plate model, etc. The simulation was performed for both a sinusoidal and square wave desired steering rate inputs, and the results can be seen in Figures 5.4 and 5.5. For both steering inputs, the Adaptive Robust Control strategy is able to track the desired steering rate with very high control accuracy despite parametric uncertainties resulting from unknown system parameters such as system inertia and fluid bulk modulus, and nonlinear uncertainties due to pump flow losses which vary depending on operating conditions.

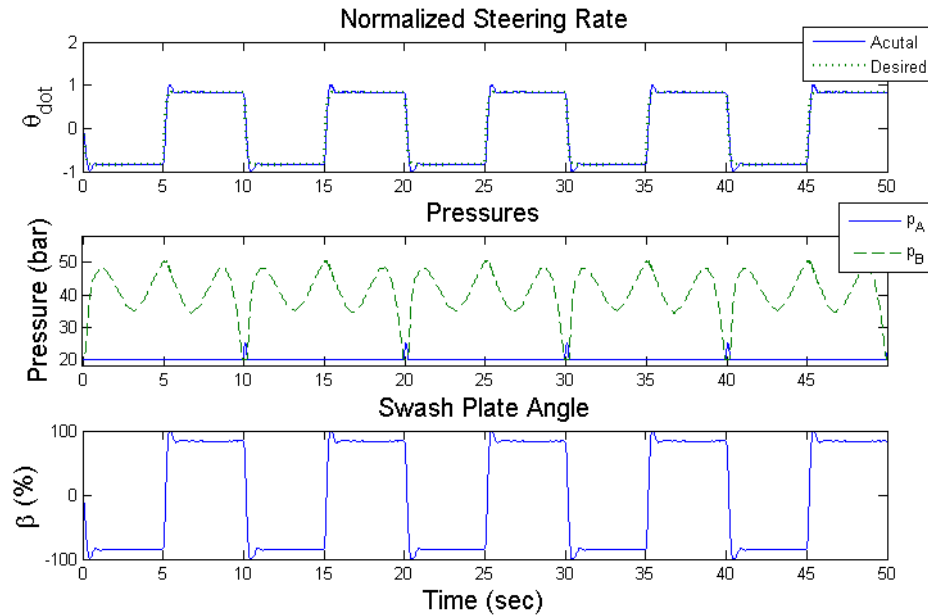


Figure 5.5. Simulation Results for a Square Desired Steering Rate.

5.2.3 Control Limitations and Challenges:

Despite the excellent performance of the ARC controller in simulation, some concerns arise about its implementation into a real physical system. Specifically, the controller presented above attempts to minimize the signal, z_3 , using a feed-forward control strategy, β_a , which contains the signal, $\dot{x}_{3,eq}$, which itself contains an acceleration term, $\dot{z}_2 = \dot{x}_2 - \dot{x}_{2,d}$. Moreover, the feedback term, β_s , also contains acceleration terms in the form of, $z_3 = x_3 - x_{3,eq}$. Consequently, the use of the acceleration signal in the control strategy can cause issues due to the noisy nature of that signal which can lead to stability issues. Typically, acceleration can be obtained either by twice differentiating a position signal, or directly from an accelerometer. Both methods, however, present challenges. Differentiating a physical signal which already contains noise results in an even noisier signal, particularly, if differentiated twice. Using low pass filters to reduce that noise can help remedy this issue but can also result in phase lag which can affect the stability of the system. On the other hand using accelerome-

ters to directly obtain the acceleration signal maybe challenging in a steering system application due to its relatively slow lateral motion which leads to a lower signal-to-noise ratio. This issue is even worsened if the acceleration signal is used to obtain the velocity signal which is also required by the proposed ARC controller. Integrating a noisy signal leads the accumulation of low frequency errors which will cause the resulting steering velocity signal to drift away from its true value as time goes on.

Additionally, all of the issues mentioned above are worsened when the steering position, rather than the steering rate, is the desired entity to be controlled. In that control mode, the proposed ARC controller will require the use of the derivative of the acceleration signal which is even noisier than the acceleration making the implementation of the controller even more challenging.

Consequently, since in a steering system application, the goal is to control the steering position or rate, and not its acceleration, the question arises: Do we really need to use the acceleration signal to control a steering system? In the next section, we attempt to answer this question by investigating the possibility of using an even simpler system model. A lower order model can result in a simpler control system that will be easier to implement into a real physical system and yield acceptable results.

5.3 An Even Simpler System Model:

Due to the high stiffness of the hydraulic system, i.e. low capacitance term, C_H , the pressure dynamics of the fluid inside the steering cylinder is relatively much faster than that of the steering system. Consequently, the pressure dynamics of the system can be neglected. Mathematically, this means we can assume that the capacitance term is negligible, i.e. $C_H \approx 0$. Consequently, the simplified model, which we repeat below for convenience, can be simplified even further.

$$\chi(s) = \frac{(1 + \alpha)A_A}{C_H m_{eq} s^3 + C_H b s^2 + (1 + \alpha^2)A_A^2 s} Q_e \quad (5.57)$$

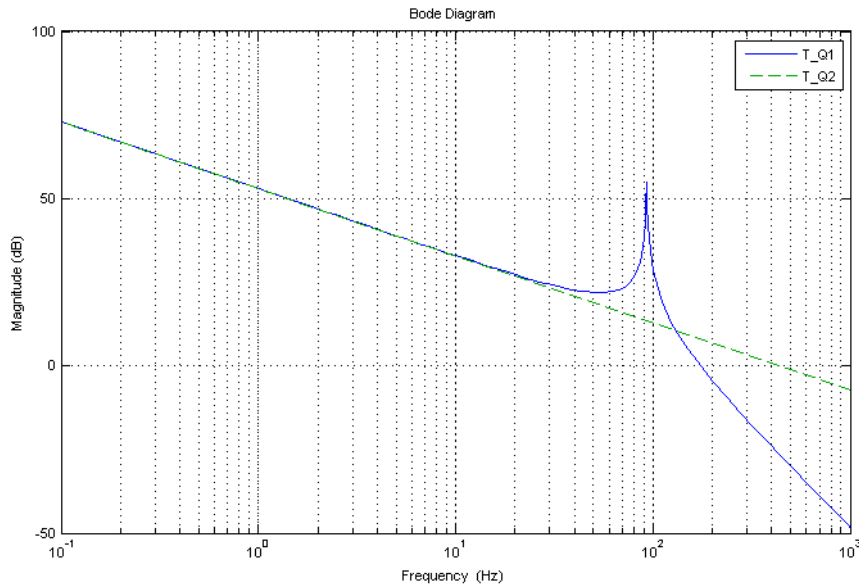


Figure 5.6. Bode Plot Comparison of the Two Simplified Models.

Which after setting $C_H = 0$ becomes:

$$\chi(s) = \frac{(1 + \alpha)}{(1 + \alpha^2)A_A s} Q_e \quad (5.58)$$

Furthermore, by looking at the bode plot of the simplified models (Figure 5.6), it can be seen that both models match over a frequency range up to about 30 Hz which is significantly higher than the typical frequency response of steering systems.

Moreover, in order to validate the new simplified model, both the complete model and the new simplified model are subjected to the same effective pump flow. The position response of both models is compared as presented in Figure 5.7 which shows a very close match between the two model responses.

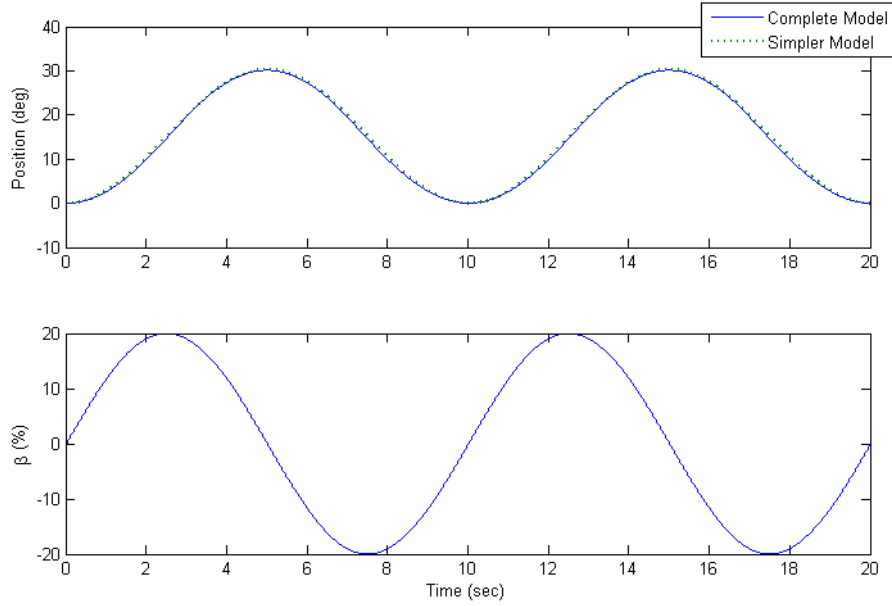


Figure 5.7. Simpler Model Validation.

5.4 Adaptive Robust Control Strategy II:

5.4.1 Controller Synthesis:

Starting with the Simpler Model equation (5.58), and plugging in the equation for the effective flow, Q_e , yields:

$$\dot{x} = \frac{(1 + \alpha)V_{sp}n_e}{(1 + \alpha^2)A_A}\beta - \frac{(1 + \alpha)}{(1 + \alpha^2)A_A}Q_s \quad (5.59)$$

Defining the state, $x_1 = x$, a known parameter $\gamma = \frac{(1+\alpha)V_{sp}n_e}{(1+\alpha^2)A_A}$, and the unknown nonlinearity, $\tilde{d} = d - d_o$, where $d = -\frac{(1+\alpha)V_{sp}n_e}{(1+\alpha^2)A_A}Q_s$, and $d_o = \eta_1$ its unknown mean value, the derived system model can be written in the following form:

$$\dot{x}_1 = \gamma\beta + \eta_1 + \tilde{d} \quad (5.60)$$

In order to control the steering position, x_1 , of the system, we define an error signal, $z_1 = x_1 - x_{1,d}$, where $x_{1,d}$ is the desired steering position which the controller needs to track.

Differentiating z_1 and noting equation (5.60), we obtain:

$$\dot{z}_1 = \gamma\beta + \eta_1 + \tilde{d} - \dot{x}_{1,d} \quad (5.61)$$

Once again, we propose an Adaptive Robust Control strategy to minimize the error signal, z_1 , while guaranteeing the boundedness of its transient and steady state response, and therefore guaranteeing the tracking of the desired steering position, $x_{1,d}$:

$$\beta = \beta_s + \beta_a \quad (5.62)$$

$$\beta_s = \beta_{s,1} + \beta_{s,2} \quad (5.63)$$

$$\beta_a = \frac{1}{\gamma}(-\hat{\eta}_1 + \dot{x}_{1,d}) \quad (5.64)$$

β_s is a robust feedback control law, while β_a a feed-forward control strategy used to directly compensate for the model uncertainties through online parameter estimation given by (5.32) with a tuning function:

$$\tau_1 = \phi_1 z_1 \quad \text{where } \phi_1 = [1] \quad (5.65)$$

β_s consists of a linear stabilizing term, $\beta_{s,1}$, and a nonlinear feedback term, $\beta_{s,2}$:

$$\beta_s = -k_{s,1}z_1 + \beta_{s,2} \quad ; \quad k_{s,1} = k_1 \frac{1}{\gamma} \quad (5.66)$$

Where $k_1 > 0$, and $\beta_{s,2}$ satisfies the following conditions:

$$i. \quad z_1 \{ \gamma\beta_{s,2} - \phi_1^T \tilde{\eta} + \tilde{d} \} \leq \epsilon_1 \quad (5.67)$$

$$ii. \quad \gamma\beta_{s,2}z_1 \leq 0 \quad (5.68)$$

Where ϵ_1 is a design parameter than can be arbitrarily small. Condition (i) guarantees that $\beta_{s,2}$ will dominate the model uncertainties due to parametric uncertainties, $\tilde{\eta}$, as well as uncertain nonlinearities \tilde{d} . On the other hand, condition (ii) guarantees that

$\beta_{s,2}$ is dissipating in nature, and thus, does not interfere with the adaptive control part β_a [41]. Moreover, $\tilde{\eta}$ is defined as:

$$\tilde{\eta} = \hat{\eta}_1 - \eta_1 = \tilde{\eta}_1 \quad (5.69)$$

Substituting the control law described by equations (5.62)-(5.64), and (5.66) into (5.61) yields:

$$\dot{z}_1 = -k_1 z_1 + \gamma \beta_{s,2} - \phi_1^T \tilde{\eta} + \tilde{d} \quad (5.70)$$

Defining a semi-positive Lyapunov function, $V_1 = \frac{1}{2}(z_1)^2$, its time derivative is expressed as:

$$\dot{V}_1 = \dot{z}_1 z_1 = -k_1 z_1^2 + z_1 \{\gamma \beta_{s,2} - \phi_1^T \tilde{\eta} + \tilde{d}\} \quad (5.71)$$

Theorem 2: [41] *Let the parameter estimates be updated by the adaptation law (5.32) in which τ_1 is given by:*

$$\tau_1 = z_1 \phi_1 \quad (5.72)$$

A. In general, the output tracking error, z_1 , is bounded. Furthermore, V_1 is bounded above:

$$V_1(t) \leq \exp(-\lambda_{v1}t) V_1(0) + \frac{\epsilon}{\lambda_{v1}} [1 - \exp(-\lambda_{v1}t)] \quad ; \quad \lambda_{v1} = 2k_1 \quad (5.73)$$

B. If after a finite time t_o , $\tilde{d} = 0$, i.e., in the presence of parametric uncertainties only, then, in addition to results in A, asymptotic output tracking is also achieved.

Proof A:

Noting the formula for $k_{s,1}$ and equations(5.67) and (5.71):

$$\dot{V}_1 = -k_1 z_1^2 + z_1 \{\gamma \beta_{s,2} - \phi_1^T \tilde{\eta} + \tilde{d}\} \quad (5.74)$$

$$\leq -k_1 z_1^2 + \epsilon_1 \quad (5.75)$$

$$\leq -\lambda_{v1} V_1 + \epsilon_1 \quad (5.76)$$

Thus, leading to the result (5.73) of Theorem 2 which can also be expressed in terms of the tracking error, z_1 :

$$|z_1|^2 \leq \exp(-2k_1 t) |z_1(0)|^2 + \frac{\epsilon_1}{k_1} [1 - \exp(-2k_1 t)] \quad (5.77)$$

As a result, the tracking error, z_1 , exponentially decays at a rate of $2k_1$ to a ball of radius, $\sqrt{\frac{\epsilon_1}{k_1}}$, which is determined by the controller parameters, ϵ_1 , and k_1 . As a result, the transient performance of the system, and boundedness of the tracking error is guaranteed even before the convergence of the parameter estimation.

Proof B:

When $\tilde{d} = 0$, (5.48) becomes:

$$\dot{V}_1 = -k_1 z_1^2 + z_1 \{ \gamma \beta_{s,2} - \phi_1^T \tilde{\eta} \} \quad (5.78)$$

Recalling the condition (ii) on the nonlinear feedback term, $\beta_{s,2}$, (5.68), and the expression for the tuning function, τ_1 , of (5.72), equation (5.78) becomes:

$$\dot{V}_1 \leq -k_1 z_1^2 - \tilde{\eta}^T \tau_1 \quad (5.79)$$

Selecting a positive semi-definite Lyapunov function, $V_{a,1} = V_1 + \frac{1}{2} \tilde{\eta}^T \Gamma^{-1} \tilde{\eta}$, with its time derivative:

$$\dot{V}_{a,1} = \dot{V}_1 + \tilde{\eta}^T \Gamma^{-1} \dot{\tilde{\eta}} \quad (5.80)$$

$$\leq -k_1 z_1^2 + \tilde{\eta}^T (\Gamma^{-1} Proj_{\hat{\eta}} (\Gamma \tau_1 - \tau_1) \tilde{\eta}^T \tau_1) \quad (5.81)$$

Noting the projection property (ii) mentioned in (5.34), we obtain:

$$\dot{V}_{a,1} \leq -k_1 z_1^2 \quad (5.82)$$

Therefore, $z_1 \in L_2$. One can also show that \dot{z}_1 is bounded, and so by Barbalat's Lemma, $z_1 \rightarrow 0$ as $t \rightarrow \infty$, which proves part B of Theorem 2.

5.4.2 Simulation Results

The new Adaptive Robust Controller designed based on the newly derived simpler model is simulated using the complete system model. The simulation is performed for two different desired steering inputs; a sinusoidal (Figure 5.8) and a square wave desired steering position (Figure 5.9) at the output shaft of the steering cylinder. In both scenarios, the ARC position controller is able to closely track the desired steering position despite the unknown pump flow losses.

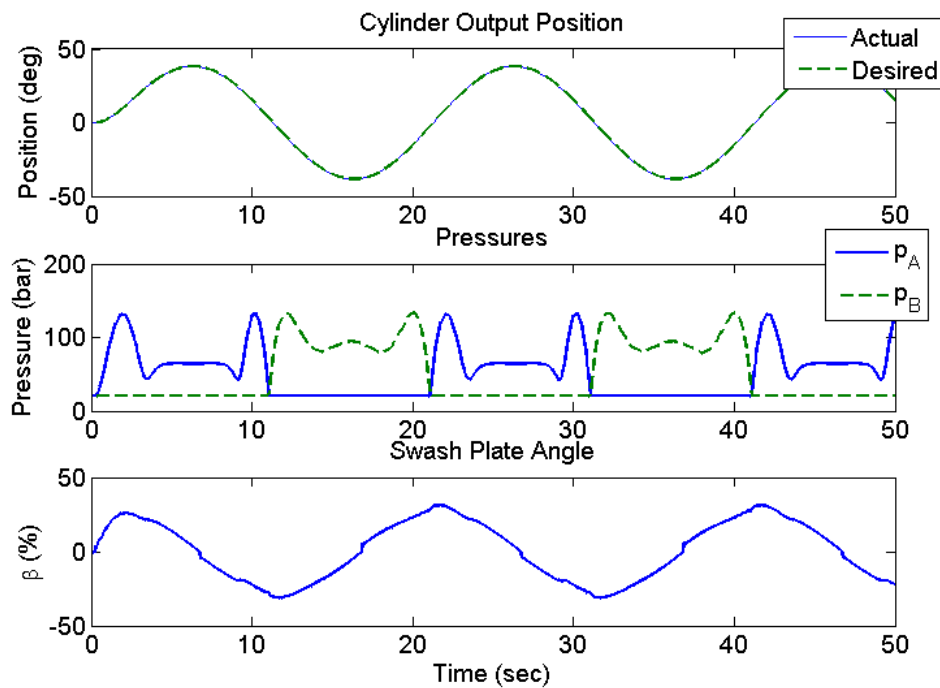


Figure 5.8. Simulation Results for a Sinusoidal Desired Steering Position

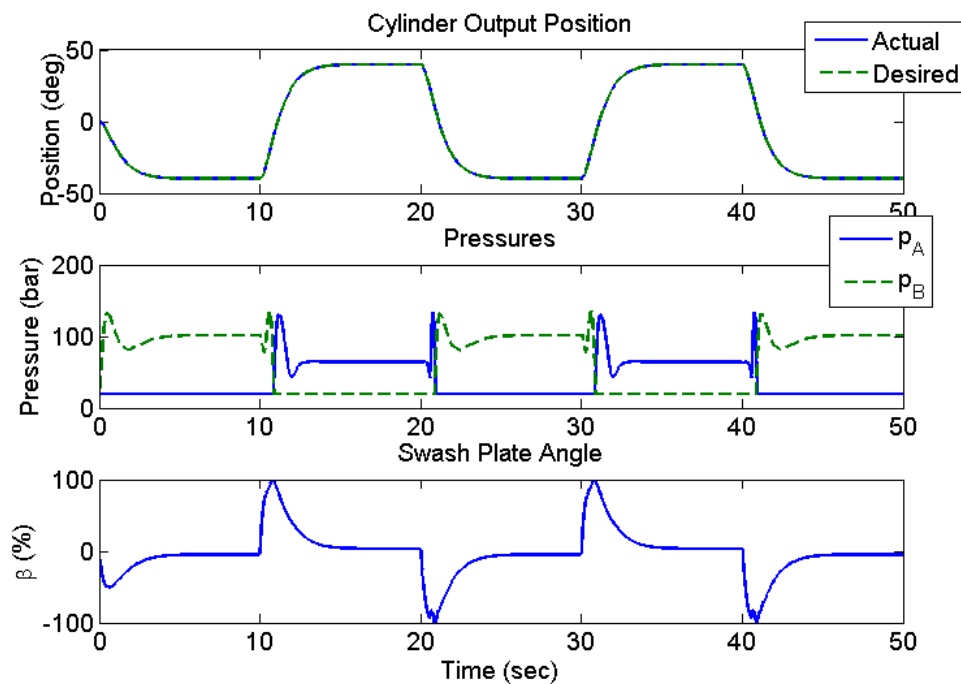


Figure 5.9. Simulation Results for a Square Desired Steering Position

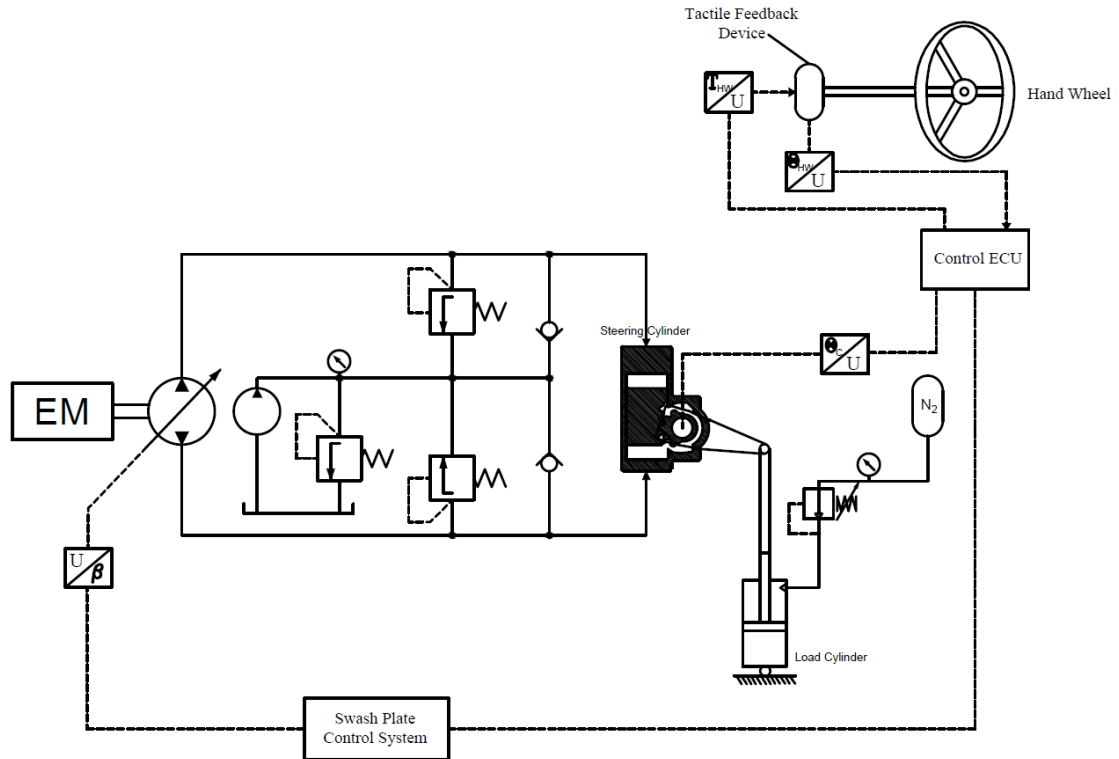


Figure 5.10. Schematics of Experimental Laboratory Setup using Single Rack Cylinder

5.4.3 Laboratory Experimental Results

Single Rack Cylinder Lab Setup

When implementing the simplified ARC control system into the laboratory single rack cylinder test setup (5.10), an excellent position control performance was achieved. As shown in Figure 5.11, the resulting tracking error was within half a degree, 0.5 deg, for the sinusoidal desired steering position. Likewise, a tracking error of less than half a degree was also achieved with the step response performance as shown in Figure 5.12.

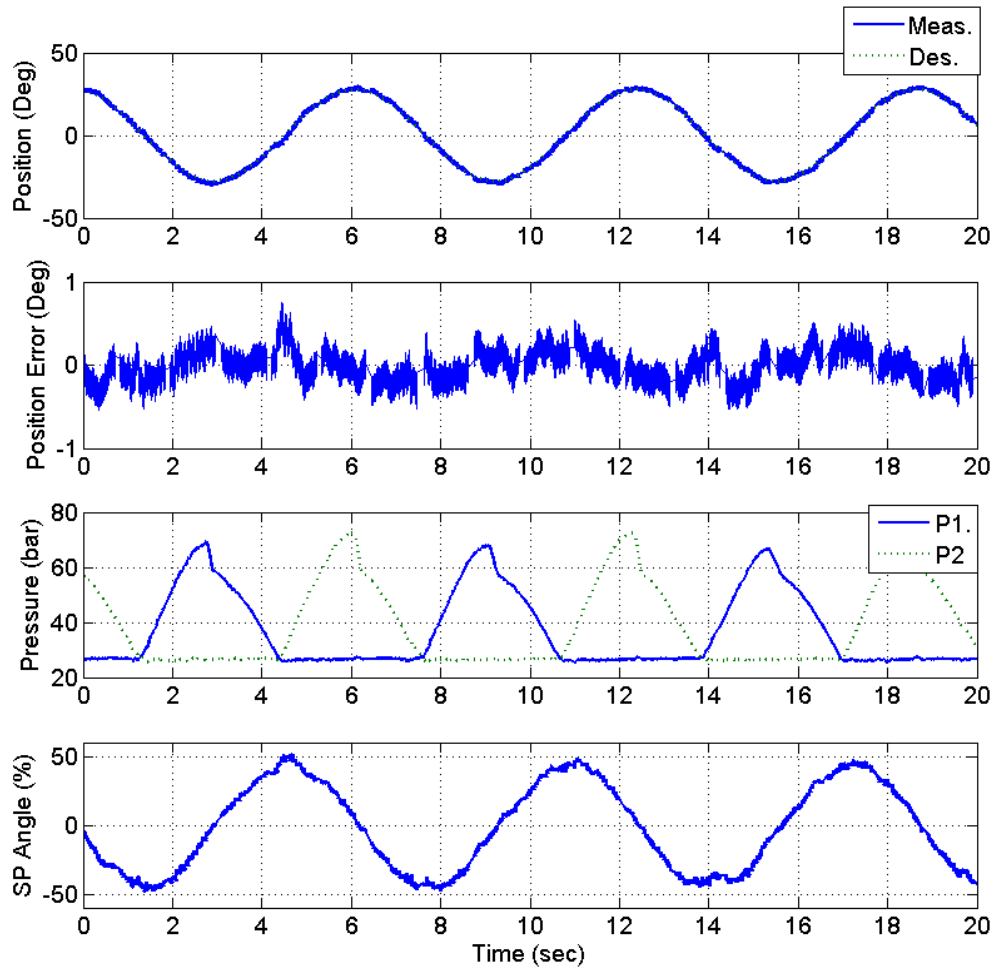


Figure 5.11. Single Rack Experimental Results for a Sinusoidal Wave Desired Steering Position

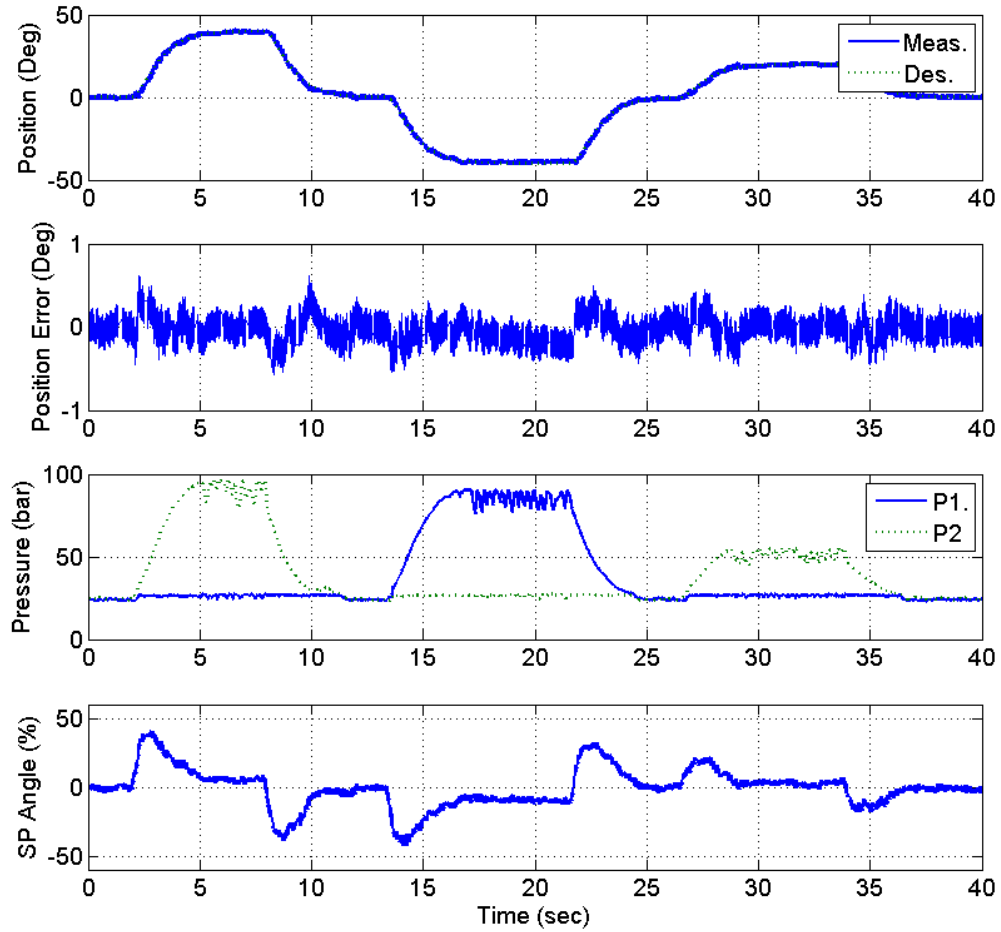


Figure 5.12. Single Rack Experimental Results for a Square Wave Desired Steering Position

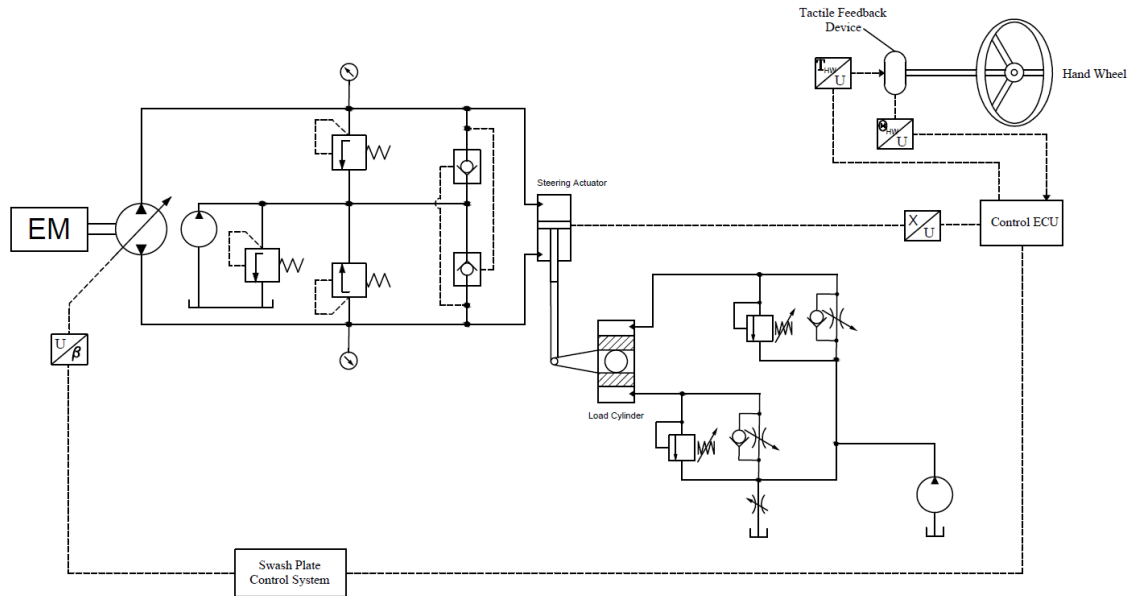


Figure 5.13. Schematics of Experimental Laboratory Setup using Linear Cylinder

Linear Cylinder Lab Setup

Similarly, when using the simplified ARC control system with the laboratory linear cylinder test setup (Figure 5.13), an excellent tracking performance was achieved. As shown in Figure 5.14, the tracking error was within one millimeter for the sinusoidal desired steering position, and even less than a millimeter at steady-state, as shown in Figure 5.15 with the step steering response performance.

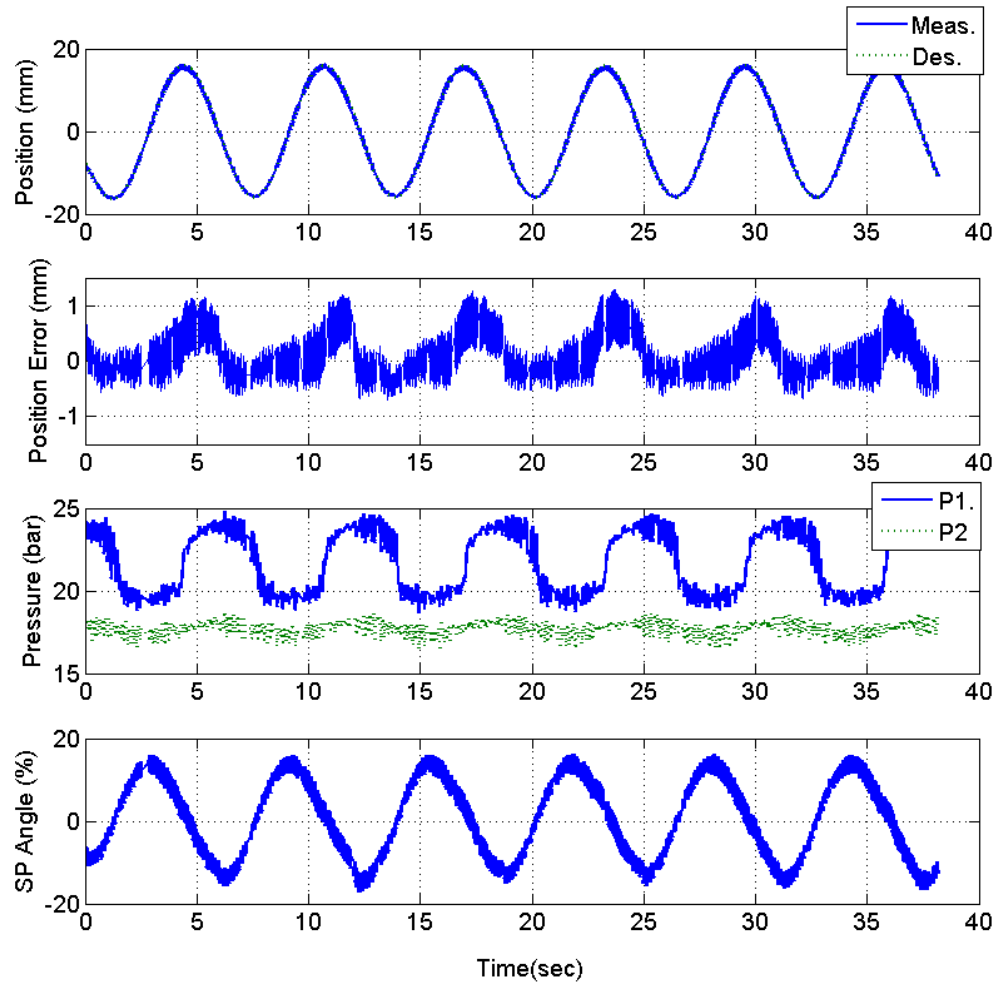


Figure 5.14. Experimental Results for a Sinusoidal Wave Desired Steering Position.

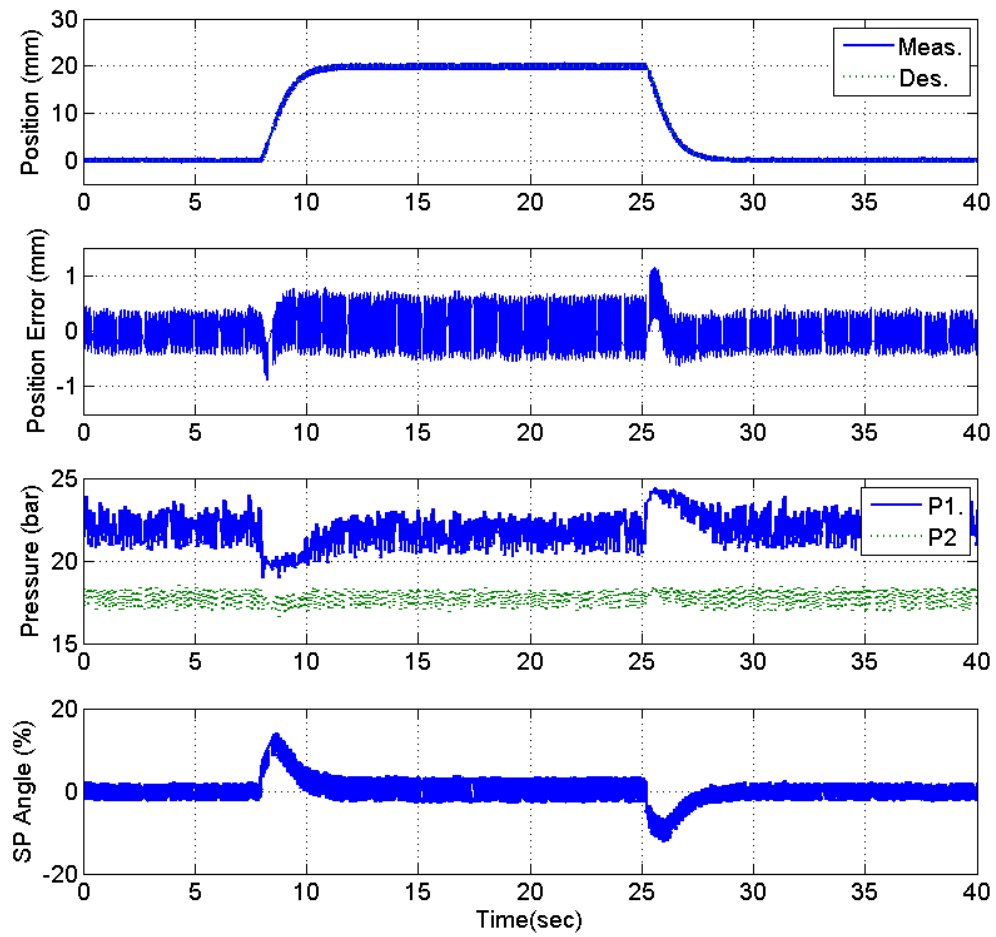


Figure 5.15. Experimental Results for a Filtered Step Desired Steering Position

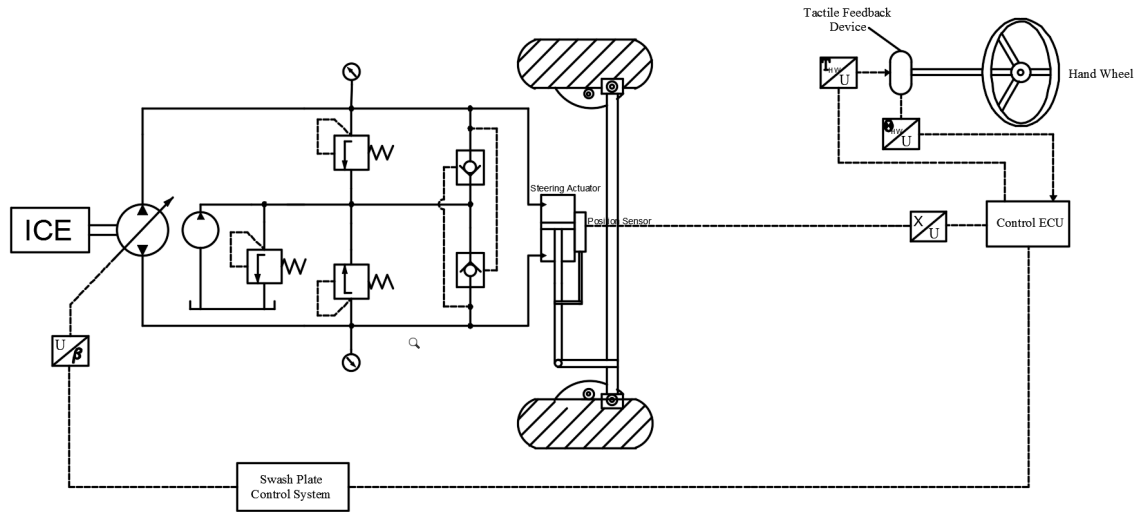


Figure 5.16. Experimental Vehicle Setup Schematics

5.4.4 Vehicle Experimental Results

When implemented on the vehicle (Figure 5.16), the DC steer-by-wire ARC control system performed just as well as in the lab setup. Performance of the system under different steering and driving conditions was analyzed. Figure 5.17 shows the performance of the system during a low speed double lane change maneuver where the steering position tracking remained well below one millimeter throughout the maneuver, highlighting the high accuracy of the ARC control system.

Similarly, when performing a static steer (stand still) maneuver which is considered the worst case scenario for a steering system due to the high static friction forces between the tires and ground, the steering position error still remained below 1 mm during transients and less 0.2 mm at steady state (Figure 5.18).

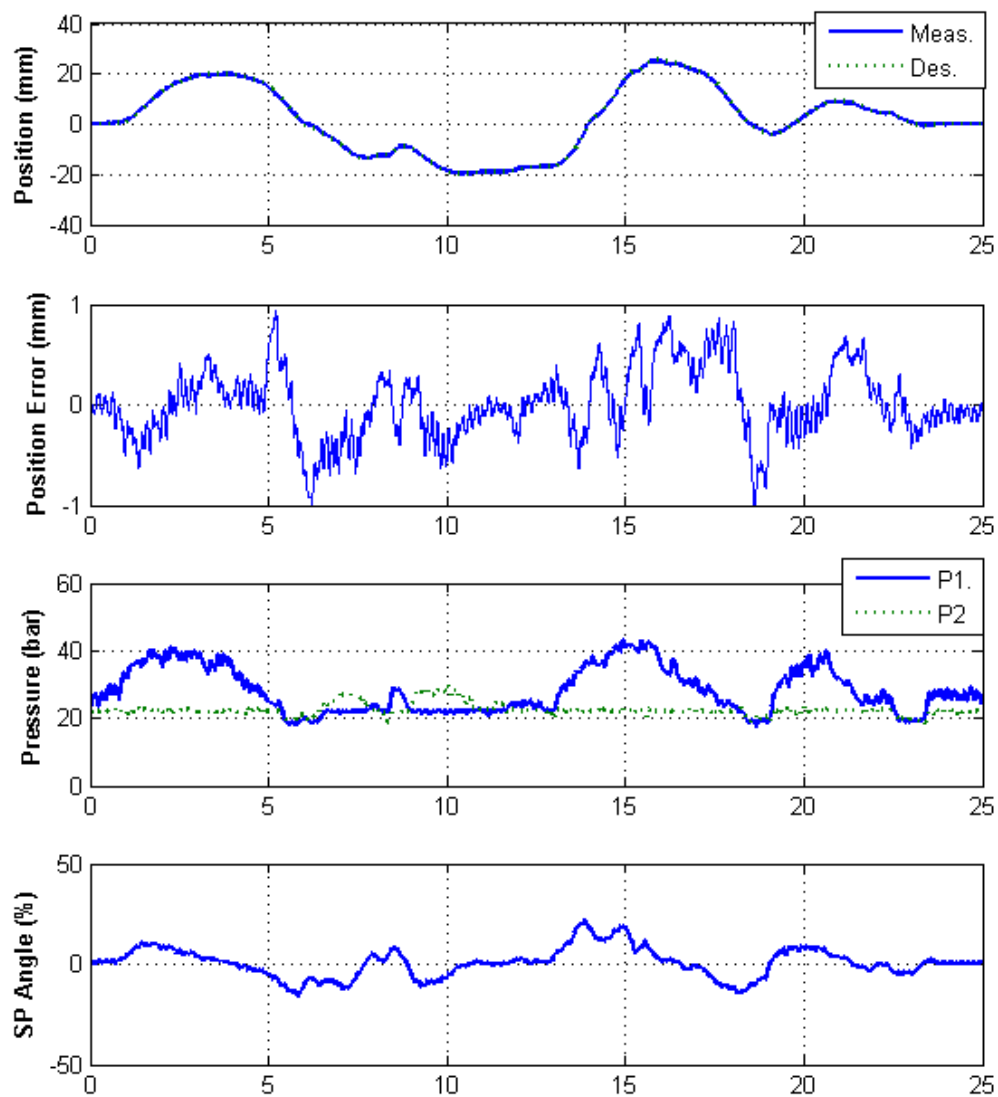


Figure 5.17. Experimental Results for a Low Speed Double Lane Change Maneuver

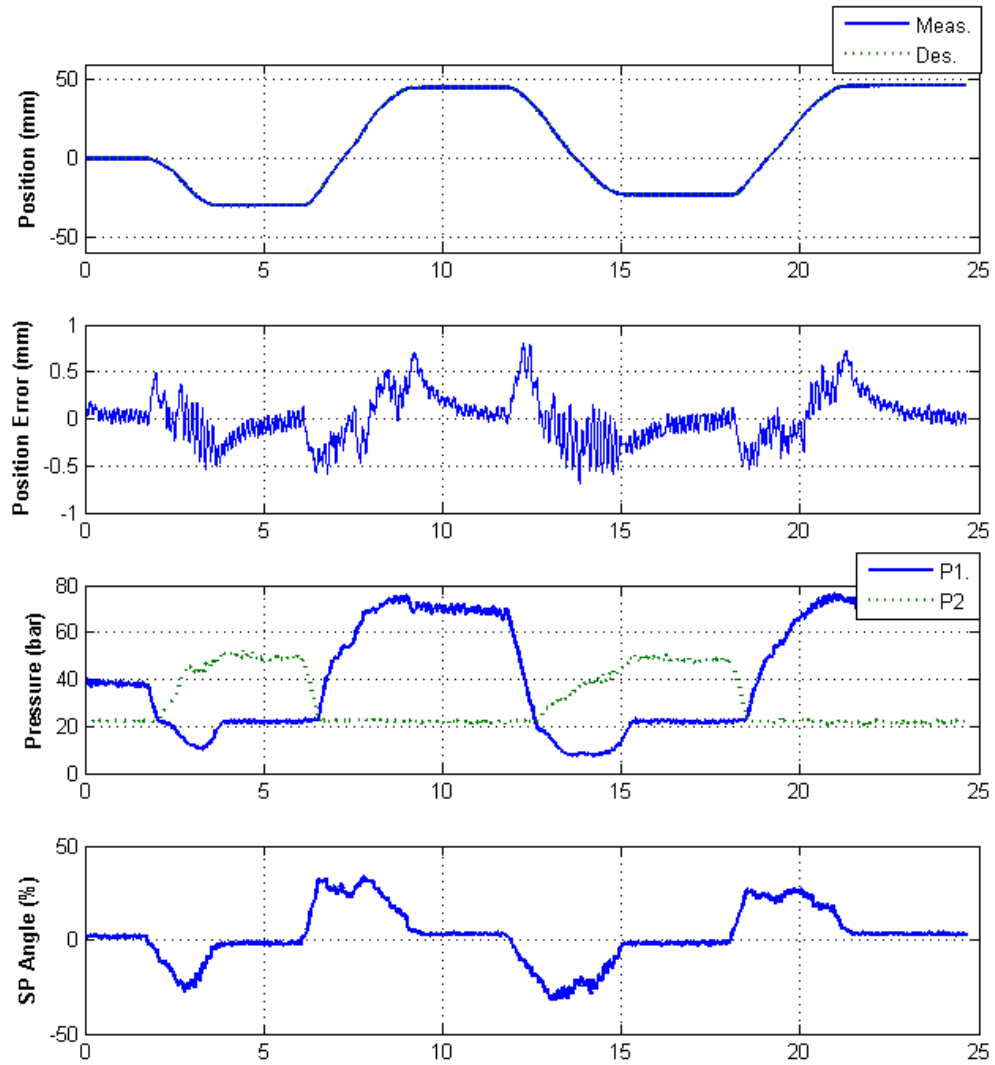


Figure 5.18. Experimental Results for a Static Steering Maneuver (Dry Park)

5.5 Performance of the Adaptive Robust Control System

As previously mentioned, the Adaptive Robust Control (ARC) system was chosen for its consistent high accuracy control that is needed for on-highway vehicles to maintain a straight lane. Such accuracy was demonstrated on the laboratory setup as well as on the test vehicle. One might wonder, however, whether a simpler control system such as a PID would have resulted in good enough control accuracy. That might be the case for a system with a particular set of hardware, for example, or under specific conditions. However, the ARC's performance stands out due to its ability to adapt and compensate for different conditions. Whether it's changes over time due to wear and tear that could worsen a pump's flow losses, or differences in pumps' performance due to manufacturing imprecisions, the ARC is able to adapt and compensate for these changes when a PID may not, at least not with the same high control accuracy.

Furthermore, the ARC control system was designed based on a very simple first order model which was obtained by simplifying a more complex model based on a set of assumptions valid throughout the range of operating conditions that the steering system will undergo. Specifically, the low compliance of the hydraulic system made it such that the effect of the external load on the position response of the steering system is negligible. Moreover, the relatively slow response of steering systems allowed for the effects of inertia and viscous damping on the position response to pump flow to be neglected as well. As a result, a simple first order system model was enough to describe the performance of the steering system. Accordingly, the resulting ARC control system was simple with only one unknown parameter, η_1 , to estimate and one unknown nonlinearity, d , for which to compensate. Consequently, tuning the ARC is not any more complicated than tuning a PID control system. In fact, one might argue that the ARC is easier to tune as the effect of each control parameter on the system is easier to understand and predict due to the simplicity of the model, and the architecture of the ARC itself which decouples the adaptation task from robustness.

Looking closely at the performance of the ARC system in Figure 5.19, one can see that the feed-forward term, β_a , constitutes the majority of the control input, $\beta = \beta_a + \beta_s$. This means that the ARC is able to estimate the unknown parameters using the adaptation law and directly compensate for them through feed-forward control, i.e. β_a . As a result, the feedback control term, β_s , does minimal work and the ARC system is able to track the desired steering inputs without using high feedback gains, and thus without the need for expensive high bandwidth actuators. The feedback term's main role is to keep the system stable using linear feedback, and compensate for model uncertainty, particularly, during the transients when the unknown parameters' estimates have not converged yet. As predicted by the theory (Theorem 2.A), such control strategy has resulted in a bounded error signal which led to a very high control accuracy of steering position during both transient (< 1 mm) and steady state (< 0.2 mm) (Figure 5.19). Although, in theory, the error can be made arbitrarily small by the decreasing the parameters, ϵ_1 . In practice, there is a limit below which the control signal starts to chatter due to amplification of noise in the measured signals.

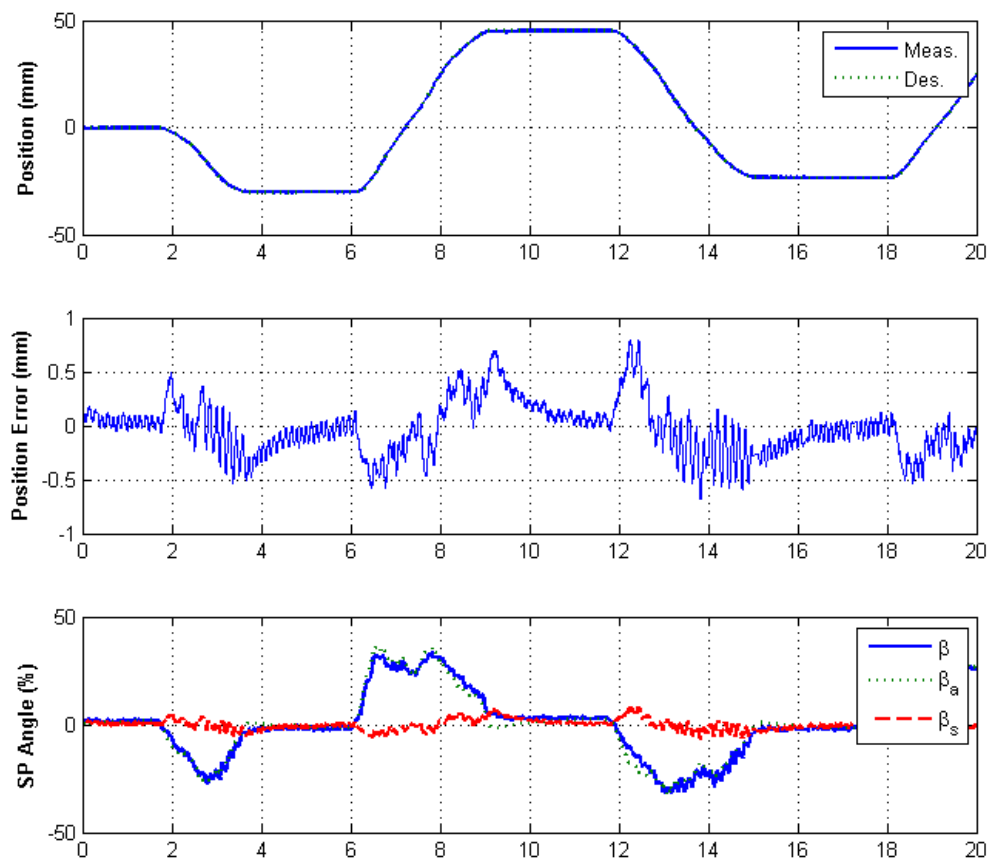


Figure 5.19. Performance of the ARC System

6. STEER-BY-WIRE FAIL SAFE MECHANISM

Having proved the feasibility the DC steer-by-wire for on-highway commercial vehicles in simulation and experimentally on a laboratory setup and on a test vehicle, the next logical step is to ensure that when a failure occurs the system enters a safe state. Due to the absence of the mechanical link between the hand-wheel and road wheels, a failure in the steering system can lead to the vehicle becoming uncontrollable in the lateral direction. As a result, when using a vehicle equipped with a steer-by-wire system on roads shared with other motorists, the steering system must be designed to fail safely. In other words, should any failure occur in the steering system, the driver shall be able to remain in control of the vehicle and steer it to safety and away from any danger to the driver and other motorists.

Failures in the steer-by-wire system can be the result of different potential issues. One of the most critical failures is a loss of power which in a hydraulic steer-by-wire system can be the result of a hydraulic failure, e.g. loss of pump flow, or an electrical failure that can lead to inability to actuate the pump or any other electrical devices on which the system relies, e.g control valve. Furthermore, a failure in the system's communication network, e.g CAN bus, can also lead to a complete failure in the steer-by-wire system.

Consequently, in this chapter, we research and propose different fail-safe concepts that allow the vehicle to remain controllable should a failure occur in the DC steer-by-wire system.

6.1 Fail-Safe Using a Clutch Mechanism:

One simple design to deal with potential loss of power in a steer-by-wire system is to use a clutch mechanism to mechanically connect the steering wheel to the road

wheels in the event of a failure. A version of this concept was proposed by Nissan in [42], and ZF in [43]. As such, the system becomes a manual steering system and allows the driver to safely steer the vehicle to safety. However, in heavy commercial vehicles such as the American class 8 tractor, manual steering can still be a difficult task, particularly at lower speeds, and nearly impossible at stand still. As a result, when using the clutch mechanism to steer the vehicle after a failure event, the driver should be aware of the limitations of the manual steering system.

Moreover, in order to implement the clutch fail-safe mechanism, the steering cylinder should be able to mechanically transfer the steering wheel motion to the road wheels. When using the single-rack hydraulic cylinder configuration as presented in Chapter 3, this can be achieved using the conventional steering gear in which a worm screw mechanically connects the input on the steering gear to its output (Figure 6.1). On the other hand, when using the linear cylinder steer-by-wire configuration, the fail-safe clutch mechanism can be implemented with a manual steering gearbox in parallel with the linear steering cylinder (Figure 6.2).

6.2 Fail-Safe Using Redundant Independent Steering Systems:

Having a redundant steering system is one solution to dealing with failures in the steer-by-wire system. Redundancy can be introduced by implementing an independent secondary steer-by-wire system either on the same steered front axle, or on a different steerable axle, e.g. rear axle steering. However, for the primary and secondary steering systems to be truly independent of each other, they must have different power sources. For example, the primary steering system can have a pump driven by the engine while the secondary system can be equipped with a pump driven by an electric motor that is activated when needed. As a result, a loss of power due an engine failure can be mitigated by the secondary steering system. Moreover, in order to mitigate any electrical failures in one of the systems, both steering systems should have independent electrical systems, e.g. different batteries to power their electron-

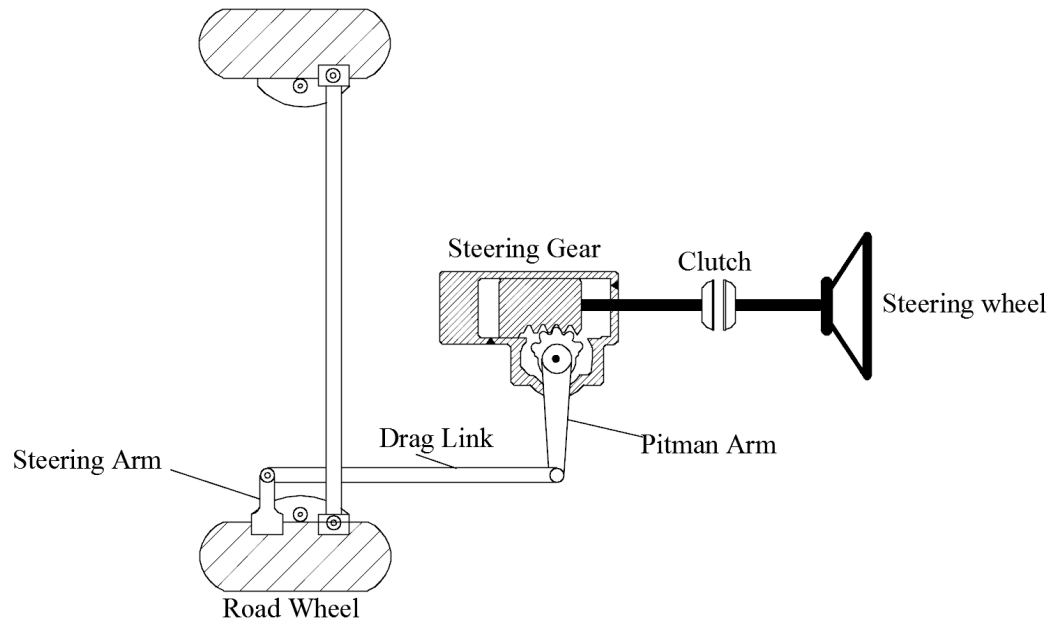


Figure 6.1. Fail-Safe Mechanism using Clutch with Modified Steering Gear.

ics, different sensors to measure their current state, and independent communication networks to relay information between system components.

One advantage of having the secondary steering system on a different axle, particularly the rear axle, is the added benefits of increased maneuverability of the vehicle, and reduction in tire wear which help justify the increased cost of the system with the added redundancy. Steering the rear axle of a vehicle helps reduce its turning radius which can be very useful when driving in urban environments such as in the narrow streets of European cities. Furthermore, steering the rear axle of the vehicle, rather than dragging it against the pavement as in conventional long wheel base vehicles, also helps reduce tire wear [44], and thus reducing vehicle maintenance costs.

Nonetheless, these advantages are not achievable in all vehicle configurations. For example, in a tractor-trailer combination, the vehicle spends most of its lifetime driving straight on highways. Consequently, steering its other axles will not result in any significant reduction in tire wear, while the improved maneuverability is unnec-

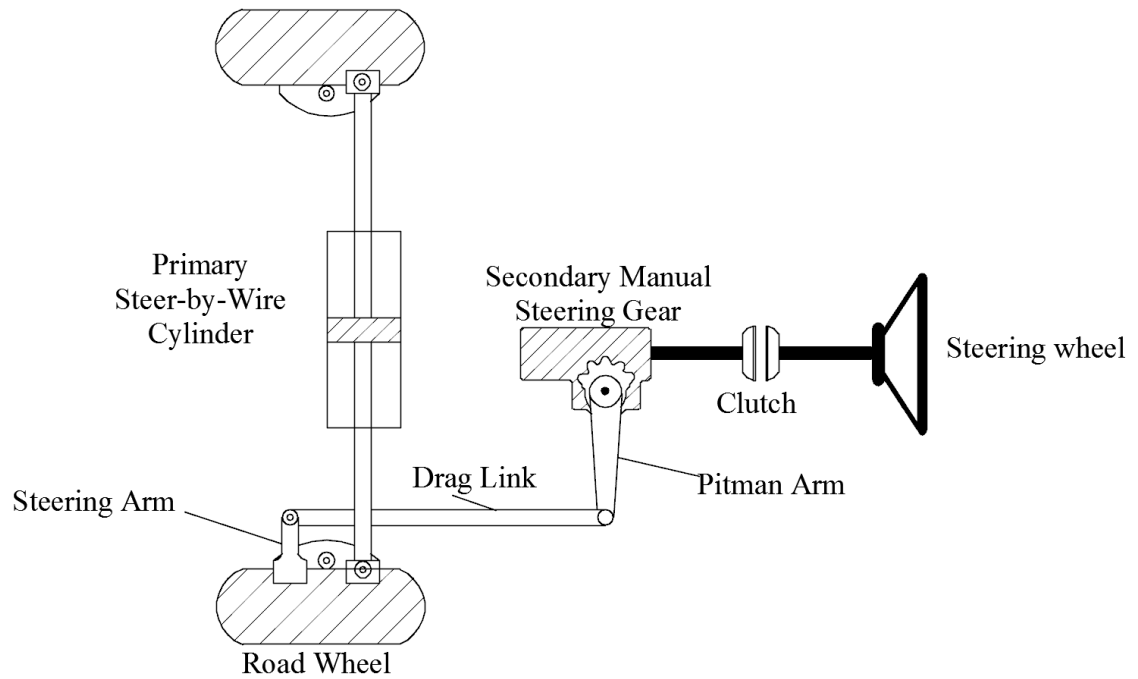


Figure 6.2. Fail-Safe Mechanism using Clutch with Linear Acting Cylinder

essary in these applications as they spend most of their duty cycle on highways. In such cases, other fail-safe mechanisms might prove more viable, e.g. using clutch mechanism.

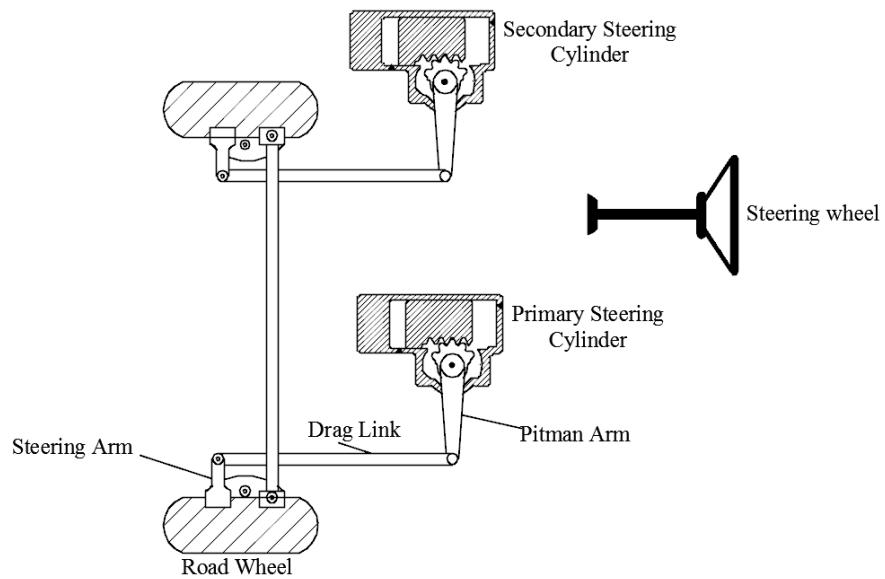


Figure 6.3. Fail-Safe Mechanism using Redundant Steering on the Same Axle

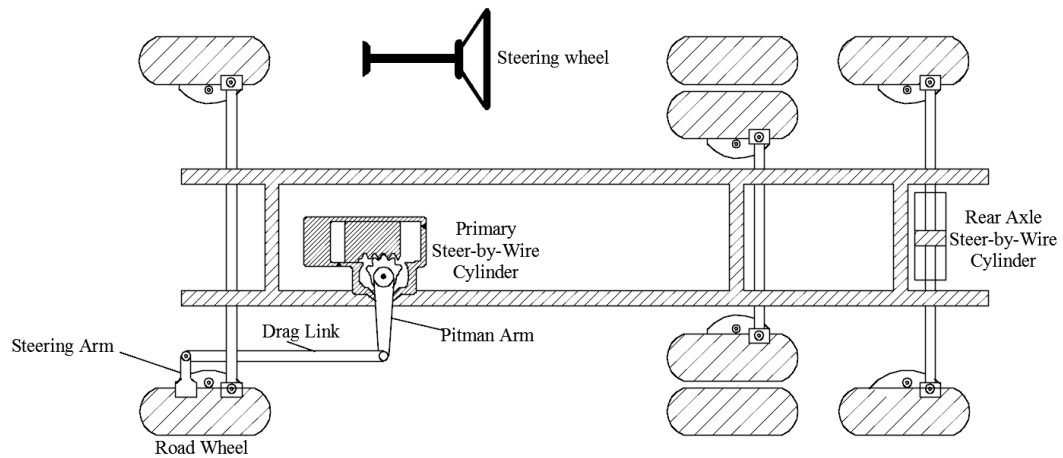


Figure 6.4. Fail-Safe Mechanism using Redundant Steering on the Rear Axle

6.2.1 Implementation of Rear Axle Steering As Fail-Safe Mechanism:

When a failure is detected in the front axle steering system, the rear axle system is responsible for steering the vehicle and achieving the same response as if the vehicle were steered by the front steering system. Since the fundamental response to steering is a change in heading, i.e. yaw rate, using the vehicle model, the vehicle's yaw rate response to a steering input at the front axle can be established in the form of transfer function. Subsequently, the task at hand would be to manipulate the rear axle steering input to obtain the same yaw rate response as if the vehicle were steered from the front [37].

Starting with the vehicle model equations developed in Chapter 4, which we repeat here for convenience:

$$\dot{v}_y = \frac{1}{m_v} \left\{ C_1 \cos(\delta_1) \left[\delta_1 - \arctan\left(\frac{v_y + x_1 \dot{\psi}}{v_x}\right) \right] - C_2 \arctan\left(\frac{v_y + x_2 \dot{\psi}}{v_x}\right) + C_3 \cos(\delta_3) \left[\delta_3 - \arctan\left(\frac{v_y + x_3 \dot{\psi}}{v_x}\right) \right] \right\} - v_x \dot{\psi} \quad (6.1)$$

$$\ddot{\psi} = \frac{1}{I_v} \left\{ x_1 C_1 \cos(\delta_1) \left[\delta_1 - \arctan\left(\frac{v_y + x_1 \dot{\psi}}{v_x}\right) \right] - x_2 C_2 \arctan\left(\frac{v_y + x_2 \dot{\psi}}{v_x}\right) + x_3 C_3 \cos(\delta_3) \left[\delta_3 - \arctan\left(\frac{v_y + x_3 \dot{\psi}}{v_x}\right) \right] \right\} \quad (6.2)$$

We consider the following definitions for brevity [38]:

$$C_a = C_1 + C_2 + C_3 \quad (6.3)$$

$$C_b = x_1 C_1 + x_2 C_2 + x_3 C_3 \quad (6.4)$$

$$C_c = x_1^2 C_1 + x_2^2 C_2 + x_3^2 C_3 \quad (6.5)$$

Making small angle approximations which is a valid assumption for typical on-highway driving conditions, and using the definitions in equations (6.3)-(6.5), the vehicle model equations are rearranged to obtain the linear state-space shown below.

$$\begin{bmatrix} \dot{v}_y \\ \dot{r} \\ \dot{\psi} \\ \dot{y} \end{bmatrix} = \begin{bmatrix} \frac{-C_1-C_2-C_3}{m_v v_x} & \frac{-x_1 C_1 - x_2 C_2 - x_3 C_3}{m_v v_x^2} - v_x & 0 & 0 \\ \frac{-x_1 C_1 - x_2 C_2 - x_3 C_3}{I_v} & \frac{-x_1^2 C_1 - x_2^2 C_2 - x_3^2 C_3}{I_v v_x} & 0 & 0 \\ 0 & 1 & 0 & 0 \\ 1 & 0 & v_x & 0 \end{bmatrix} \begin{bmatrix} v_y \\ r \\ \psi \\ y \end{bmatrix} + \begin{bmatrix} \frac{C_1}{m_v} & \frac{C_3}{m_v} \\ \frac{x_1 C_1}{I_v} & \frac{x_3 C_3}{I_v} \\ 0 & 0 \\ 0 & 0 \end{bmatrix} \begin{bmatrix} \delta_1 \\ \delta_3 \end{bmatrix} \quad (6.6)$$

Using the Laplace transform on the derived state-space model above, the response of the vehicle's yaw rate, r lateral velocity, v_y , heading, ψ , and lateral position, y , can be expressed in terms of the steering inputs δ_1 and δ_3 as shown in [37].

$$r(s) = \frac{C_1 v_x (s x_1 m_v v_x + x_1 C_a - C_b) \delta_1(s) + C_3 v_x (s x_3 m_v v_x + x_3 C_a - C_b) \delta_3(s)}{s^2 m_v v_x^2 I_v + s v_x (m_v C_c + I C_a) + C_a C_c - C_b^2 - C_b m_v v_x^2} \quad (6.7)$$

$$\psi(s) = \frac{C_1 v_x (s x_1 m_v v_x + x_1 C_a - C_b) \delta_1(s) + C_3 v_x (s x_3 m_v v_x + x_3 C_a - C_b) \delta_3(s)}{s (s^2 m_v v_x^2 I_v + s v_x (m_v C_c + I C_a) + C_a C_c - C_b^2 - C_b m_v v_x^2)} \quad (6.8)$$

$$v_y(s) = \frac{v_x C_1 (s I_v v_x + C_c - x_1 (C_b + m_v v_x^2)) \delta_1(s)}{s^2 m_v v_x^2 I_v + s v_x (m_v C_c + I C_a) + C_a C_c - C_b^2 - C_b m_v v_x^2} \quad (6.9)$$

$$+ \frac{v_x C_3 (s I_v v_x + C_c - x_3 (C_b + m_v v_x^2)) \delta_3(s)}{s^2 m_v v_x^2 I_v + s v_x (m_v C_c + I C_a) + C_a C_c - C_b^2 - C_b m_v v_x^2} \quad (6.10)$$

$$y(s) = \frac{C_1 v_x (s^2 I_v v_x + s (C_c - x_1 C_b) + x_1 v_x C_a - v_x C_b) \delta_1(s)}{s^2 (s^2 m_v v_x^2 I_v + s v_x (m_v C_c + I C_a) + C_a C_c - C_b^2 - C_b m_v v_x^2)} + \frac{C_3 v_x (s^2 I_v v_x + s (C_c - x_3 C_b) + x_3 v_x C_a - v_x C_b) \delta_3(s)}{s^2 (s^2 m_v v_x^2 I_v + s v_x (m_v C_c + I C_a) + C_a C_c - C_b^2 - C_b m_v v_x^2)} \quad (6.11)$$

As the objective here is to use the rear-axle steering system to achieve the same yaw response as if the vehicle were steered from the front, first the desired yaw rate response to a steering input from the front is characterized by taking equation (6.7) and setting the steering input of the rear-axle to zero, i.e. $\delta_3 = 0$:

$$\frac{r(s)}{\delta_c(s)} = \frac{C_1 v_x (s x_1 m_v v_x + x_1 C_a - C_b)}{s^2 m_v v_x^2 I_v + s v_x (m_v C_c + I C_a) + C_a C_c - C_b^2 - C_b m_v v_x^2} \quad (6.12)$$

Where $\delta_c = \delta_1$ is the steering command from the driver whose intent is to steer the wheels on the front axle. δ_c will then be used to generate a steering command, δ_3 , at the rear axle which should result in the desired yaw rate response shown in equation (6.12).

The yaw response of the vehicle to a steering input from the rear, δ_3 , depends on whether or not the front axle wheels are generating side forces. Two different scenarios are explored here: (1) the front tires are locked in the straight-ahead position, i.e. $\delta_1 = 0$, and as a result, are able to generate cornering forces at the front axle, and (2) just like the front wheels of a shopping cart, the front tires of the vehicle are allowed to freely pivot without any constraints, and therefore, do not generate any side forces, i.e. $C_1 = 0$. This is also referred as caster steering.

Scenario 1: Front Wheel Locked at Straight-Ahead

Setting $\delta_1 = 0$ in the general yaw rate response equation (6.7) yields the vehicle's yaw rate response to a steering input from the rear axle:

$$\frac{r(s)}{\delta_3(s)} = \frac{C_3 v_x (s x_3 m_v v_x + x_3 C_a - C_b)}{s^2 m_v v_x^2 I_v + s v_x (m_v C_c + I C_a) + C_a C_c - C_b^2 - C_b m_v v_x^2} \quad (6.13)$$

The goal here is to take the yaw rate response to a rear steering input, $\frac{r(s)}{\delta_3(s)}$, and determine the transfer function, $\frac{\delta_3(s)}{\delta_c(s)}$, by which it needs to be multiplied to obtain the yaw rate response that the driver would be expecting if he or she were to steer the front axle, $\frac{r(s)}{\delta_c(s)}$, that is:

$$\frac{r(s)}{\delta_3(s)} \frac{\delta_3(s)}{\delta_c(s)} = \frac{r(s)}{\delta_c(s)} \quad (6.14)$$

Equation (6.14) is then solved for $\frac{\delta_3(s)}{\delta_c(s)}$:

$$\frac{\delta_3(s)}{\delta_c(s)} = \frac{r(s)}{\delta_1(s)} \left(\frac{r(s)}{\delta_3(s)} \right)^{-1} = \frac{C_1 x_1 (s m_v v_x + C_a - \frac{C_b}{x_1})}{C_3 x_3 (s m_v v_x + C_a - \frac{C_b}{x_3})} \quad (6.15)$$

Which then results in the desired steering input at the rear axle, δ_3 :

$$\delta_3(s) = \frac{C_1 x_1 (s m_v v_x + C_a - \frac{C_b}{x_1})}{C_3 x_3 (s m_v v_x + C_a - \frac{C_b}{x_3})} \delta_c \quad (6.16)$$

Equation (6.16) represents the necessary steering input at the rear axle, δ_3 , that will result in the same yaw rate response the driver would expect if the vehicle were steered from the front.

If the yaw rate responses for steering the vehicle from the front and the rear are identical, then so are their time integrals, i.e. heading responses. On the other hand, it has been shown in [37] that the other vehicle state variables, namely, lateral velocity and position, while they do not match the desired response of the front steered vehicle, they do start to converge toward it at higher speeds if the vehicle is neutrally steered, i.e. $C_b = 0$, and balanced, i.e. $x_1 = -x_3$.

Simulation Results:

Using the previously built vehicle model simulation program and subjecting it to a sinusoidal driver steering command, δ_c . The steering input at the front wheels, δ_1 , was set to 0 to simulate the front wheels being locked in the straight-ahead position. The driver steering intent, δ_c , was then processed by the transfer function described in equation (6.16) which generated a steering input at the rear axle, δ_3 . As shown in Figure 6.5, the resulting yaw rate response was identical to what the vehicle would exhibit if it were steered with the same driver steering command at the front axle. It can also be seen that, as expected, the steering input at the rear is in the opposite direction as the driver steering input.

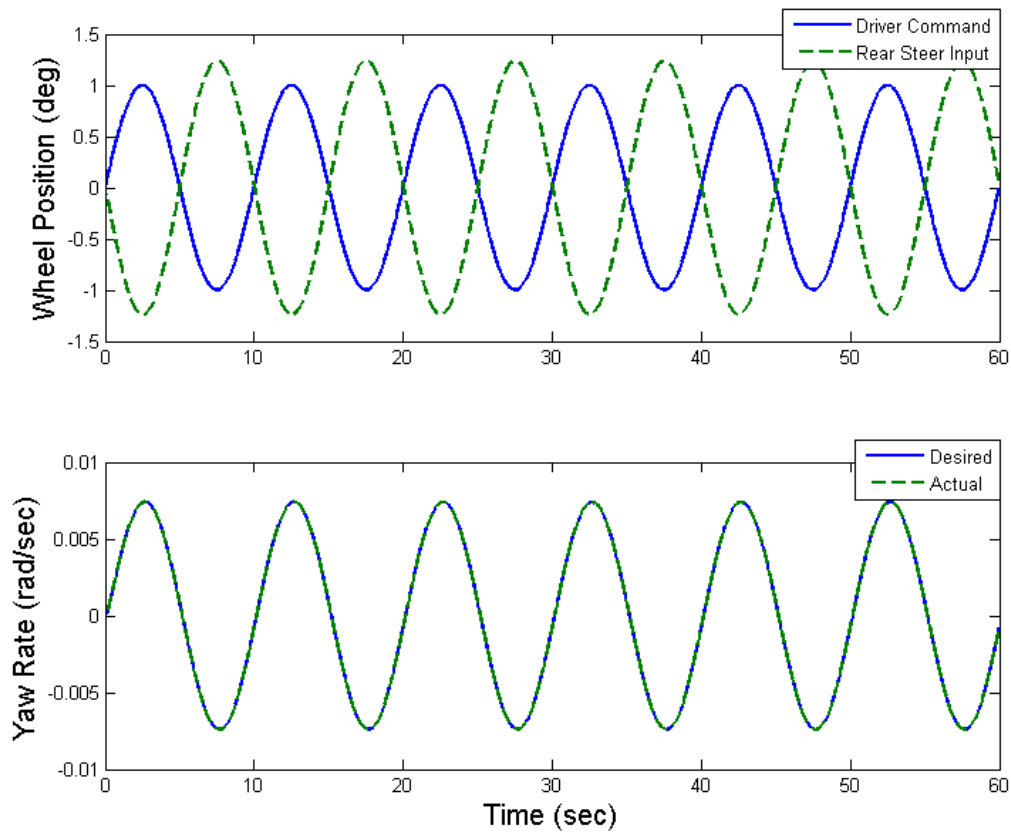


Figure 6.5. Vehicle Yaw Rate Simulation Response when Rear Wheels Steered and Front Wheels Locked in Straight-Ahead Position

Scenario 2: Caster Steered Front:

When the front wheels are allowed to freely pivot, they do not generate side forces. As a result, C_1 can be assumed to be null:

$$C_1 = 0 \quad (6.17)$$

Updating the definitions for C_a , C_b , C_c accordingly yields:

$$C'_a = C_2 + C_3 \quad (6.18)$$

$$C'_b = C_2 + x_3 C_3 \quad (6.19)$$

$$C'_c = x_2^2 C_2 + x_3^2 C_3 \quad (6.20)$$

To determine the vehicle's yaw rate response to a rear steering input when the front wheels are castered, equations (6.17)-(6.20) are plugged into equation (6.13):

$$\frac{r(s)}{\delta_3(s)} = \frac{C_3 v_x (s x_3 m_v v_x + x_3 C'_a - C'_b)}{s^2 m_v v_x^2 I_v + s v_x (m_v C'_c + I C'_a) + C_a C'_c - C_b'^2 - C'_b m_v v_x^2} \quad (6.21)$$

Once again, the goal is to process the driver's command, δ_c , and obtain a steering input at the rear axle, δ_3 , such that the yaw rate response is equivalent to that of the vehicle steered by the front wheels. In other words, we need to find the relationship, $\frac{\delta_3(s)}{\delta_c(s)}$ such that the yaw rate response is equivalent to equation (6.12). This can be expressed again mathematically as follows:

$$\frac{r(s)}{\delta_3(s)} \frac{\delta_3(s)}{\delta_c(s)} = \frac{r(s)}{\delta_c(s)} \quad (6.22)$$

As a result,

$$\frac{\delta_3(s)}{\delta_c(s)} = \frac{r(s)}{\delta_1(s)} \left(\frac{r(s)}{\delta_3(s)} \right)^{-1} \quad (6.23)$$

Which yields:

$$\frac{\delta_3(s)}{\delta_c(s)} = \left(\frac{s^2 m_v v_x^2 I_v + s v_x (m_v C'_c + I C'_a) + C_a C'_c - C_b'^2 - C'_b m_v v_x^2}{s^2 m_v v_x^2 I_v + s v_x (m_v C_c + I C_a) + C_a C_c - C_b^2 - C_b m_v v_x^2} \right) \times \left(\frac{C_1 x_1 (s m_v v_x + C_a - \frac{C_b}{x_1})}{C_3 x_3 (s m_v v_x + C'_a - \frac{C'_b}{x_3})} \right) \quad (6.24)$$

Equation (6.24) represents a third order filter which when applied to the driver command will result in a yaw rate response equivalent to (6.12) when the front wheels are caster steered.

Simulation Results:

To simulate the castered front wheels scenario, the front tires cornering stiffness, C_1 , is set to 0. The driver steering input is processed by the transfer function shown

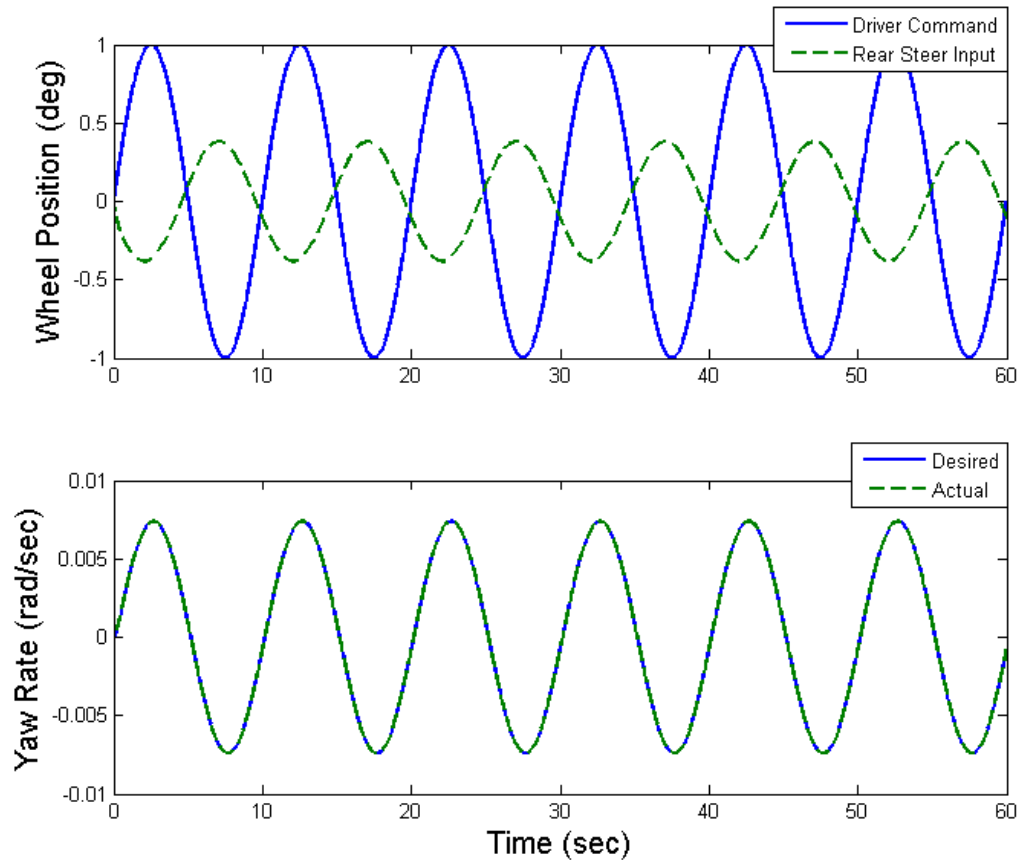


Figure 6.6. Vehicle Yaw Rate Response when Rear Wheels Steered and Castered Front Wheels

in equation (6.24) which generates the appropriate steering input at the rear axle which in turn results in a vehicle yaw rate response identical to the desired yaw rate response (Figure 6.6). It can be seen from the simulation results that the steering input at the rear for the castered front wheels scenario is less than the rear steering input for locked front wheels scenario. This is a result of allowing the front wheels to freely pivot which prevents them from resisting the motion of the vehicle. As a result the rear wheels do not have to compensate for those resisting forces.



Figure 6.7. Test Vehicle Equipped with Rear Axle Steering System

6.2.2 Experimental Results:

A vehicle equipped with a rear axle steering system (Figure 6.7) was used to experimentally validate the proposed fail-safe mechanism presented above. Unlike the front steer-by-wire system, the rear axle steering system is made of an electric motor placed at the input of the steering gear. Steering position commands can be sent to the rear axle via the vehicle CAN communication bus. The presented concept, however, can be implemented with any type of active steering system whether electric or hydraulic. In fact, the same hydraulic DC steer-by-wire system used on the front can be replicated in the rear as long as the power sources, i.e, pump and battery, and communication systems are kept independent between the front and rear steering systems.

Vehicle Model Validation:

As presented above, in order to obtain a yaw response when steering the rear axle similar to that of the vehicle steered from the front, the driver steering command is processed by a transfer function that depends on some vehicle parameters, namely, vehicle mass, m_v , and moment of inertia, I_z , tires' cornering stiffnesses, C_i , and distances between the vehicle axles and its center of gravity, x_1 , x_2 , and x_3 . The vehicle mass and lengths, x_i , can be easily measured. However, the vehicle's moment of inertia depends on the mass and the complex weight distribution of the vehicle, and thus, cannot be directly measured either. Similarly, the tires' cornering stiffnesses are highly dependent on the type of tires used, as well as the load on the tires, and therefore, cannot be directly measured. As a result, these parameters have to be determined empirically.

The previously built vehicle simulation model is again used in an optimization routine that uses previously measured front and rear steering inputs to excite the model. The routine compares the measured and simulated yaw rate responses and accordingly adjusts the unknown parameters, namely the vehicle's moment of inertia and tires' cornering stiffnesses, and runs the simulation again. This process is run iteratively until the optimization routine's cost function is minimized down to a specified tolerance.

In order to obtain a set of model parameters that will represent the behavior of the vehicle's yaw rate response under different conditions, the simulation model is validated using two steering scenarios: (1) steering the front axle and rear axle sequentially, and (2) steering the front and rear axle simultaneously. After running the optimization routine, a set of parameters for the vehicle's moment of inertia and tires' cornering stiffnesses was obtained which resulted in a simulated yaw rate response that closely matches the measured yaw rate of the vehicle for both steering scenarios (Figures 6.8 and 6.9).

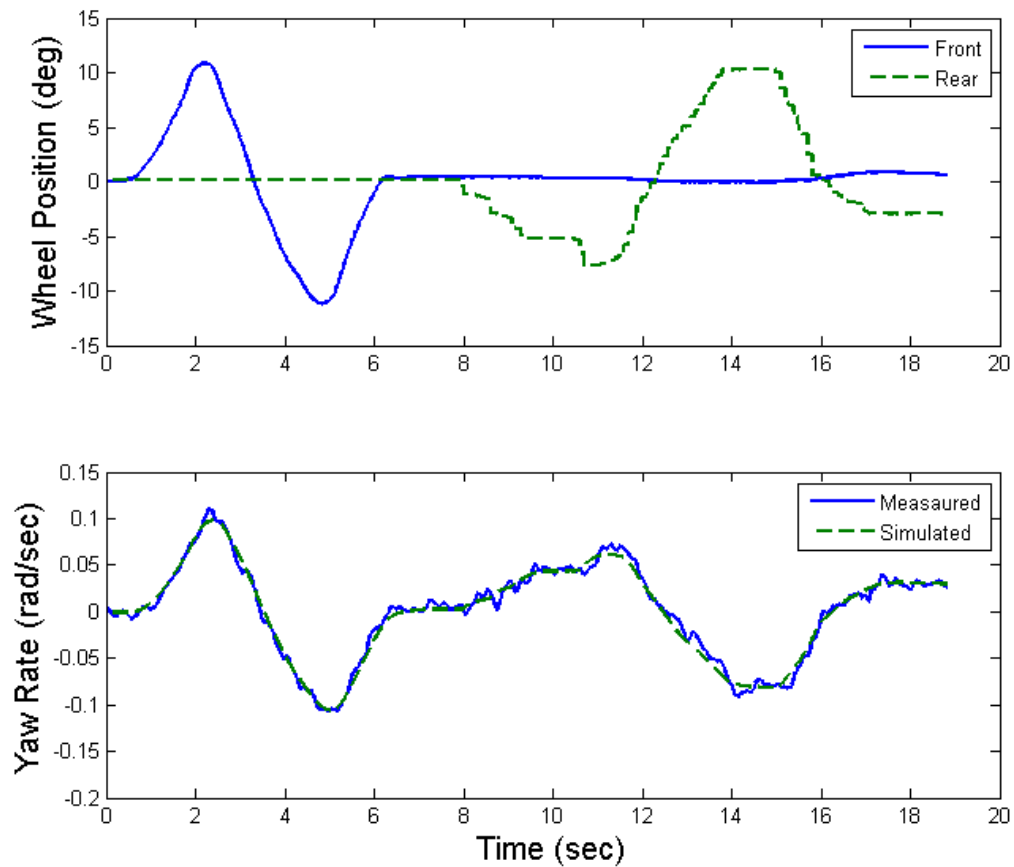


Figure 6.8. Model Validation Results with Front and Rear Steered Sequentially

Once the vehicle model is validated and the necessary parameters needed to implement the fail-safe mechanism using rear axle steering are determined, the validation of the fail-safe mechanism is performed:

Scenario 1: Front Wheel Locked at Straight-Ahead

In this scenario, the front wheels are locked in straight-ahead position and the driver's steering command is processed by the transfer function (Eq. 6.16) which generates a steering input at the rear axle which in theory should result in a yaw rate

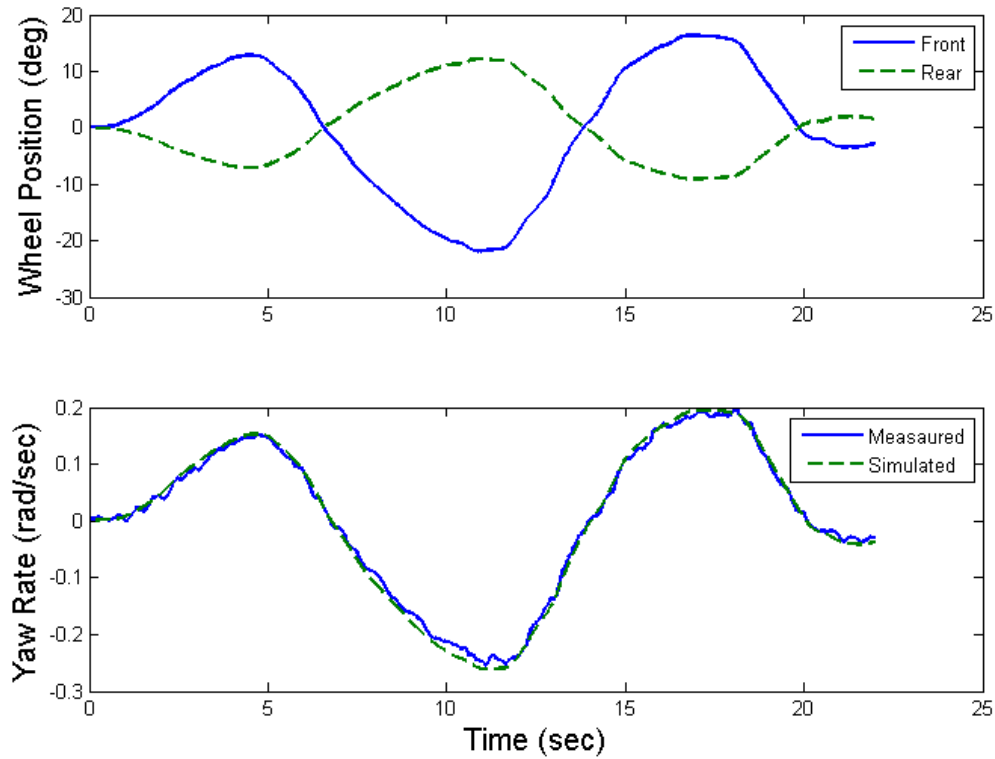


Figure 6.9. Model Validation Results with Front and Rear Steered Simultaneously

response identical to that of a front steering vehicle. For convenience we show that transfer function here again:

$$\delta_3(s) = \frac{C_1 x_1 (s m_v v_x + C_a - \frac{C_b}{x_1})}{C_3 x_3 (s m_v v_x + C_a - \frac{C_b}{x_3})} \delta_c \quad (6.25)$$

To validate the fail-safe mechanism in this scenario, the vehicle is driven on a straight road lane inside a closed low speed test area away from any vehicles. The front wheels are locked in the straight ahead position by commanding a zero position to the front steering system. While moving at low speed, the driver attempts to steer the vehicle to make a double lane change maneuver by steering the hand wheel (which is mechanically disconnected from the front steering system), the fail-safe control system then takes in the driver command and generates a steering command to the rear axle

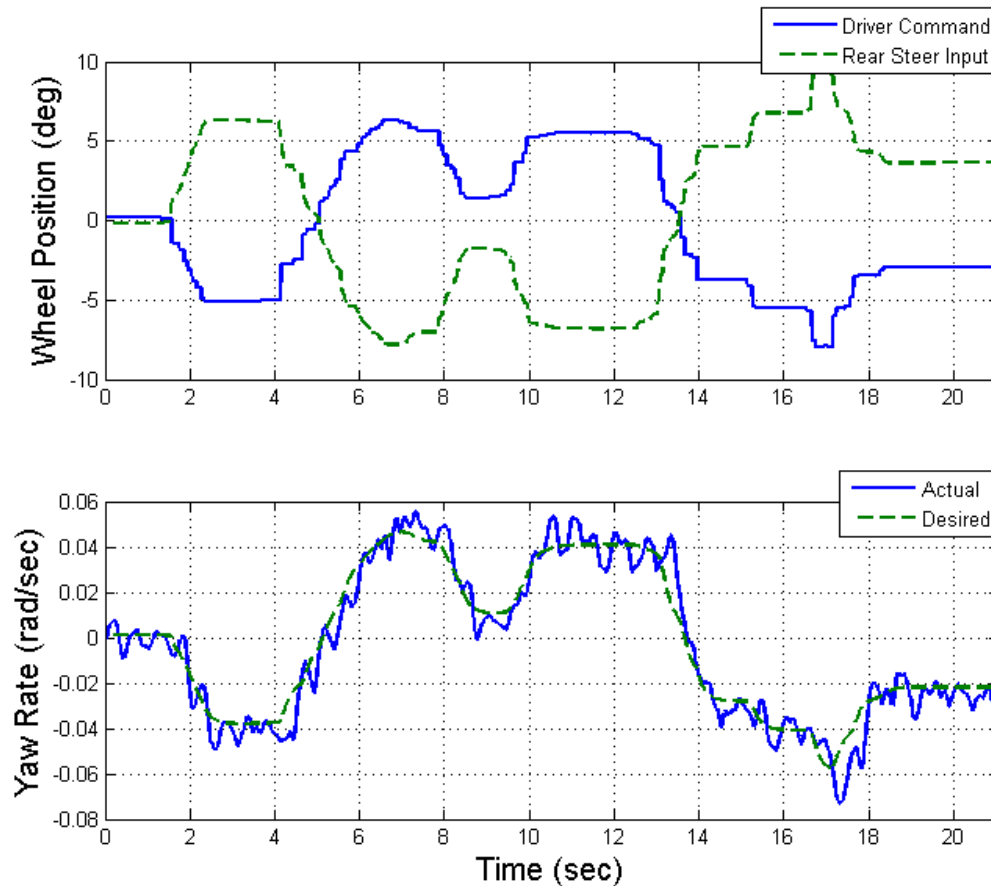


Figure 6.10. Experimental Validation Results for Fail-Safe Using Steering: Typical Steering Maneuvers

using equation (6.25). Figure 6.10 shows the driver command and resulting rear axle steering input. More importantly, it shows that, as predicted, the measured yaw rate response of the vehicle very closely tracks the desired yaw rate (Equation 6.12) which is what the driver would feel if he/she were steering the vehicle from front. This is a major result that shows that, indeed, the rear axle steering system can be used to generate a similar response to that of a front steered vehicle in case of failure of the front steering system.

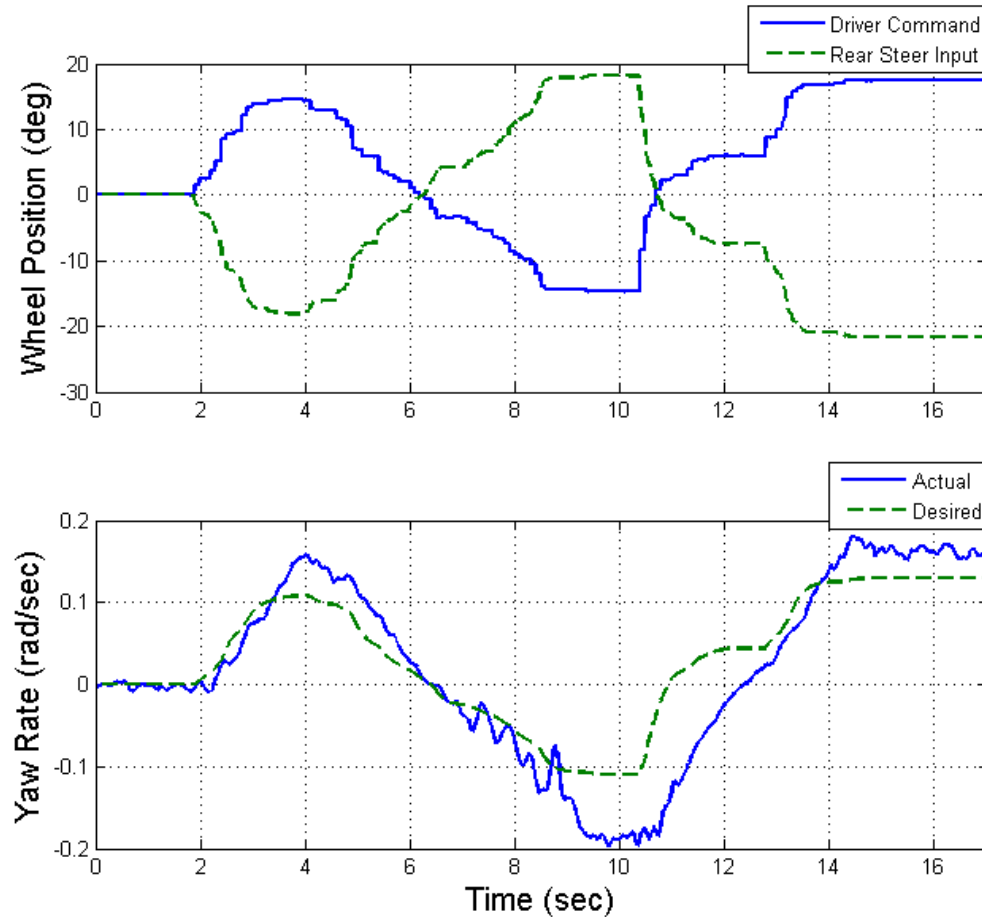


Figure 6.11. Experimental Validation Results for Fail-Safe Using Steering: Large Steering Maneuvers

However, when attempting to make large steering maneuvers, it can be noticed that the measured yaw rate response of the vehicle starts to deviate from the desired yaw rate (Figure 6.11). This is due to the fact that at large slip angles, the tires' cornering forces start to saturate and are no longer proportional to the slip angle. Due to this nonlinear tire behavior, the response of the derived linear model of the vehicle will be different from the actual response of the vehicle.

Up to this point, the strategy for using the rear axle steering system to generate the desired vehicle yaw rate response has been to assume that the vehicle is a linear

system, and to directly use the reciprocal of the yaw rate response transfer function to a front steering input (Eq.6.7) to process the driver steering command to generate the appropriate steering input at the rear axle. This is essentially a feed-forward strategy which only works if the model used exactly describes the plant. However, as with any real-world system, there will always be uncertainties in the model and possible unmodeled dynamics such as the previously observed saturation of the tire forces. Consequently, in order to make the fail-safe mechanism more robust against these deviations from the linear model, a feedback term is added to the rear steering command. This will help minimize the error between the measured and desired yaw rate response and keep the system stable when the vehicle dynamics diverge from the linear model. As a result, the proposed steering input command to the rear axle is of the form:

$$\delta_3(s) = \frac{C_1 x_1 (s m_v v_x + C_a - \frac{C_b}{x_1})}{C_3 x_3 (s m_v v_x + C_a - \frac{C_b}{x_3})} \delta_c + k_{yr} (\dot{\psi}_d - \dot{\psi}) \quad (6.26)$$

Where k_{yr} is the yaw rate feedback gain.

As can be seen from Figure 6.12, the feedback term helps keep the yaw rate response of the vehicle close to the desired yaw rate, and corrects the steering command to the rear axle when necessary to keep the system stable and near the desired response. This is more evident when the driver commands large steering inputs that may cause the tire forces to saturate resulting in the rear axle to start sliding outward. This is effectively a simple stability control system.

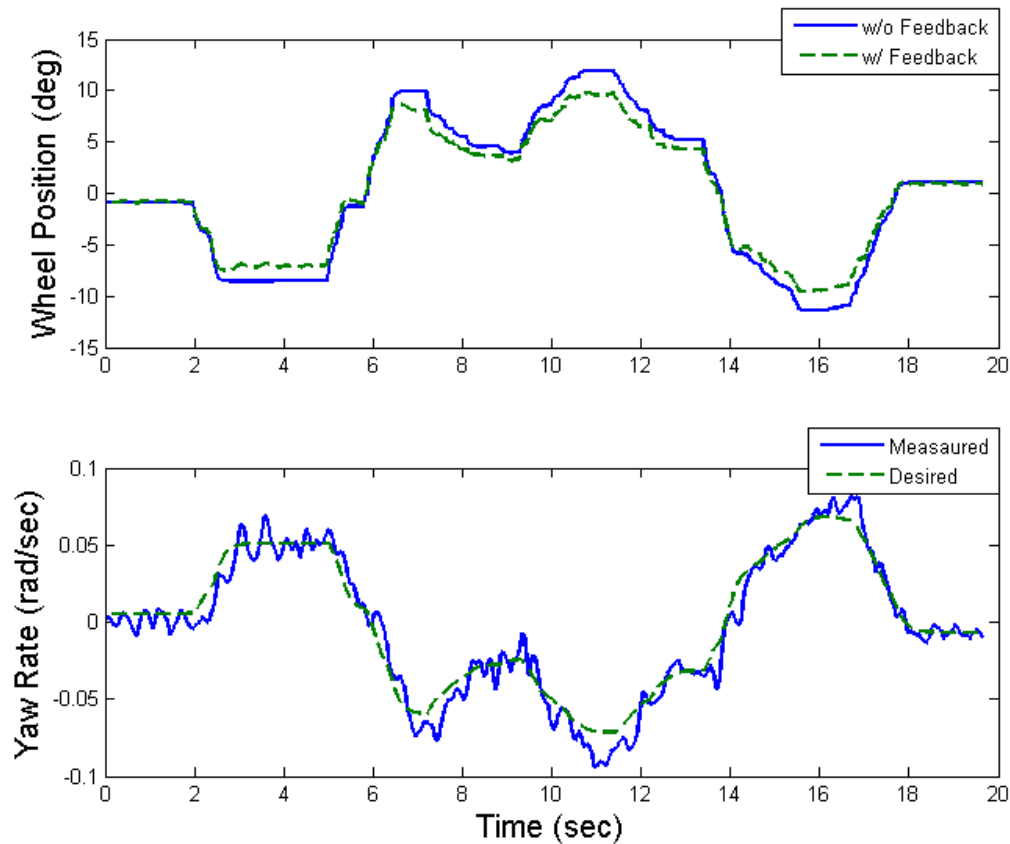


Figure 6.12. Experimental Validation Results for Fail-Safe Using Steering with Feedback Term

Scenario 2: Caster Steered Front:

In this scenario, the front wheels are left to freely pivot around their axis of rotation. As a result, it is assumed that they don't generate any side forces, i.e. $C_1 = 0$. With the following experiment, we verify whether such assumption is valid. Similar to the previous experiment, the vehicle is driven at low speed in a straight road lane with the front tires left unconstrained. While maintaining a constant speed, the driver attempts to make a double lane change maneuver by steering the hand wheel.

The fail-safe control system then takes in the driver command and generates a steering command to the rear axle using equation (6.24) which we repeat here for convenience:

$$\delta_3(s) = \left(\frac{s^2 m_v v_x^2 I_v + s v_x (m_v C'_c + I C'_a) + C_a C'_c - C_b'^2 - C'_b m_v v_x^2}{s^2 m_v v_x^2 I_v + s v_x (m_v C_c + I C_a) + C_a C_c - C_b^2 - C_b m_v v_x^2} \right) \times \left(\frac{C_1 x_1 (s m_v v_x + C_a - \frac{C_b}{x_1})}{C_3 x_3 (s m_v v_x + C'_a - \frac{C'_b}{x_3})} \right) \delta_c(s) \quad (6.27)$$

Figure 6.13 shows that despite processing the driver's steering command using the transfer function above, the vehicle yaw rate response does not track the desired response very well. The main assumption in this scenario was that because the front tires are unconstrained, they are free to pivot, and thus, do not generate any cornering forces. However, it turns out that this assumption is not valid. In fact, during these steering maneuvers, the front wheels did not rotate, and were therefore, resisting motion, and thus, generating cornering forces. This is due to what's called the back efficiency of the front steering system. Steering systems are designed to efficiently transfer driver torque from steering wheel to road wheels. However, they are also designed to minimize road noise transfer to the hand wheel, and therefore, do not transfer forces up through the steering system as efficiently. As a result, the forces at the front tires did not dissipate up through the front steering system, and thus cornering forces were generated at the front, and the assumption initially made is not valid.

Next, in this scenario, i.e. castered front wheels, the filter input from the previous scenario (locked front axle) with the combination of feedback term is used resulting in a better response than in the previous experiment, as the front wheels stayed near the on-center position and the feedback control strategy took care of any unmodeled dynamics and nonlinear behavior.

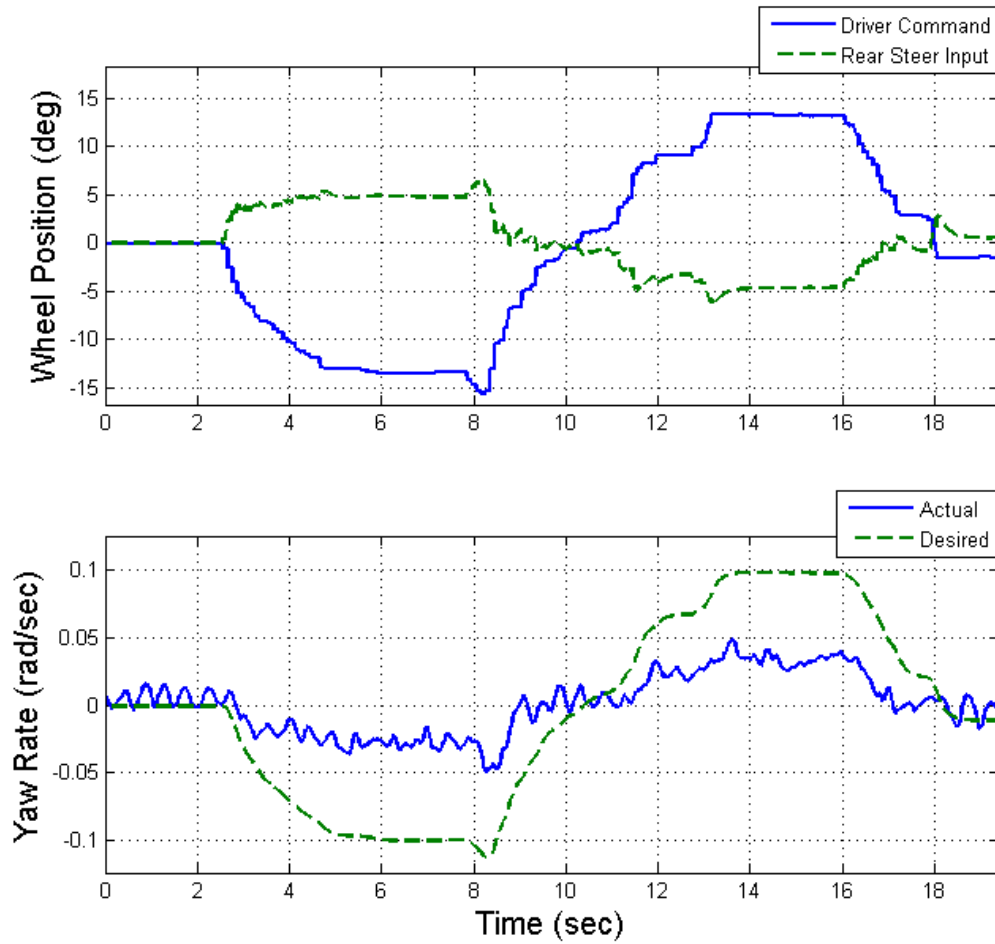


Figure 6.13. Experimental Validation Results for Fail-Safe Using Steering Equation 6.27 With Castered Front Axle

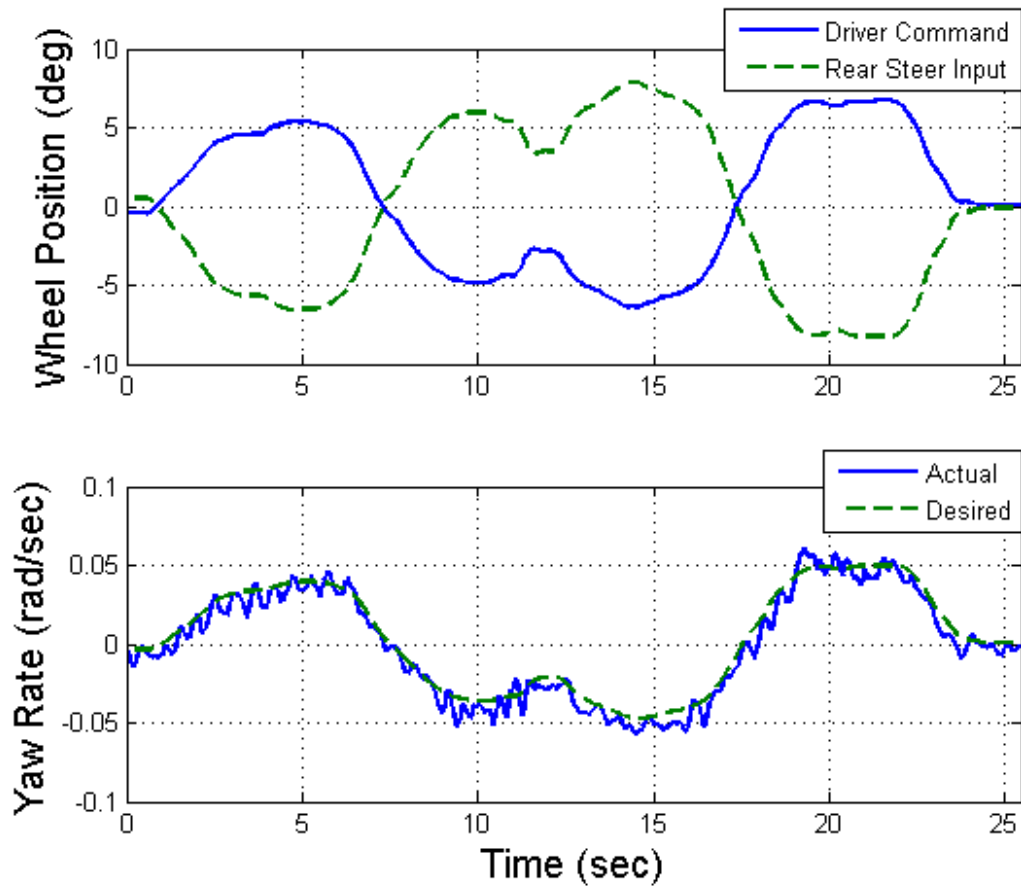


Figure 6.14. Experimental Validation Results for Fail-Safe Using Steering Equation 6.26 With Castered Front Axle

Conclusions:

Using rear axle steering as a fail-safe mechanism to mitigate failures in the front steer-by-wire system, different scenarios were explored. First, with the front wheels locked in the on-center position, a control strategy that includes both feed-forward and feedback terms worked best, particularly, when commanding large steering inputs where the tires' cornering forces start to saturate and the system can no longer be considered linear. On the other hand, in the scenario where the front wheels are left to freely pivot around their axis of rotation, the computed theoretical steering angle at the rear based on the driver command did not result in the desired vehicle yaw rate response. This is likely due to the fact that the front wheels are not truly unconstrained as a result of the back efficiency of the steering system which is designed to minimize the load transfer from the wheels to the driver. In this same scenario, when using the control strategy from the previous scenario, i.e. wheels locked on-center, in addition to feedback control, the vehicle's yaw rate response closely matched the desired response. Consequently, the same control strategy can be used for both scenarios and the feedback control term can be used to deal with any system uncertainties or unmodeled dynamics. While other control strategies may prove more suitable, the goal here was to show the potential utilization of the rear axle steering system as a fail-safe mechanism in addition to all the other benefits it offers. Other control strategies to enable this fail-safe mechanism can be further investigated.

6.3 Fail-Safe Using Differential Braking for Steering:

Differential braking has been used to affect the cornering response of vehicles where the distribution of braking forces is altered to induce the desired lateral response in a vehicle [45]. Typically, differential braking can be used to enhance the stability of a vehicle by using braking forces to control the yaw rate response of the vehicle. Differential braking has also been proposed as a way to preventing unintended lane departures [46].

In the context of steer-by-wire, differential braking might offer a viable way to mitigate failures in the steering system. For example, in the case of loss of power in the steer-by-wire system, the steering wheel position signal can be used to infer the intended steering direction of the driver. As a result, after detecting a steering system failure, the steering controller will send the appropriate braking commands to the brake controller which then distributes the braking force between left and right wheels, resulting in the desired yaw rate response of the vehicle, and thus, effectively steering the vehicle.

Nevertheless, it has been shown that using braking to affect the lateral dynamic response of the vehicle is not as efficient as steering the road wheels [30]. Steering requires only a fraction of the tire force compared to braking, leaving more tire force for the driver to operate the vehicle. As a result, in the case of failure of the steering systems, differential braking should only be used temporarily to keep the vehicle under control and safely move it away from the road and other motorists.

7. INSTRUMENTATION AND EXPERIMENTAL SETUP

The experimental validation of the DC steer-by-wire system is implemented in two separate steps. First, the system is implemented in a laboratory environment where the different subsystems, i.e. the swash plate control system and steer-by-wire control system are built and validated. Subsequently, the DC steer-by-wire system is implemented onto a test vehicle to validate its performance under real world conditions. Moreover, two of proposed fail-safe mechanisms for the steer-by-wire system are implemented and validated on the test vehicle.

7.1 Laboratory Setup

Before implementing the new steer-by-wire system on a vehicle, the initial proof of concept of the system and its subsystems is performed in the laboratory first. Specifically, the swash plate control system and steering actuator position control system were designed, tuned, and tested on the laboratory test bench first.

To validate the DC steer-by-wire system, two different configurations with different actuators are considered. The first configuration uses a single rack cylinder as the steering actuator which is most advantageous when replacing an existing conventional steering system where the steering gear is directly replaced by the single rack cylinder, and thus making use of the existing steering geometry. To simulate the load on the steering actuator, a pressurized pneumatic load cylinder is used. The pressure inside the pneumatic cylinder is set using a pressure regulator placed between the load cylinder and a tank of pressurized nitrogen.

The second laboratory setup configuration uses a linear cylinder as the steering actuator. Such configuration can be used as the primary steer-by-wire system with the conventional steering system replaced by mechanical gear box in series with a

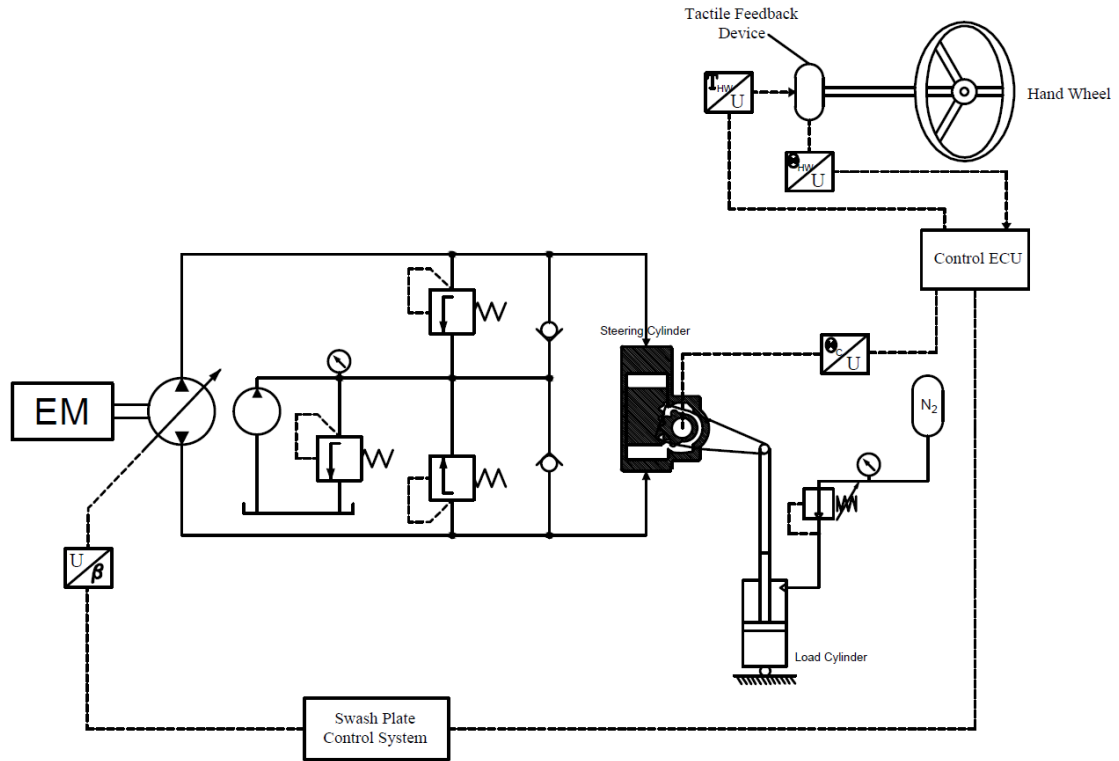


Figure 7.1. Schematics of Experimental Laboratory Setup using Single Rack Cylinder

clutch to create a fail-safe mechanism (See Chapter 6). The linear cylinder can also be used as the redundant and independent secondary steer-by-wire system which can be used in either the front or rear steered axle. In addition to being a redundant steer-by-wire, implementing a secondary steering system on the rear axle also offers improved maneuverability and decreased tire wear.

In both lab setups, the DC pump is driven by an electric motor. Flow from the pump then actuates the steering cylinder, and the direction and amount of steering is dictated by the swash plate angle of the pump which is commanded by the steer-by-wire control system, and delivered by the swash plate control system. A CAN controlled electrically driven 2-cc gear pump is used as the charge pump to compensate for hydraulic losses and as the power source for the swash plate control system.

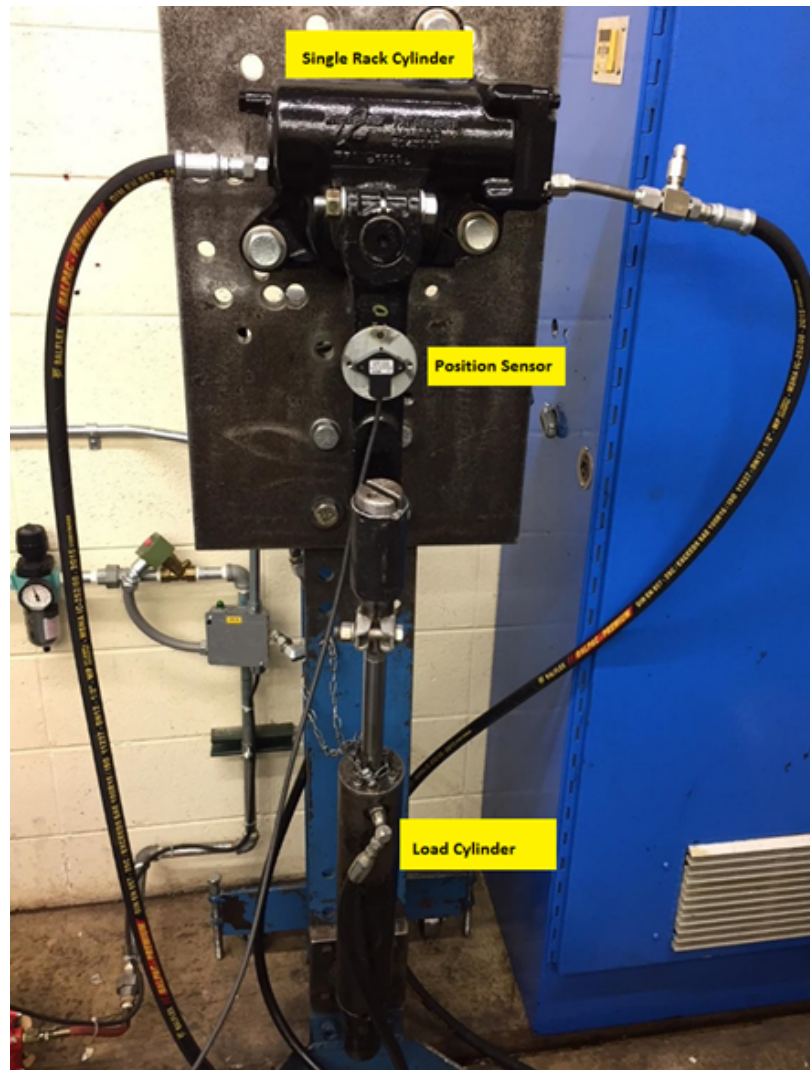


Figure 7.2. Experimental Laboratory Setup using Single Rack Cylinder

Furthermore, flow from the charge pump is controlled by a proportional directional valve which meters and direct flow to either side of the swash plate control cylinder, resulting in the actuation of the DC pump's swash plate. Moreover, a torque feedback device attached to a hand wheel is used to give steering feedback to the driver and to relay the steering intention of the driver to the steer-by-wire system by broadcasting the steering wheel position signal over the CAN communication network. Additionally, position sensors are used to measure the state of the steering actuator as well as the state of the pump's swash plate angle. And finally, the logic for both the

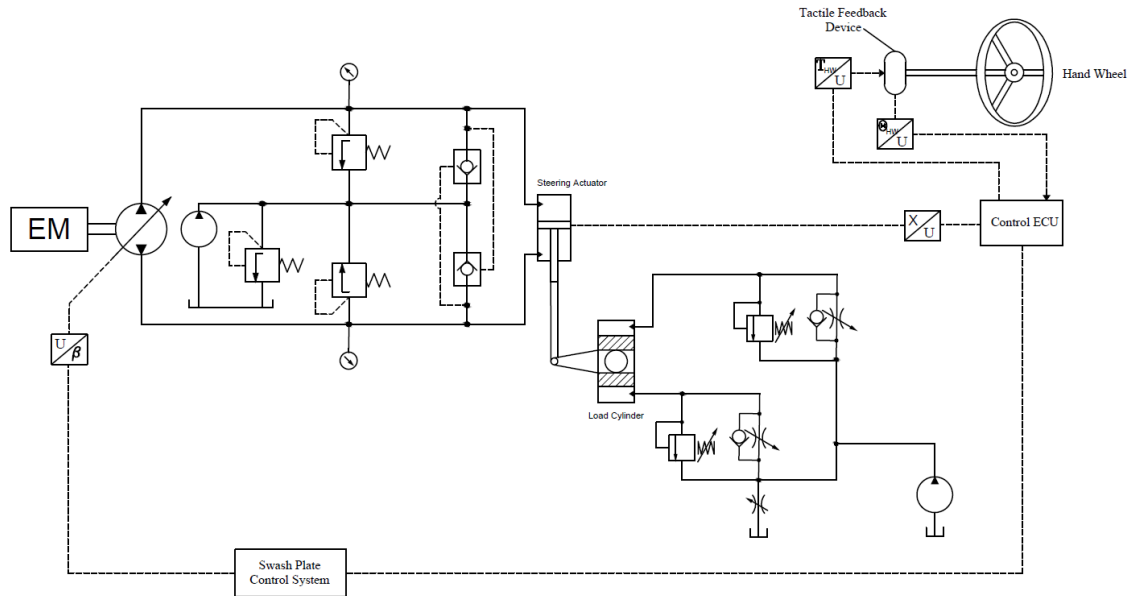


Figure 7.3. Schematics of Experimental Laboratory Setup using Linear Cylinder

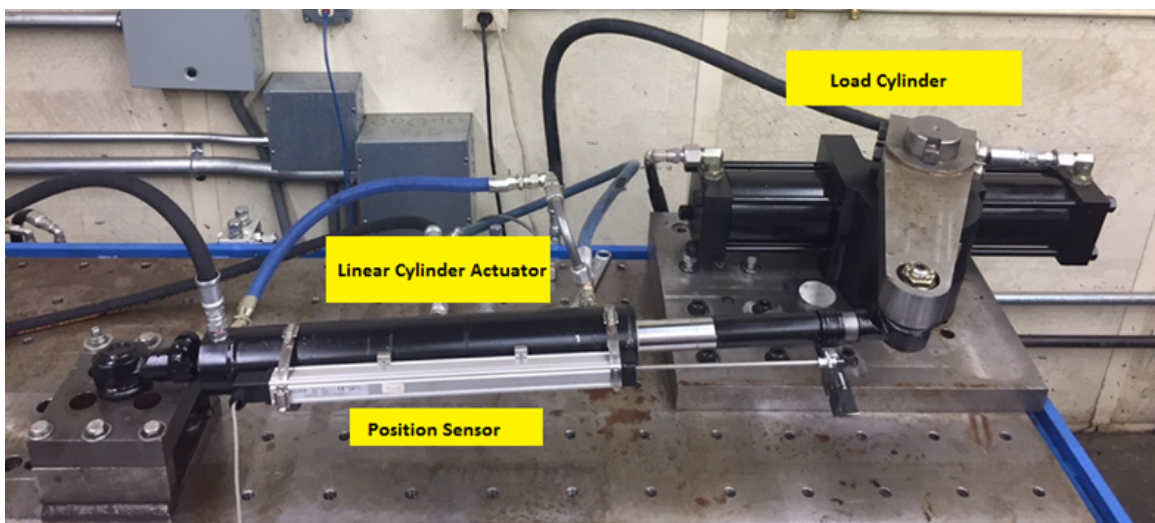
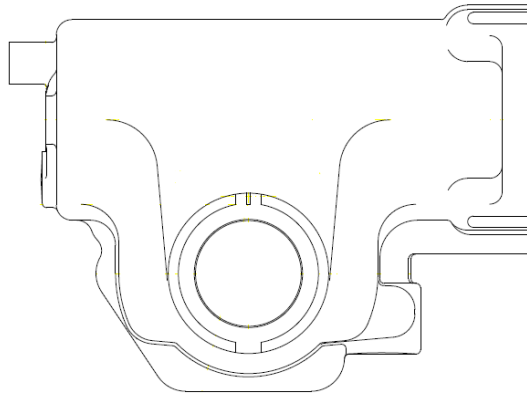
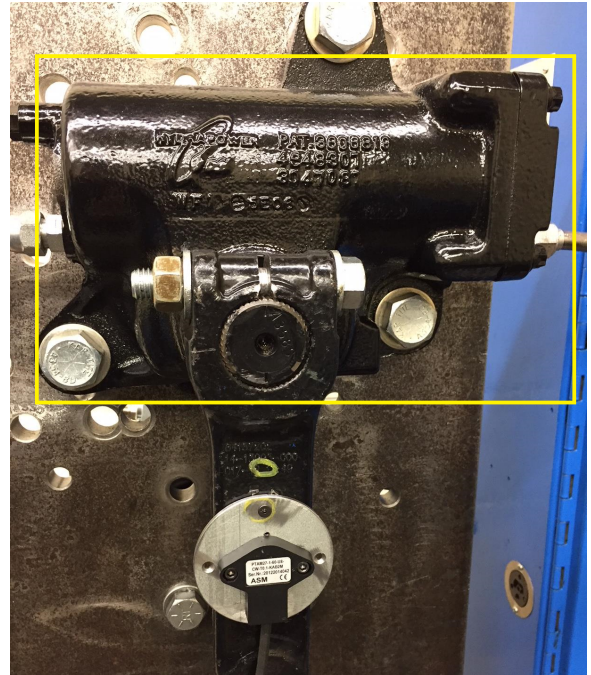


Figure 7.4. Experimental Laboratory Setup using a Linear Cylinder

steer-by-wire and swash plate control systems resides inside a dspace MicroAutobox controller which also interfaces with the different system sensors, and actuators.



(a)

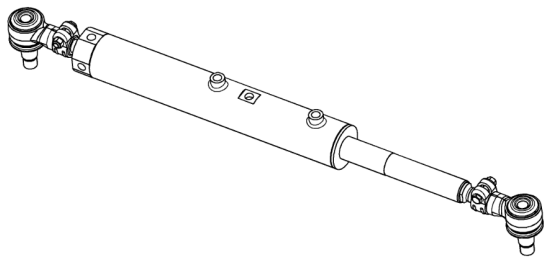


(b)

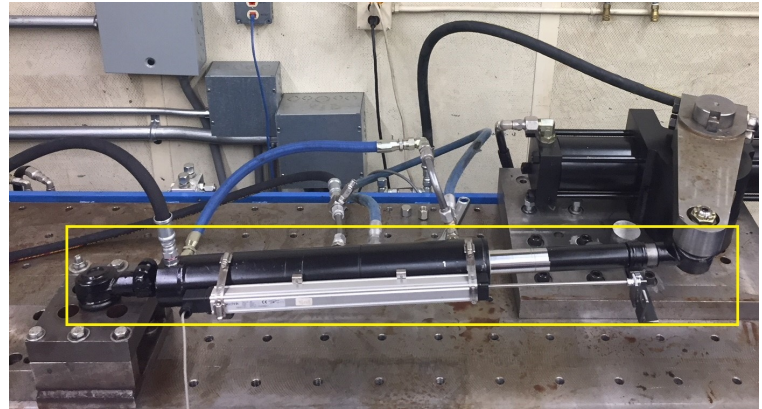
Figure 7.5. Single Rack Steering Actuator

7.1.1 Single Rack Steering Actuator

A production single rack cylinder (ZF RCS40) was chosen as the steering actuator for the experimental proof of concept. This cylinder is typically used in a dual steering master-slave configuration, with the conventional steering gear as the primary actuator, to steer vehicles with heavy front axles. However, in this application, the single rack cylinder will be the primary steering actuator and directly replaces the existing conventional steering gear of the vehicle, thus taking advantage of the already existing steering system architecture. Moreover, the new cylinder is chosen to be the same size as the baseline steering gear, and is therefore properly sized to steer the vehicle.



(a)



(b)

Figure 7.6. Linear Steering Actuator

7.1.2 Linear Steering Actuator

Due to its availability in the laboratory, a production steering cylinder typically used for rear-axle steering applications is used as the primary front steering actuator. Although unnecessary for this application, the cylinder's complex design with its five chambers is due to the need for the production rear-axle steering system to recenter and remain in that position in case of failure. In that application, an accumulator is used to provide the energy to recenter the cylinder. In this setup, only the two main chambers of the cylinder are used to steer the vehicle and the other three are connected to the return reservoir. ‘

7.1.3 Position Sensor for Linear Steering Actuator

In order to measure and control the motion of the linear steering cylinder a potentiometric linear transducer is attached the cylinder.

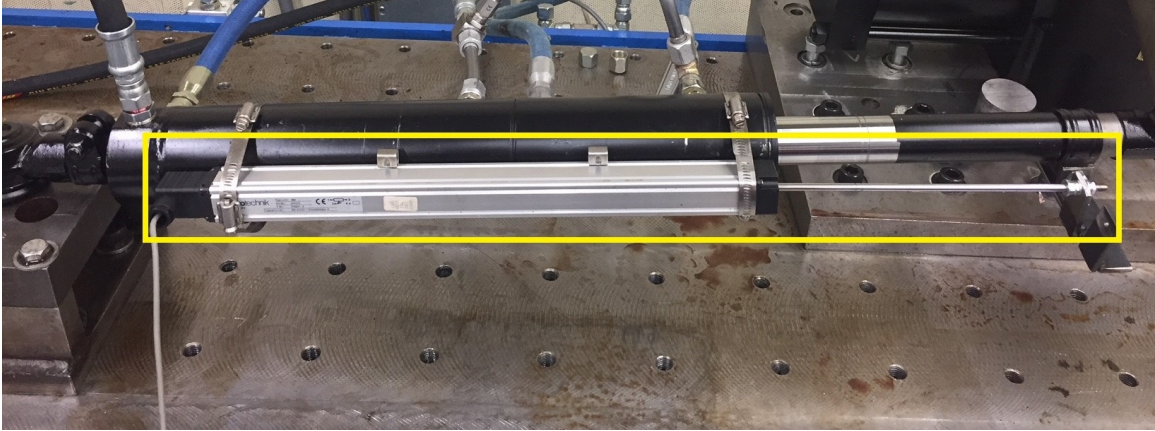


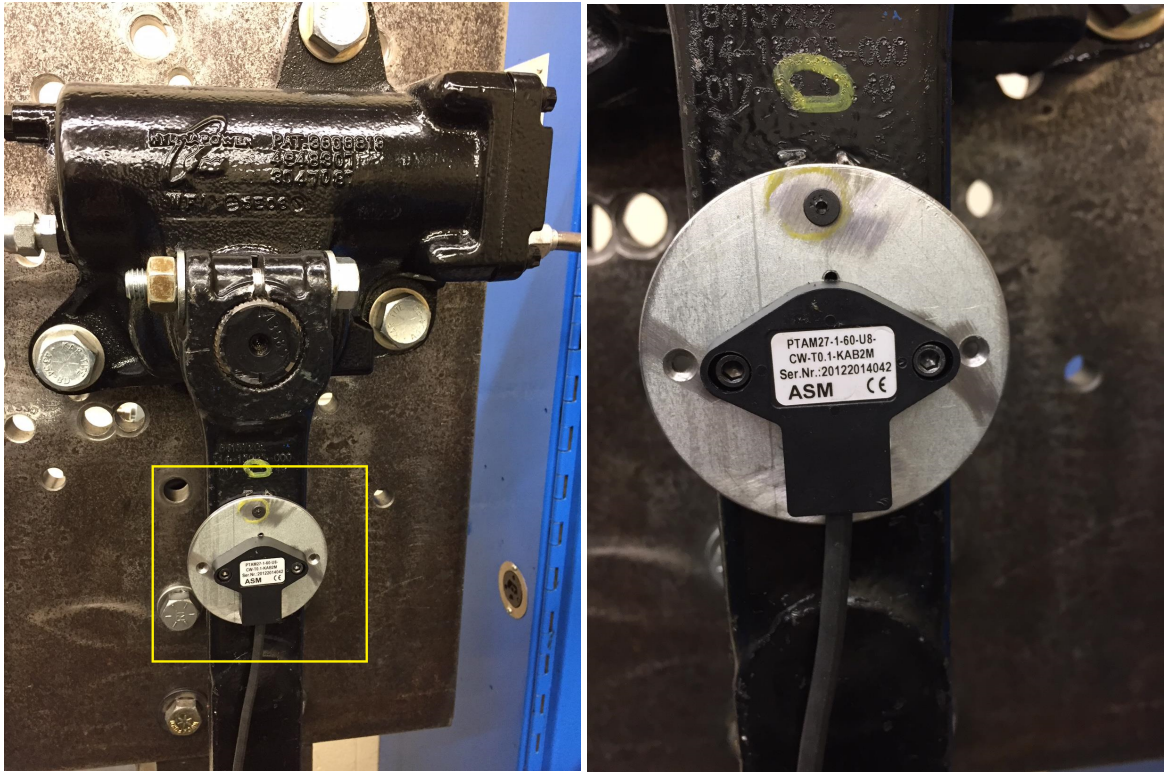
Figure 7.7. Linear Position Transducer

Table 7.1. Linear Position Sensor Specifications

| | |
|-------------------------------------|---|
| Range | 360 mm |
| Nominal resistance | 5 kohms |
| Resistance tolerance | $\pm 20 \%$ |
| Independent linearity | $\pm .05 \%$ |
| Repeatability | $< .01 \text{ mm}$ |
| Temperature range | $-30 \dots +100 \text{ }^\circ\text{C}$ |
| Maximum permissible applied voltage | 42 V |

7.1.4 Position Sensor for Single Rack Steering Actuator

A tilt sensor is placed on the Pitman arm at the output of the single rack cylinder in order to measure the steering position (Figure 7.8). The sensor specification are shown in the table below.



(a)

(b)

Figure 7.8. Tilt Sensor for Measuring Pitman Arm Position

Table 7.2. Rotary Position Sensor Specifications

| | |
|-------------------|-----------------------------------|
| Range | $\pm 60^\circ$ |
| Resolution | 0.1° |
| Linearity | $\pm 0.5^\circ$ |
| Settling Time | 0.1 ... 10 s / 90 %, configurable |
| Output/Excitation | 0.5...5 V |
| Protection Class | IP67 |

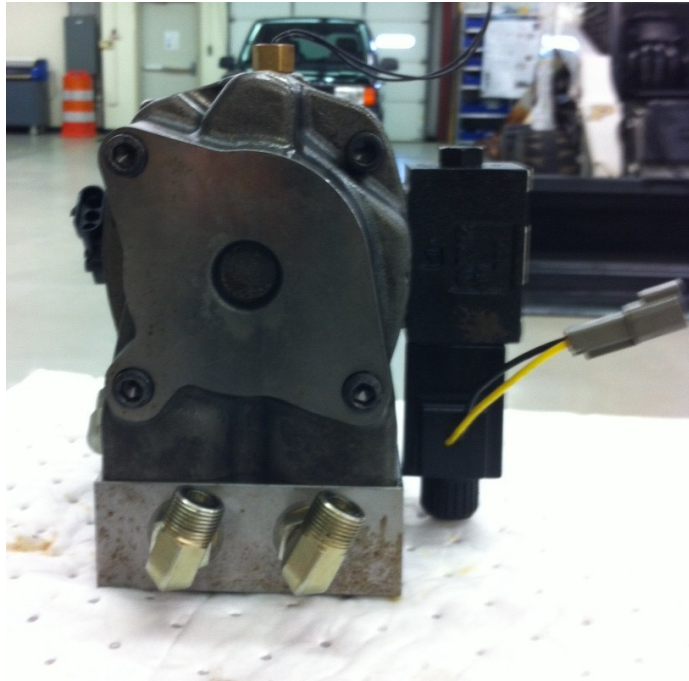


Figure 7.9. DC Steering Variable Displacement Pump

7.1.5 Steering Pump

Based on the sizing procedure shown in appendix A, an $18 \text{ cm}^3/\text{rev}$ P1 Parker variable displacement axial piston pump is selected as the main flow source for the steer-by-wire system (Figure 7.9).

Table 7.3. DC Pump Specifications

| | |
|----------------|----------------------------|
| Type | Variable Axial Piston Pump |
| Displacement | $18\text{cc}/\text{rev}$ |
| Mounting | SAE A Pilot |
| Ports | SAE Threaded Work Ports |
| Shaft Option | Slined Shaft - SAE A 9T |
| Shaft Rotation | Clockwise |

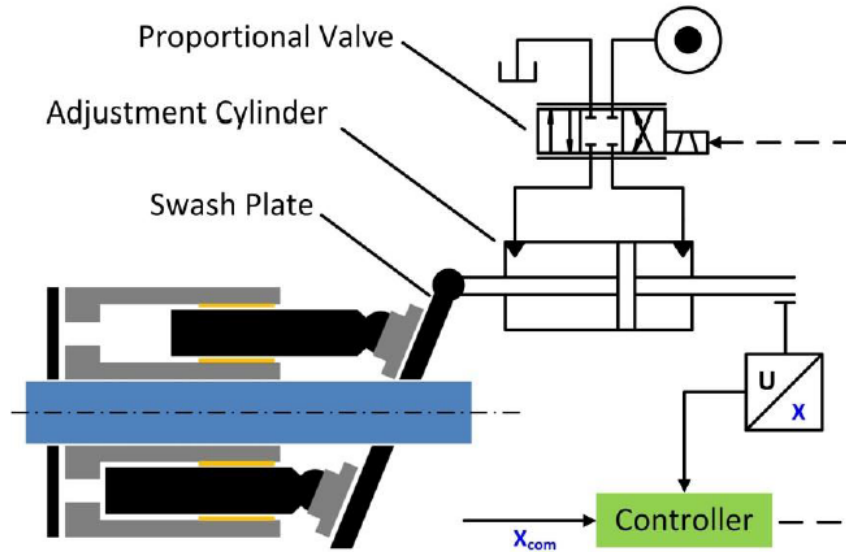


Figure 7.10. Swash Plate Control System.

7.1.6 Swash Plate Control System

In order to control the flow output of the pump, a swash plate control system need to be designed and implemented. Specifically, the control valve, charge pump, and swash plate position sensor need to be sized, selected, and implemented.

Control Valve

A 40 L/min proportional directional control valve with over 100 Hz bandwidth was selected. 40 L/min is more than what is needed for this application but due to the high cost of such valves and availability of the selected valve in the laboratory, the decision was made to use the already available valve.

Charge Pump

A 2-cc fixed-displacement pump driven by a variable speed electric motor is used as the charge pump to provide flow for the swash plate control system and compensate

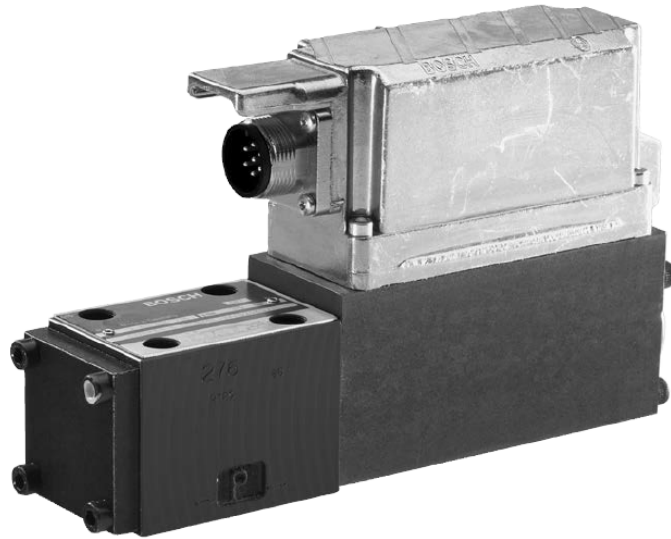


Figure 7.11. Proportional Directional Control Valve

Table 7.4. Control Valve Specifications

| | |
|---|---------------|
| Rated Flow | 40 L/min |
| Flow characteristics | Linear |
| Maximum operating pressure | 315 bar |
| Ambient temperature range | -20 ... +50 C |
| Actuating time for signal step 0...100% | < 10 ms |
| Supply voltage | 24 V |
| Command value input | +/- 10 V |

for hydraulic losses within the steering system. The pump/motor combination comes in one single compact package and is typically used for the main flow source for light to medium weight vehicle steering systems. The speed of the motor can be electronically controlled via Control Area Network (CAN) communication which makes it very a convenient plug-and-play type of system.



Figure 7.12. ZF TRW EPHS Pump

Table 7.5. Charge Pump Specifications

| | |
|-----------------------------|----------------|
| Pump Flow | 12.0 l/min |
| Max Pump Pressure | 120 bar |
| Hydraulic Power | 1000 W |
| Max Current @ 13.5V | 115 A |
| Stand-by Current @ 13.5V | <2.5 A |
| Operating Temperature Range | -40 C to 105 C |
| Dry Weight | 5 kg |

Swash Plate Angle Position Sensor

To measure the position of the pump's swash plate, a simple potentiometer-based sensor is used. The swash plate is mechanically connected to a shaft that emerges out of the pump's drain case and rotates with the swash plate. As a result, the position sensor is attached to that same shaft which moves the wiper of the potentiometer as it rotates, and thus changing the resistance between the wiper and the two end

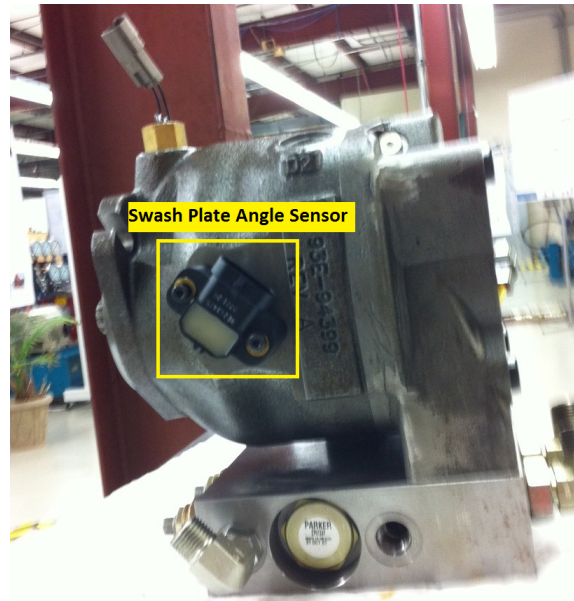


Figure 7.13. Swash Plate Angle Position Sensor

connections of the sensor. As such, the output signal changes linearly with the motion of the swash plate, resulting in a position reading. The sensor is powered with 5 Volts from the control ECU and the resistance between its end points is $10\text{ k}\Omega$.

7.1.7 Control ECU

A dspace MicroAutobox II is used to receive and process all raw sensor data, as well as the steering inputs from the driver. The proposed control systems are implemented in a Matlab Simulink environment using dspace program which then generates and loads the control software into the MicroAutobox. The MicroAutobox controls the charge pump by sending its motor speed commands using SAE J1939 CAN (Control Area Network) communication protocol. The dspace box also controls the DC pump's swash plate system by receiving an analog signal from the swash plate position sensor, and sending an analog output command to actuate the control valve which in turn actuates the swash plate, thus inducing steering motion of the cylinder based on



Figure 7.14. dSPACE MicroAutobox



Figure 7.15. Test Vehicle: Freightliner FL60

vehicle operating conditions. The MicroAutobox also receives vehicle information such as vehicle speed, and yaw rate from the vehicle's CAN communication bus.

7.2 Vehicle Setup

To complete the validation of the DC steer-by-wire system, implementation and testing on an vehicle was performed. For this purpose, a Freightliner FL60 three-axle vehicle was used as the test vehicle. In this validation, the DC steer-by-wire configuration using the linear cylinder was chosen for its ease of installation in parallel with the existing conventional steering system. Moreover, using the linear cylinder

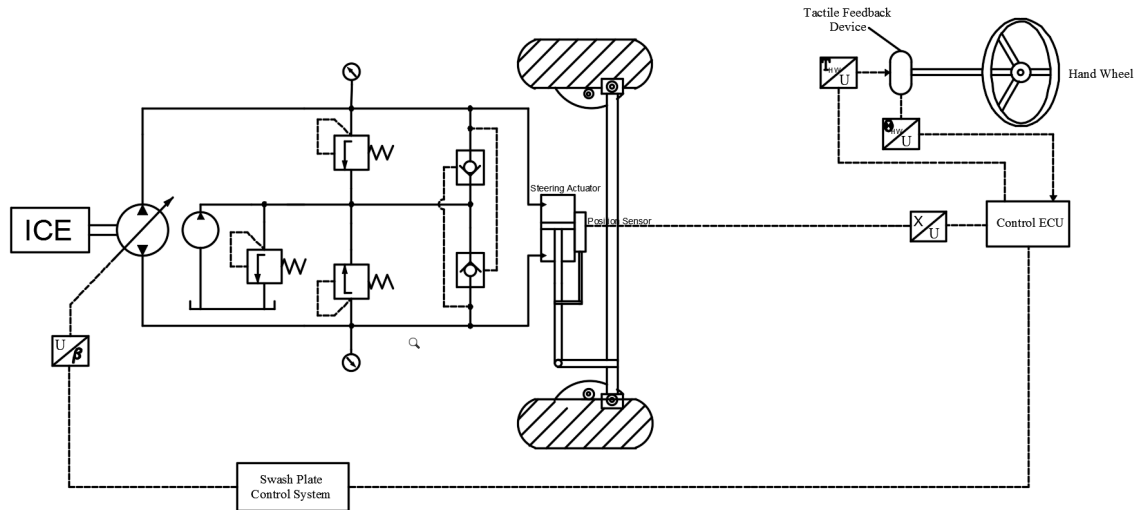


Figure 7.16. Experimental Vehicle Setup Schematics

rather than the single rack cylinder allows for the conventional steering gear to remain on the vehicle, and along with a pneumatic clutch, can be used as part of one of the two proposed fail-safe mechanisms to mitigate failures in the steer-by-wire system (see Chapter 6). However, in normal conditions, the clutch is disengaged, allowing the system to steer by wire. Keeping the conventional steering gear also allows the vehicle to remain drivable while the steer-by-wire system is being installed.

7.2.1 System Architecture:

The steering cylinder is actuated using the 18-cc DC pump which due to its large physical size did not fit in the engine compartment, and thus could not be run using the vehicle's engine. Instead, a separate gasoline engine was placed in the back of the vehicle and used to run the pump. Moreover, the same electrically driven gear pump previously used in the lab setup as a charge pump was used in the vehicle setup. The charge pump electric motor is powered by the vehicle's battery and receives speed command from the the control ECU over the vehicle's CAN communication bus.

Similarly, the same proportional directional valve is used to control the DC pump's swash plate angle. The valve requires 24 Volts power source, and as a result an electric converter is used to convert from the vehicle's 12 Volts power to the required 24 Volts. Finally, to control the steer-by-wire system, the same dspace MicroAutobox control ECU was used to interface with the different systems and sensors installed on the vehicle. The MicroAutobox is connected to the vehicle's CAN bus over which it receives information on the state of the vehicle, such as vehicle speed, yaw rate, and lateral acceleration, which can be used to affect the steering behavior of the steer-by-wire system. Additionally, the MicroAutobox also communicates with the rear axle steering system via CAN as part of the fail-safe mechanism.

7.2.2 Wiring Schematics

A Mototron hub is used to interface between the dspace MicroAutobox and the vehicle signals, namely, power, ground, ignition and CAN signals. The charge pump is also connected to the same hub. The dspace ECU interfaces directly with the different system sensors, i.e. swash plate position sensor, pressure sensors, and steering cylinder position sensor. The dspace controller is also responsible for actuating the directional valve that controls the DC pump's swash plate, as well as sending speed commands the charge pump's driving motor.

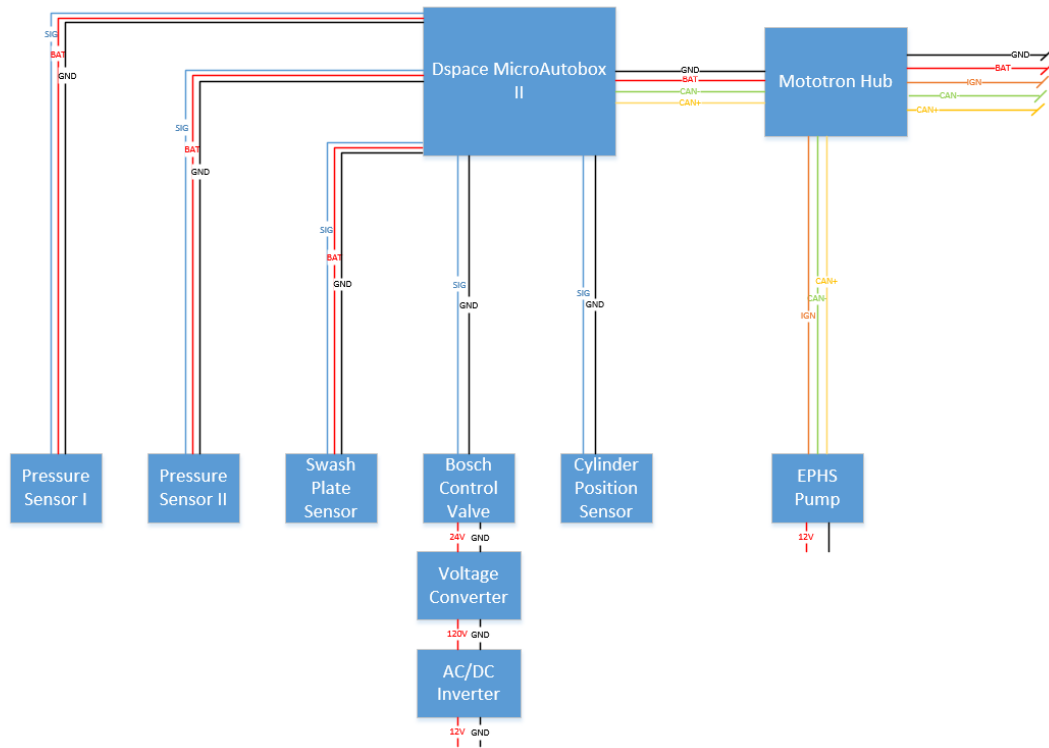


Figure 7.17. Vehicle Setup Wiring Schematics of DC Steer-by-Wire

7.2.3 Cylinder Installation

The steer-by-wire actuating cylinder is attached on one end to the front axle and to the tie rod on the other end. As such, the steer-by-wire system is installed in parallel with the vehicle's original steering system which has been modified to act as one of the proposed fail-safe mechanisms. Just like in the lab setup, the steering position sensor is attached to the cylinder as shown in Figure 7.19. The hydraulic lines are then run to the pump which is driven by the external gasoline engine located behind the cab.



Figure 7.18. Cylinder Installation on Vehicle

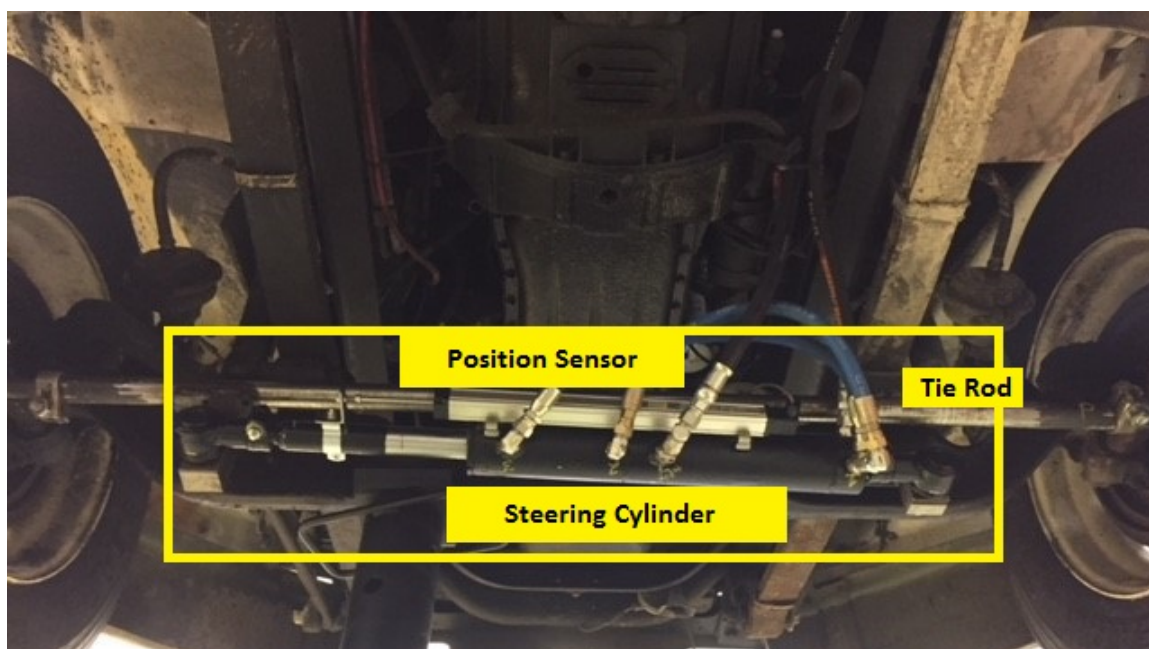


Figure 7.19. Cylinder Installation on Vehicle Close-Up

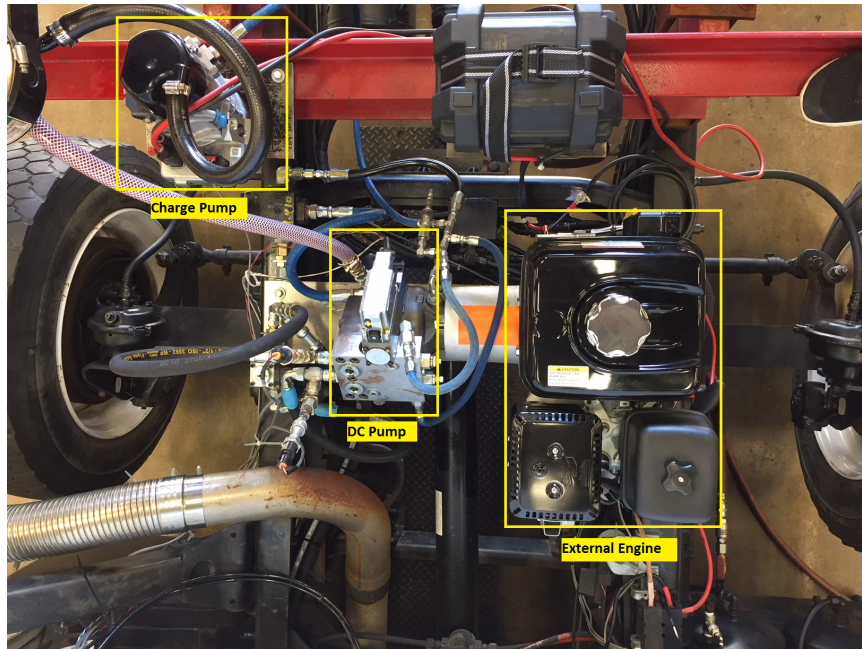


Figure 7.20. Engine-Pump Installation on Vehicle: Top View

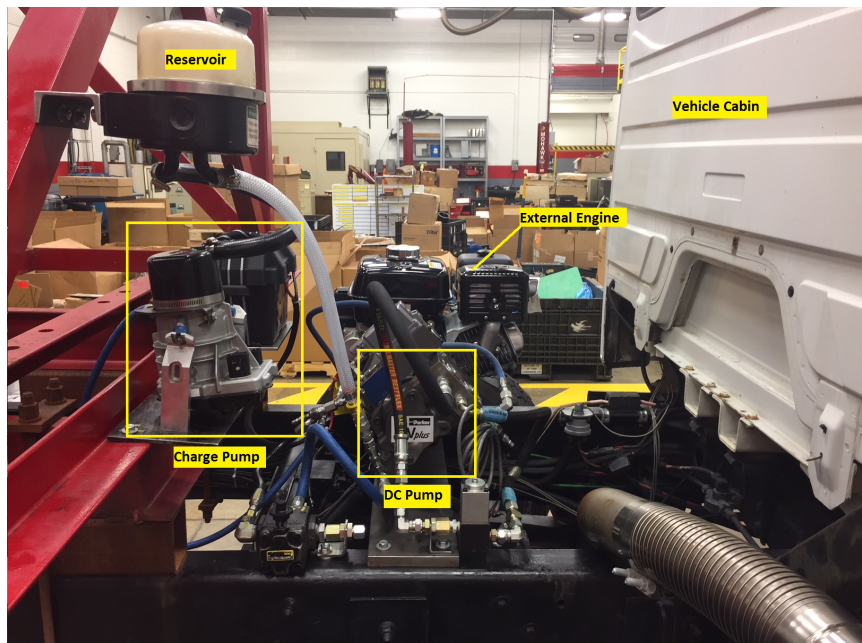


Figure 7.21. Engine-Pump Installation on Vehicle: Side View

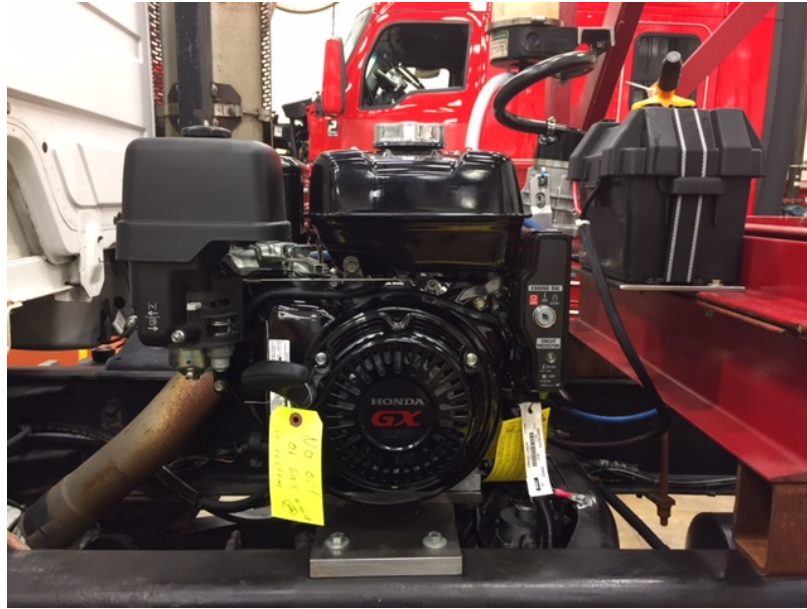


Figure 7.22. Honda GX270 External Gasoline Engine

7.2.4 Pump Installation

Due to lack of space in the engine compartment of the test vehicle and the DC pump's large physical size, an external gasoline engine is used to drive the DC pump. The engine-pump assembly along with the charge pump are placed behind the vehicle cabin and the hydraulic lines are run to the front axle where the steering cylinder is located.

7.2.5 External Gasoline Engine

A 4-stroke external Honda GX270 gasoline engine is used to drive the pump. The engine has been chosen based on the power requirements of the steering system at static dry park maneuver which constitutes the most power demanding scenario for steering systems.

Table 7.6. External Engine Specifications

| | |
|--------------------|--|
| Engine Type | Air-cooled 4-stroke OHV |
| Displacement | 270 cm^3 |
| Net Power Output | 8.5 HP (6.3 kW) @ 3,600 rpm |
| Net Torque | 14.1 lb-ft (19.1 Nm) @ 2,500 rpm |
| Dry Weight | 55 lb (25 kg) |
| PTO Shaft Rotation | Counterclockwise (from PTO shaft side) |

7.2.6 Driver Torque Feedback System

In a steer-by-wire system it is important to send steering feel feedback to the driver through the hand wheel so that he or she is aware of the vehicle's state and operating conditions. In order to do so, a ZF ReAX torque overlay system installed on the steering column of the vehicle was used. The ReAX has a closed-loop hand wheel torque control system that allows accurate control of the driver's torque in the presence of external disturbances [21]. Consequently, whether the ReAX is mechanically connected to vehicle's road wheels, and thus loaded, or completely disconnected from them as in the case of a steer-by-wire, the driver will always experience the desired torque feel in his or her hands as computed by the ReAX system.

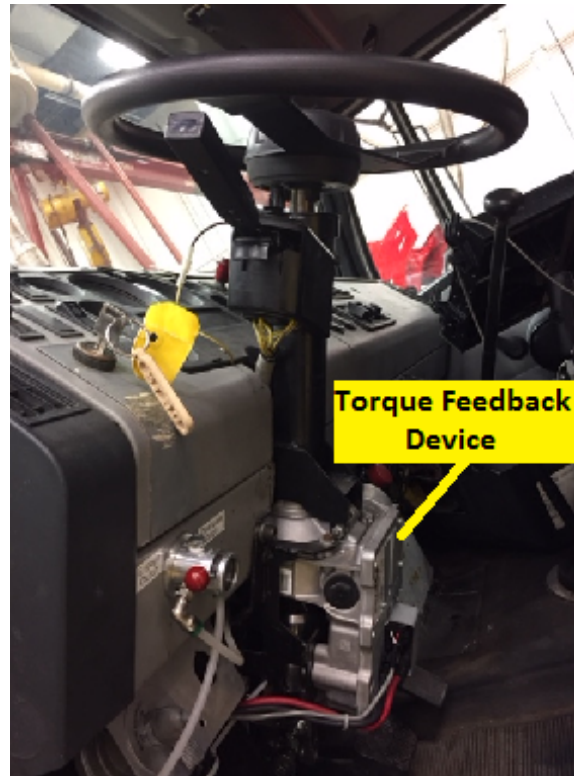


Figure 7.23. ZF ReAX Torque Overlay Steering System Used as Torque Feedback Device

7.2.7 Voltage Inverter

In the lab setup a voltage converter was used to convert voltage input from 110V AC to the 24V DC required by the proportional directional valve used by the swash plate control system. As a result, in the interest of saving time, that same converter is used in the vehicle setup along with voltage inverter that converts the battery's 12V DC to the 110V AC required by the first converter.



Figure 7.24. Xantrex PROwatt Voltage Inverter

7.3 Fail-Safe Mechanisms Implementation Into Vehicle

Two of the fail-safe mechanisms for steer-by-wire proposed in Chapter 6 are implemented into the test vehicle. The first one uses a pneumatic clutch to mechanically connect the steering wheel to the road wheels in case of failure of the front steer-by-wire system. On the other hand, the second proposed fail-safe mechanism takes advantage of an existing steering system on the rear axle to help steer the vehicle in case of failure of the front steering system.

7.3.1 Fail-Safe Mechanism Using a Clutch

When a failure is detected in the steer-by-wire system, the steering controller engages the pneumatic clutch, and thus mechanically connecting the steering wheel to the road wheels which allows the driver to manually steer the vehicle to safety. A mechanical gearbox is used to amplify the driver's steering torque. In fact, for this

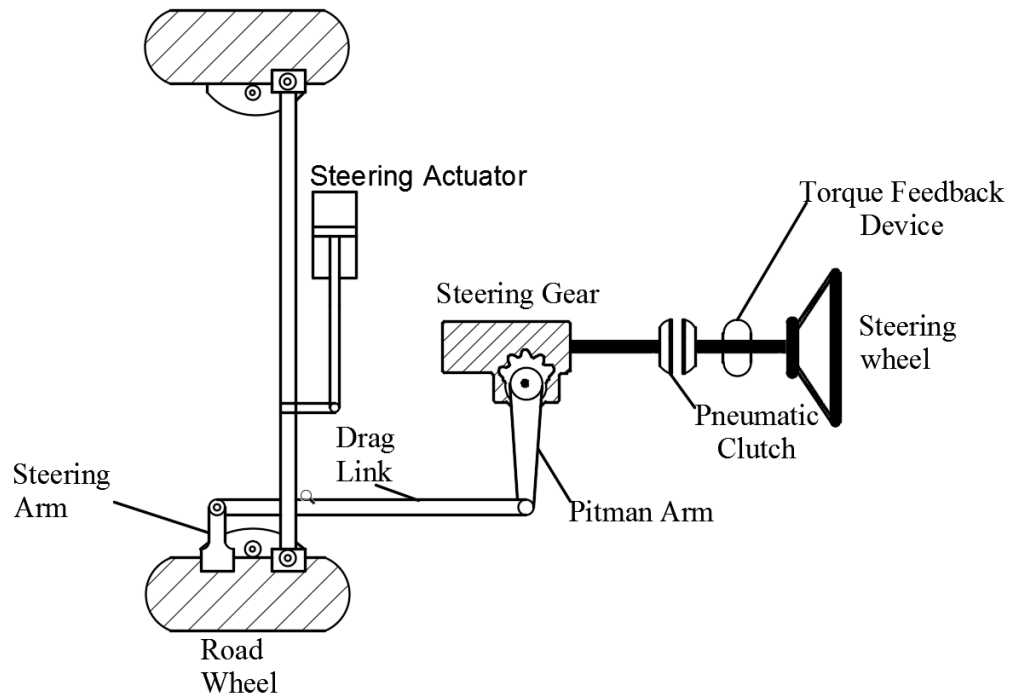


Figure 7.25. Vehicle Fail-Safe Mechanism Using a Pneumatic Clutch

implementation the vehicle's original steering gearbox was used which offers both mechanical and hydraulic assistance.



Figure 7.26. Fail-Safe Mechanism Using a Clutch: Inside Cab.

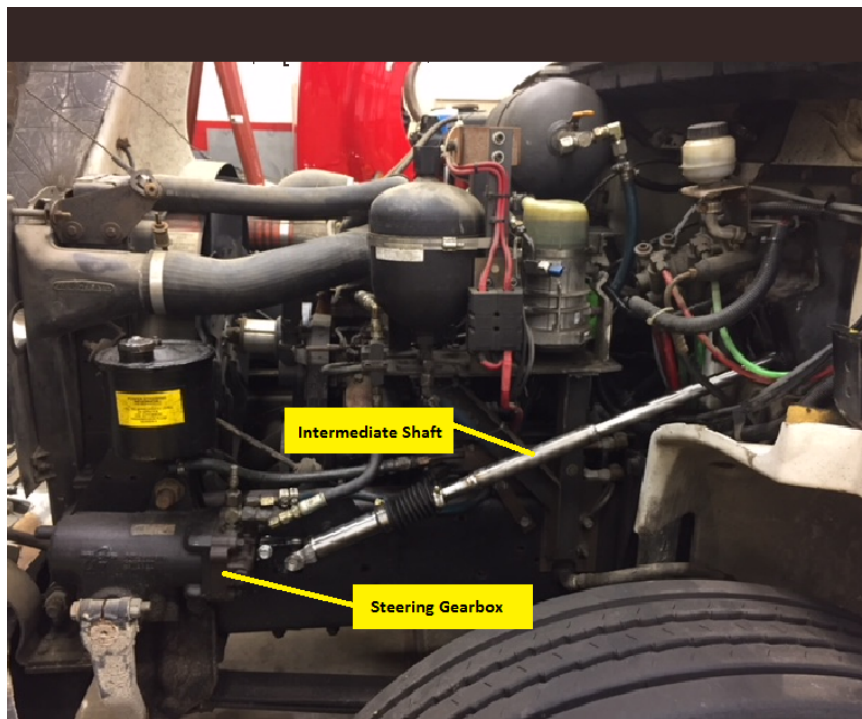


Figure 7.27. Fail-Safe Mechanism Using a Clutch: Engine Compartment.

7.3.2 Fail-Safe Mechanism Using Rear Axle Steering System

The test vehicle used for this project comes equipped with an electro-hydro-mechanical rear axle steering system. To steer the rear wheels, an electric motor is placed at the input of a conventional steering gear which in turn is connected to the road wheels via a series of linkages. The electric motor actuates the rotary valve at the steering gear input which pressurizes fluid inside its chambers, and thus actuating the steering gear and in turn the wheels on the rear axle. It must be noted that the type of steering system used, whether it's electro-mechanical, hydro-mechanical, or electro-hydro-mechanical, is irrelevant to the fail-safe mechanism. In fact, the same DC steer-by-wire system implemented in the front axle can be replicated in the rear, providing improved energy efficiency and added functionality, i.e decrease in turning radius and tire wear, in addition to being a fail-safe mechanism to the front steer-by-wire system. The rear axle steering system is connected to the vehicle CAN communication bus, and therefore can be controlled by steer-by-wire control ECU (dpsace MicroAutobox).

System Architecture

The rear axle steering system is controlled by the MicroAutobox ECU via the vehicle CAN communication network. In the event of a failure of the front steer-by-wire system, the steering controller receives the driver's steering command via CAN from which it infers the desired vehicle yaw rate response using the transfer functions shown in chapter 6, and generates the feedforward term of steering command. The measured yaw rate is also received through the CAN bus from the standard SAE J1939 Vehicle Dynamics and Controls message 2 (VDC2), and is used as part of the feedback control strategy. The feedforward and feedback control terms are then combined and sent to the rear axle steering system via the vehicle CAN.



Figure 7.28. Rear Axle Steering System on Test Vehicle

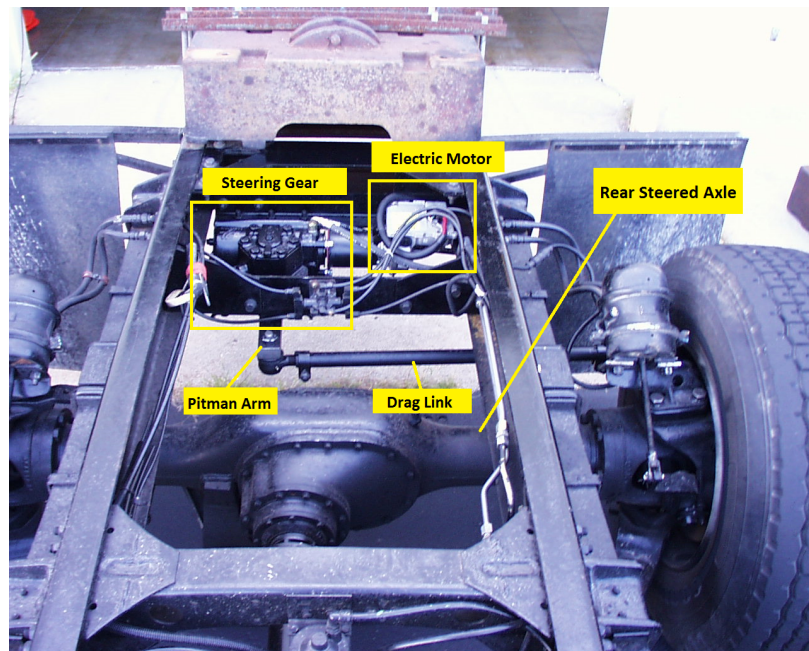


Figure 7.29. Rear Axle Steering System on Test Vehicle : Top View.

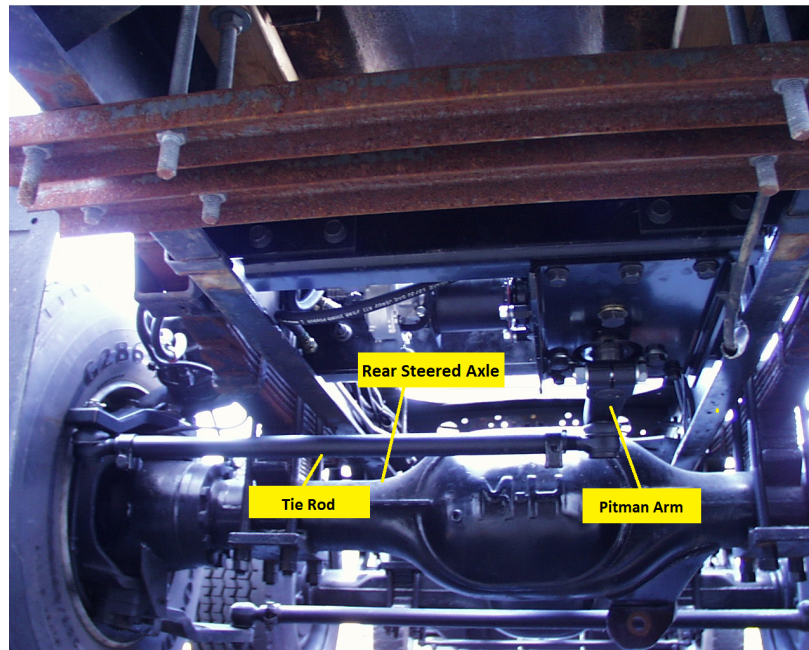


Figure 7.30. Rear Axle Steering System on Test Vehicle : Bottom View.

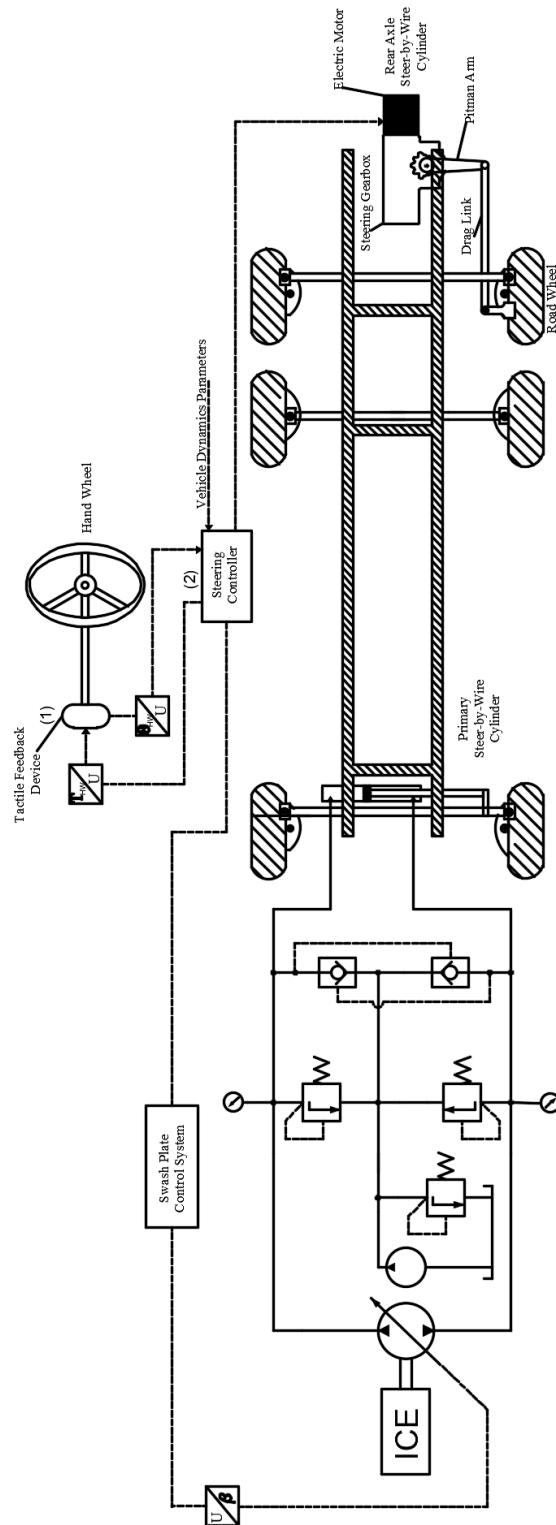


Figure 7.31. System Architecture of Fail-Safe Using Rear Axle Steering

8. ACTIVE CONTROL OF STEERING EFFORT USING DISPLACEMENT CONTROLLED PUMPS

So far in this dissertation, the DC steer-by-wire system was presented as one of the possible ways to use Displacement Controlled pumps to steer on-highway commercial vehicles. For that system, different possible configurations were proposed and a proof of concept using simulation and experimental validation was performed in the laboratory and on a test vehicle to prove the feasibility of the concept. Moreover, different steer-by-wire fail-safe mechanisms were proposed and implemented on the same test vehicle to demonstrate how the vehicle remain controllable should the steer-by-wire system fail.

In this chapter, we propose another way of using DC pumps to steer on-highway commercial vehicles, namely, the concept of active control of steering effort using DC pumps while maintaining the mechanical link between the hand-wheel and the road wheels. Due to time limitations and the scope of this project, in this dissertation, we only introduce this new concept with the understanding that further simulation and experimental work is be needed to prove its feasibility. Such work will be the subject of future publications.

8.1 The Concept of Active Control of Steering Effort

The concept of active of control of driver steering effort has been around for a few decades now after it was first proposed in [19]. It is achieved by constantly measuring the driver's torque input at the hand wheel and comparing it against a computed desired torque that the system designer would like the driver to experience at the hand-wheel based on some particular steering and vehicle operating conditions, e.g. steering wheel position and rate, vehicle speed, etc. A torque control system takes the

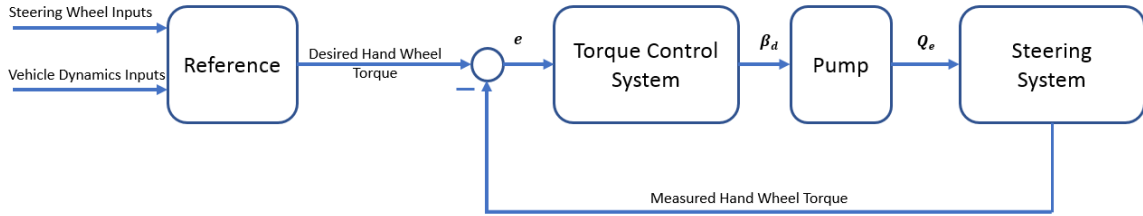


Figure 8.1. Proposed Torque Control Block Diagram

desired and measured hand wheel torque input and attempts to minimize the error signal between them in the presence of external disturbances. A near zero error signal means that the measured driver torque tracks the computed desired torque which in turn means that the driver is experiencing the computed desired torque at the hand wheel regardless of the external forces acting on the steering system.

8.2 Advantages of Active Control of Steering Effort

The ability to closely control the driver's steering feel despite external disturbances on the system offers significant flexibility to the steering system designers and simplifies many of the design aspects of the system. Typically, when designing a conventional hydro-mechanical steering system for commercial vehicles, the steering feel of the system is heavily dependent on the design of the control valve inside the steering gear which determines the steering feel of the system. Consequently, to closely design the steering feel for these systems, precise manufacturing of the control valve metering edges is necessary which increases the complexity and cost of the system. Nonetheless, despite a high precision manufactured valve, in conventional steering systems, the steering feel cannot be designed to actively vary with operating conditions such as vehicle speed. Ideally, the steering system should be designed to provide low steering efforts at low vehicle speed as in low speed maneuvering situations, e.g. truck yard or delivery depot, and a stiffer stable feel on-center at highway speeds.

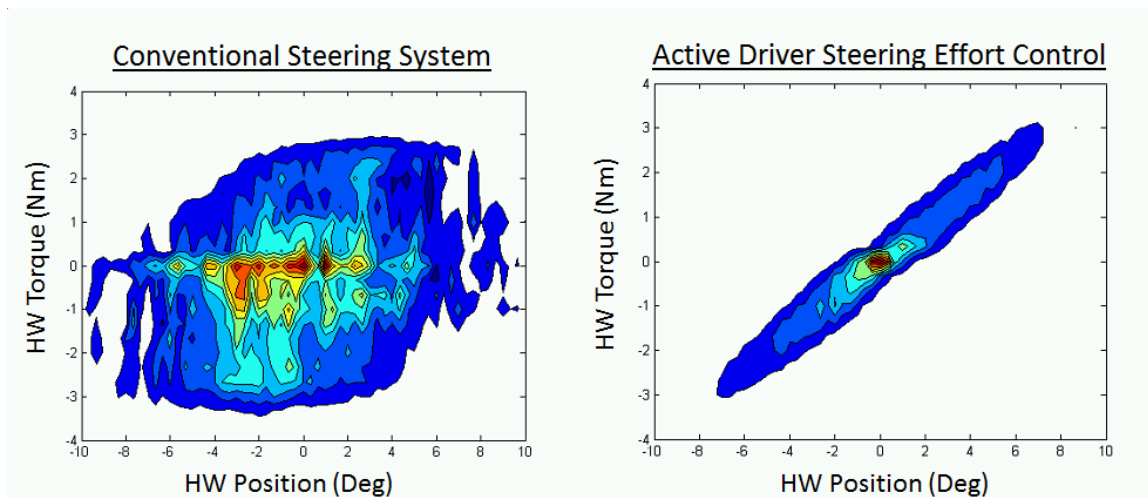


Figure 8.2. Hand Wheel Torque Response with and without an Active Steering Effort Control system

These are fundamentally conflicting design requirements that a mechanical control valve cannot achieve. As a result, in reality a compromise is achieved between the two requirements and a conventional steering system is designed to give acceptable relatively low efforts at low speeds, and its on-center behavior is tweaked to provide acceptable stable on-center feel at highway speeds. However, with the active torque control concept, the two aforementioned design requirements can both easily be achieved by adjusting the computed desired driver torque based on a vehicle speed measurements which will result in the driver experiencing low efforts at low speeds and a stiffer stable feel when driving at highway speeds.

Moreover, with active driver torque control, the hard requirements that are typically imposed on the steering system components to improve steering feel, i.e. low friction and lash can be relaxed as these undesired effects can be compensated for by the torque control system 8.2. Additionally, as the driver torque feel can be controlled regardless of external loads on the steering systems, when a desired torque feel is decided on by the system designer, the same system can be installed on different vehicle platforms and consistently provide the desired steering feel regardless of

difference in the steering geometry of the vehicle or front axle load. This is not the case for conventional steering systems which need to have their components tailored and tuned for every vehicle platform, e.g. different steering gear sizes and different control valves for different applications.

In summary, the active control of driver steering effort offers consistency in the driver steering experience despite external disturbances on the system, and simplifies many aspects of the steering system design by allowing more flexibility in the steering feel design, as well as in the implementation into different vehicle platforms.

8.3 Active Control of Steering Effort Using DC Pumps

The concept of active control of driver steering effort using a variable displacement pump is similar to the torque overlay concept in which an electric motor is placed in series with the conventional steering system and used to actively control the driver's hand wheel torque, and as a result offering steering assistance. However, a major drawback of the current torque overlay systems is their use of conventional steering gears and pumps which already suffer from significant inefficiencies that result from flow metering through the use of control valves. Such inefficiencies is what the new proposed concept aims to improve on by eliminating the control valve inside the steering gear and providing steering assistance by directly varying the flow output of the pump to help displace the steering gear piston, and ultimately control the driver's steering effort.

To control driver steering effort using a DC pump, a torque sensor (Figure 8.3) is placed at the hand wheel to measure driver's torque input, and a desired driver torque is computed based on the steering system and vehicle operating conditions. A control system is then designed to minimize the error signal between the measured and desired hand wheel torque, and outputs a desired pump displacement that is sent to the pump's displacement control system. The pump then delivers the desired flow output to the steering gear and helps apply a hydraulic force on its piston, thus

providing steering assistance. With a well designed torque control system, the error signal between measured and desired torque can be made to converge to zero under all operating conditions, leading the driver's steering effort to track the computed desired hand wheel torque.

8.4 Other Possible Implementations:

8.4.1 Variable Displacement Pump in a Open-Circuit Configuration:

Driver Steering effort can also be implemented with a variable displacement pump in an open circuit configuration in which the torque control system will send the desired pump displacement command to the pump to vary its flow output, while a three way valve is used to direct the flow to the appropriate chamber of the steering gear based on the system's operating conditions (Figure 8.4).

8.4.2 Fixed Displacement Pump in a Open-Circuit Configuration with a Variable Speed Electric Motor:

Alternatively, a fixed displacement pump driven by a variable speed electric motor can be used to control the driver's steering effort. The speed of the motor will be adjusted by the torque control system in order to track the desired steering feel while the three way control valve is used to send the pump's flow output to appropriate side of the steering gear depending on operating conditions (Figure 8.5).

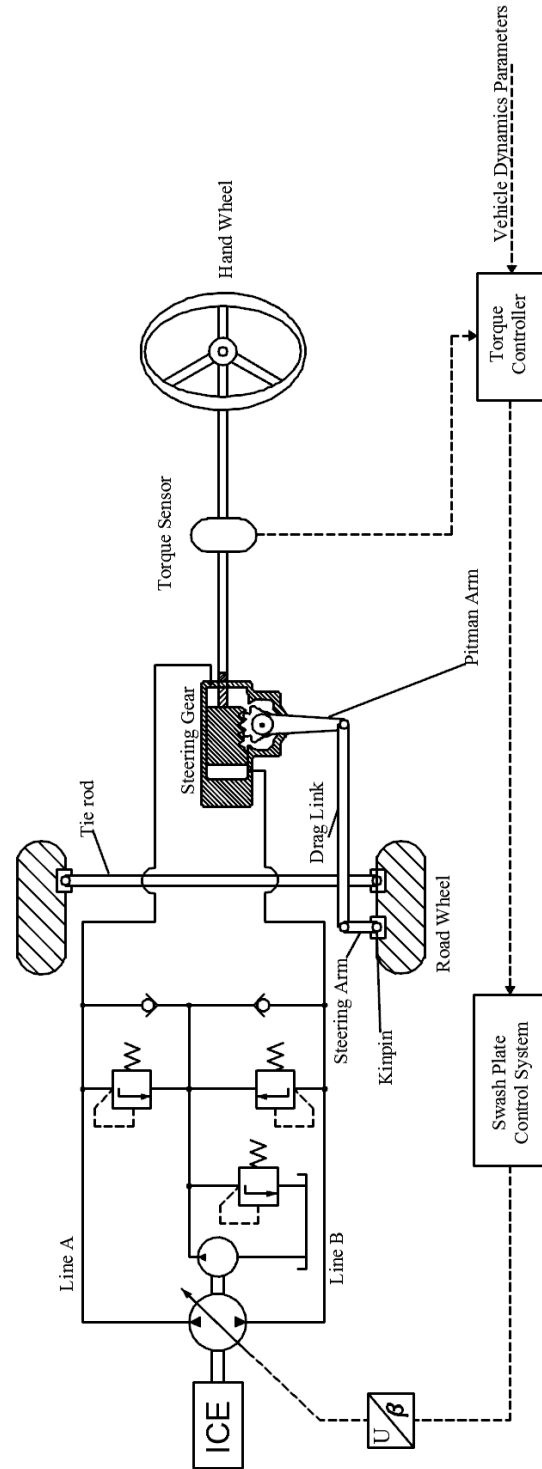


Figure 8.3. Active Steering Effort Control Using Displacement Controlled Pump in Closed-Circuit Configuration

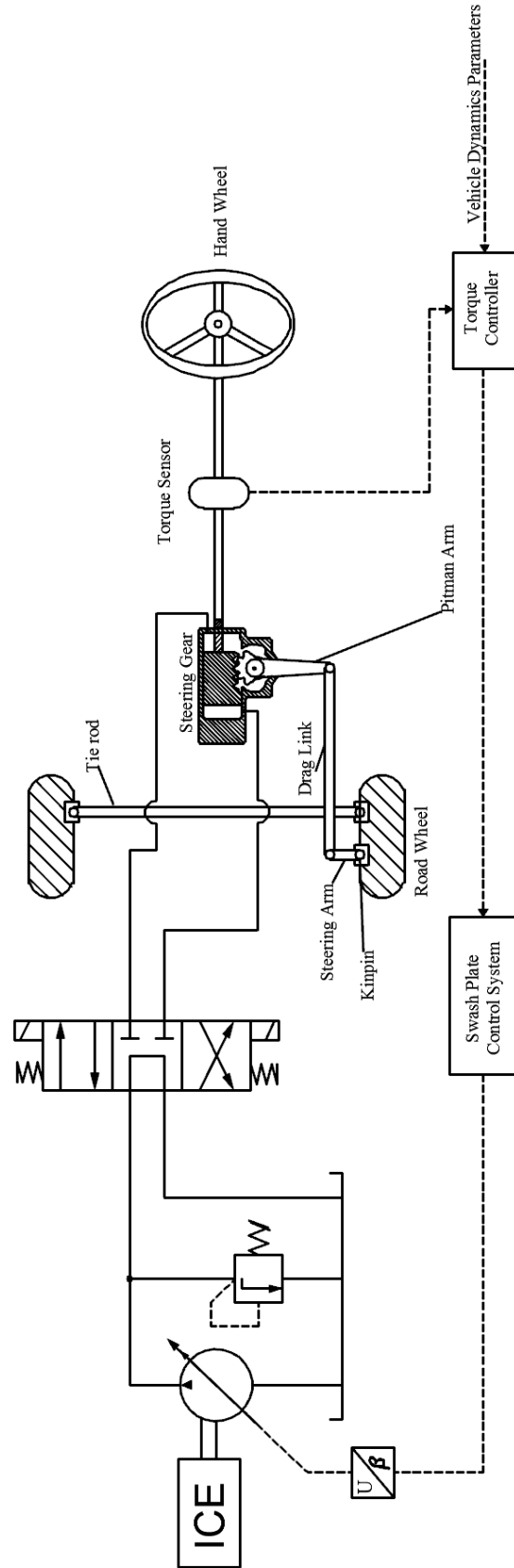


Figure 8.4. Active Steering Effort Control Using Displacement Controlled Pump in Open-Circuit Configuration

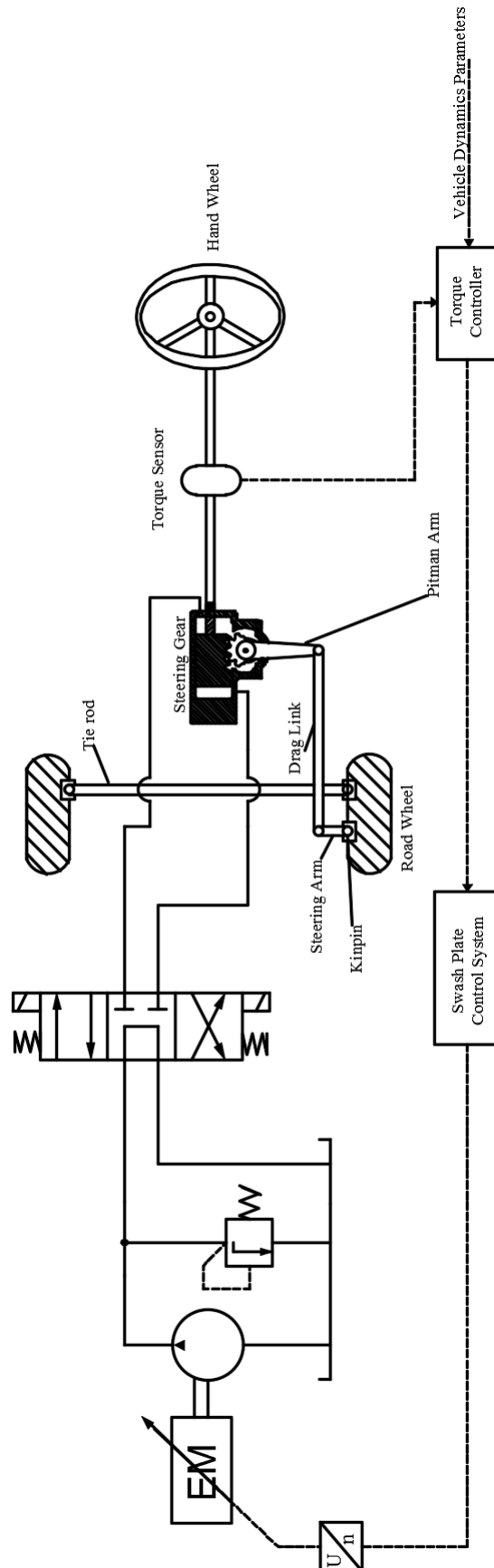


Figure 8.5. Active Steering Effort Control Using Fixed Displacement Pump with Variable Speed Motor in Open-Circuit Configuration

9. CONCLUSIONS AND FUTURE WORK

9.1 Conclusions

In this research project, the potential use of Displacement Controlled (DC) pumps in enabling active steering in on-highway commercial vehicles while improving efficiency was researched. First, a steer-by-wire concept for commercial vehicles was proposed with different potential mechanical and hydraulic configurations accommodating different applications. Next, one of the proposed steer-by-wire configurations was designed, modeled, and validated using high fidelity commercial software. From the complete model, a simplified mathematical model of the system was derived based on which an Adaptive Robust Controller (ARC) was designed and validated in simulation and shown to closely track the desired steering motion in the presence of unknown parametric and nonlinear uncertainties resulting from pump flow losses. Subsequently, due to potential implementation challenges, an even simpler system model and a lower order ARC controller were proposed, validated and shown to meet performance requirements with very high accuracy.

Subsequently, experimental validation of the steer-by-wire system was performed in two steps. First, a laboratory setup was designed and built to implement the pump's swash plate control system, and ensure proper operation and control of the pump and other system components. Implementation and validation of the steer-by-wire ARC control system was also performed on the lab setup for two different configurations; a linear cylinder configuration and a single rack cylinder configuration.

Next, implementation of the steer-by-wire system into a test vehicle was performed. Due to the relatively large physical size of the available DC pump, a separate small gasoline engine was purchased and installed in the back of the vehicle on which the pump was mounted. Once all the components were installed and wired,

implementation and validation of the steer-by-wire control system was performed to ensure that the required performance is achieved.

Moreover, different possible fail-safe mechanisms have been proposed to mitigate any potential steer-by-wire system failures in order to maintain safe operation of the vehicle at all times. Two of the proposed fail-safe mechanisms have been implemented into the test vehicle. The clutch fail-safe mechanism mechanically connects the steering wheel to the road wheel through a steering gearbox that allows the driver to manually steer the vehicle should the steer-by-wire system fail. The second implemented fail-safe mechanism uses the rear axle steering system of the vehicle, typically used to improve maneuverability and reduce tire wear, to take over the steering task when the front steer-by-wire system fails. It has been shown that by manipulating the driver's steering command using specific transfer functions, the vehicle yaw rate response can be made to closely match the response of the vehicle as if it were steered from the front, and thus providing a way to steer the vehicle to safety if the front steer-by-wire system fails.

9.2 Future Work

For safety reasons, all of the vehicle validation work conducted so far in this project has taken place in a low speed closed course environment. Once the steer-by-wire system is more mature, high speed testing will need to be conducted to validate the system performance in those operating conditions. Particularly, one need to ensure that the lateral response of the system is acceptable and is achieved with high enough accuracy. Low accuracy of the control system may result in a dead-band between the the steering wheel inputs from the driver and the resulting lateral response of the vehicle which would be equivalent to mechanical lash in the steering system. Such behavior could lead to dangerous situations and is mitigated by high accuracy control system which the Adaptive Robust Control (ARC) attains

as previously shown. However, high speed testing will demonstrate whether that accuracy is high enough or whether it needs to be improved upon.

Additionally, high speed testing of the fail-safe mechanism using the rear axle steering shall also be performed to validate its response. Specifically, the yaw rate response of the vehicle when steered from the rear needs to match the desired yaw rate response of the vehicle when steered from the front. When performing this test, a limit of the steering command to the rear axle needs to be applied to avoid any dangerous situations. Specifically, such limit shall decrease with the square term of the vehicle which directly correlates with the lateral acceleration of the vehicle.

Before testing the steer-by-wire system at high speeds, a health monitoring and fault management system should be implemented. The system would constantly check the health of the system and its different components to ensure they are operating properly and within predetermined safe boundaries. One method to ensure the system is operating properly is to implement a type of watchdog system which typically runs the same sort of calculations and routines in parallel with the main ECU and compares its outputs to those of the main ECU. If the difference between the outputs are outside some predefined thresholds, the system raises a fault and takes the appropriate action. If the fault is critical then the system shall enter a predetermined safe state, e.g. engage the pneumatic clutch. Once the health monitoring and fault management system is implemented, it would need to be incorporated with the fail-safe mechanism which will ensure the system fails safely and the vehicle remains controllable at all times.

Furthermore, an investigation shall be conducted on the concept of using pump displacement control to provide steering assistance by directly controlling driver steering effort and without breaking the mechanical link between steering wheel and road wheels. In order to validate this concept, first the steering control system will need to be designed and validated in simulation. For this task, parts of the mathematical system model built for this project can be reused while some of its other subsystems will need to be modified to account for the differences between the steer-by-wire sys-

tem model and this new concept steering system which has a full mechanical link between steering wheel and road wheels. Once the model and control system are validated in simulation and the active steering effort using displacement control is deemed feasible, the experimental validation shall then be performed. If successful, this method of steering will allow for a more efficient way to do active steering without the inefficiencies of throttling losses resulting from the use of control valves and without the safety concerns imposed by the steer-by-wire concept, specifically, in the event of a failure.

In addition to the added functionality of using displacement controlled pumps in steering, namely, the advantages of both the concept of steer-by-wire and that of the active control of steering effort, it has been claimed that using DC pumps in steering would also improve their energy efficiency as throttling valves are no longer needed to control pressure inside the steering gear, or the flow output of the pump as in conventional steering systems. As such, an energy efficiency study shall be conducted to confirm the efficiency benefits of DC pumps in steering on-highway commercial vehicles. This study can first be conducted in simulation using known duty cycles and characteristics of different commercial vehicles. An experimental energy consumption study can also be conducted although instrumentation of different types of vehicles with different operating conditions would need to be performed. Such experimental study might be challenging as energy savings of steering systems are hard to measure due to their low energy consumption relative to that of the entire vehicle. Nonetheless, it is expected that the energy savings will mostly be on vehicles that negotiate turns throughout their duty cycle such as transit buses and vocational vehicles, as opposed to long haul vehicles which spend the majority of their duty cycle driving straight. However, the advantages of DC pumps in steering on-highway commercial vehicles are far more than just energy savings as stated in previous chapters.

REFERENCES

REFERENCES

- [1] M Ivantysynova. Energy saving hydraulic actuators for mobile machines. In *Proc. of 1st Bratislavian Fluid Power Symposium*, pages 47–58, 1998.
- [2] Naseem Daher. *Novel energy efficient electrohydraulic steer-by-wire technology*. PhD thesis, Purdue University, 2014.
- [3] John W Durstine. The truck steering system from hand wheel to road wheel. Technical report, SAE Technical Paper, 1973.
- [4] Kenichi Fukumura, Kyousuke Haga, Mikio Suzuki, and Katuhisa Mori. Center-closed rotary servo valve for power steering. Technical report, SAE Technical Paper, 1996.
- [5] Daniel E Williams. Power steering apparatus, April 19 2016. US Patent 9,315,208.
- [6] Daniel E Williams and Amine Nhila. Power steering apparatus, April 11 2017. US Patent 9,616,920.
- [7] Herbert E Merritt. *Hydraulic control systems*. John Wiley & Sons, 1967.
- [8] J Berbuer. *New electro-hydraulic servo technology with displacement controlled pump*. PhD thesis, Aachen: RWTH, 1988.
- [9] Rolf Ziegler. *Auslegung und Optimierung schneller Servopumpen*. PhD thesis, Institut für Werkzeugmaschinen und Betriebstechnik, Universität Karlsruhe, 1990.
- [10] J Lodewyks. *Der Differentialzylinder im geschlossenen hydrostatischen Kreislauf*. PhD thesis, Dissertation, RWTH Aachen, Germany, 1994.
- [11] Vladimir Pastrakuljic. *Design and modeling of a new electro hydraulic actuator*. PhD thesis, National Library of Canada= Bibliothèque nationale du Canada, 1995.
- [12] Saeid Habibi and Andrew Goldenberg. Design of a new high performance electrohydraulic actuator. In *Advanced Intelligent Mechatronics, 1999. Proceedings. 1999 IEEE/ASME International Conference on*, pages 227–232. IEEE, 1999.
- [13] Kim Heybroek, Jonas Larsson, and Jan-Ove Palmberg. Open circuit solution for pump controlled actuators. In *4th FPNI-PhD Symposium Sarasota 2006*. Sarasota: Coastal Printing, 2006.
- [14] Kim Heybroek and Jan-Ove Palmberg. Evaluating a pump controlled open circuit solution. 2008.

- [15] M Ivantysynova, O Kunze, and H Berg. Energy saving hydraulic systems in aircraft way to save fuel. In *4th Scandinavian International Conference on Fluid Power, Tampere, Finland*, pages 1000–1014, 1995.
- [16] Jean-Charles Maré and Marc Budinger. Comparative analysis of energy losses in servo-hydraulic, electro-hydrostatic and electromechanical actuators. In *The 11th Scandinavian International Conference on Fluid Power, SICFP*, volume 9, pages 2–4, 2009.
- [17] Fredrik Roos. Design and theoretical evaluation of electric power steering in heavy vehicles. *Royal Institute of Technology, Stockholm2005*, 2005.
- [18] S.J. Collier-Hallman and J.A. Kleinau. Closed-loop torque control for electric power steering, March 30 1993. US Patent 5,198,981.
- [19] D.E. Williams. Method of controlling a vehicle steering apparatus, April 8 2003. US Patent 6,546,322.
- [20] J. Ekmark and J. Pohl. Control strategy for computer-controlled steering, June 23 2004. EP Patent App. EP20,020,028,566.
- [21] DE Williams. Synthetic torque feedback to improve heavy vehicle drivability. *Proceedings of the Institution of Mechanical Engineers, Part D: Journal of automobile engineering*, 223(12):1517–1527, 2009.
- [22] Malte Rothhämel, Jolle IJkema, and Lars Drugge. A method to find correlations between steering feel and vehicle handling properties using a moving base driving simulator. *Vehicle system dynamics*, 49(12):1837–1854, 2011.
- [23] A. Dell’Amico. *On Electrohydraulic Pressure Control for Power Steering Applications: Active Steering for Road Vehicles*. Linköping Studies in Science and Technology. Dissertations. Department of Management and Engineering, Linköping University, 2016.
- [24] S Haggag. *Development of fault-tolerant steer-by-wire system for earth moving equipment*. PhD thesis, Ph. D. thesis, University of Illinois at Chicago, Chicago, IL, 2002.
- [25] Paul Yih. Steer-by-wire: Implications for vehicle handling and safety. 2005.
- [26] Kenneth A Sherwin. Steering apparatus, July 10 2007. US Patent 7,240,760.
- [27] Eric Fischer, André Sitte, Jürgen Weber, Erhard Bergmann, and Markus de la Motte. Performance of an electrohydraulic active steering system. In *10th International Fluid Power Conference. Dresden*, 2016.
- [28] Amine Nhila, Daniel Williams, and Vishi Gupta. Integration of lane keeping assistance with steering. *SAE International Journal of Commercial Vehicles*, 6(2013-01-2389):394–399, 2013.
- [29] Han-Shue Tan, Rajesh Rajamani, and Wei-Bin Zhang. Demonstration of an automated highway platoon system. In *American Control Conference, 1998. Proceedings of the 1998*, volume 3, pages 1823–1827. IEEE, 1998.
- [30] J Ackermann, T Bünte, and D Odenthal. Advantages of active steering for vehicle dynamics control. 1999.

- [31] Taehyun Shim and Daniel Toomey. Investigation of active steering/wheel torque control at the rollover limit maneuver. Technical report, SAE Technical Paper, 2004.
- [32] Juergen Ackermann. Robust decoupling of car steering dynamics with arbitrary mass distribution. In *American Control Conference, 1994*, volume 2, pages 1964–1968. IEEE, 1994.
- [33] Jurgen Ackermann and Tilman Bunte. Yaw disturbance attenuation by robust decoupling of car steering. *Control Engineering Practice*, 5(8):1131–1136, 1997.
- [34] Bilin Aksun Guvenc, Tilman Bunte, Dirk Odenthal, and Levent Guvenc. Robust two degree-of-freedom vehicle steering controller design. *IEEE Transactions on Control Systems Technology*, 12(4):627–636, 2004.
- [35] Shuibo Zheng, Houjun Tang, Zhengzhi Han, and Yong Zhang. Controller design for vehicle stability enhancement. *Control Engineering Practice*, 14(12):1413–1421, 2006.
- [36] Craig E Beal and J Christian Gerdes. Predictive control of vehicle roll dynamics with rear wheel steering. In *American Control Conference (ACC), 2010*, pages 1489–1494. IEEE, 2010.
- [37] Daniel E Williams and Amine Nhila. Directional dynamics of steering the third axle. *SAE International Journal of Commercial Vehicles*, 8(2015-01-2747):323–331, 2015.
- [38] Daniel Williams. Multi-axle vehicle dynamics. Technical report, SAE Technical Paper, 2012.
- [39] S Sastry and M Bodson. Adaptive systems: stability, convergence and robustness, 1989.
- [40] GC Goodwin, ME Salgado, and DQ Mayne. A bayesian approach to estimation with restricted complexity models. *Tech. Rep. EE8953*, 1989.
- [41] Bin Yao and Li Xu. Adaptive robust control of linear motors for precision manufacturing. *IFAC Proceedings Volumes*, 32(2):25–30, 1999.
- [42] Kazuo Hara, Hitoshi Ono, Kiyotaka Shitamitsu, Takaaki Eguchi, Yuusuke Katou, and Toshiaki Kasahara. Fail-safe steering system for a vehicle, March 7 2006. US Patent 7,007,769.
- [43] Daniel E Williams. Steer-by-wire steering apparatus with actuatable mechanism, September 21 2010. US Patent 7,798,279.
- [44] Daniel Williams. Tire wear improvement by steering a third axle. *SAE International Journal of Commercial Vehicles*, 4(2011-01-2148):1–12, 2011.
- [45] Naoki Matsumoto and Masayoshi Tomizuka. Vehicle lateral velocity and yaw rate control with two independent control inputs. *Journal of Dynamic systems, measurement, and Control*, 114(4):606–613, 1992.
- [46] Tom Pilutti, Galip Ulsoy, and Davor Hrovat. Vehicle steering intervention through differential braking. *Journal of dynamic systems, measurement, and control*, 120(3):314–321, 1998.

- [47] Nicoleta Minoiu Enache, Saïd Mammar, Benoit Lusetti, and Yazid Sebsadji. Active steering assistance for lane keeping and lane departure prevention. *Journal of Dynamic Systems, Measurement, and Control*, 133(6):061003, 2011.
- [48] N Minoiu Enache, Mariana Netto, Said Mammar, and Benoît Lusetti. Driver steering assistance for lane departure avoidance. *Control engineering practice*, 17(6):642–651, 2009.
- [49] Massayoshi Tomizuka. Advanced vehicle control systems (avcs) research for automated highway systems in california path. In *Vehicle Navigation and Information Systems Conference, 1994. Proceedings., 1994*, pages PLEN41–PLEN45. IEEE, 1994.
- [50] Roy McCann and Anh Le. Electric motor based steering for jackknife avoidance in large trucks. In *Vehicle Power and Propulsion, 2005 IEEE Conference*, pages 7–pp. IEEE, 2005.
- [51] Wentao William Yu and William Szabela. Energetic efficiency analysis and performance evaluation for a closed center steering system. Technical report, SAE Technical Paper, 2007.
- [52] Thomas D Gillespie. Vehicle dynamics. *Warren dale*, 1997.
- [53] Caizhen Cheng, Richard Roebuck, Andrew Odhams, and David Cebon. High-speed optimal steering of a tractor–semitrailer. *Vehicle system dynamics*, 49(4):561–593, 2011.
- [54] Richard Roebuck, Andrew Odhams, Kristoffer Tagesson, Caizhen Cheng, and David Cebon. Implementation of trailer steering control on a multi-unit vehicle at high speeds. *Journal of Dynamic Systems, Measurement, and Control*, 136(2):021016, 2014.
- [55] Keiji Suzuki, Yoshiharu Inaguma, Kyosuke Haga, and Tomomi Nakayama. Integrated electro-hydraulic power steering system with low electric energy consumption. Technical report, SAE Technical Paper, 1995.
- [56] G Burgio and P Zegelaar. Integrated vehicle control using steering and brakes. *International Journal of Control*, 79(05):534–541, 2006.
- [57] Hao Fang, Lihua Dou, Jie Chen, Roland Lenain, Benoit Thuilot, and Philippe Martinet. Robust anti-sliding control of autonomous vehicles in presence of lateral disturbances. *Control Engineering Practice*, 19(5):468–478, 2011.
- [58] Haiping Du, Nong Zhang, and Guangming Dong. Stabilizing vehicle lateral dynamics with considerations of parameter uncertainties and control saturation through robust yaw control. *IEEE Transactions on Vehicular Technology*, 59(5):2593–2597, 2010.
- [59] Jianyong Wu, Qingping Wang, Xue Wei, and Houjun Tang. Studies on improving vehicle handling and lane keeping performance of closed-loop driver–vehicle system with integrated chassis control. *Mathematics and Computers in Simulation*, 80(12):2297–2308, 2010.

APPENDIX

A. STEER-BY-WIRE SYSTEM SIZING METHODOLOGY

A.1 System Sizing Methodology:

Proper sizing of the system is the first step in designing the DC steer-by-wire system in order to insure proper operation. An undersized system can result in insufficient torque levels to actuate the road wheel or insufficient flow to support fast steering maneuvers. Conversely, an over-sized system will result in unnecessary torque or flow levels and will also likely lead to inefficient use of the already scarce space in the engine compartment. Consequently, this section will be devoted to presenting the methodology for sizing the different system components, i.e. cylinder, DC pump, charge pump, displacement control system.

A.1.1 Cylinder Sizing

The steering gear of the test vehicle is replaced by a rotary cylinder of the same size and shape such that the new cylinder can be mounted in exactly the same location as the old steering gear. Such configuration makes use of the already existing steering system architecture, namely, the geometry layout of the linkages from the pitman arm to the steering arm on the road wheel. Typically, the steering gear is sized based the amount of torque, T_{max} , required to steer the loaded steered axle of the vehicle. With a known maximum system pressure difference, Δp_{max} , the required piston area is determined:

$$A_{piston} = \frac{T_{max}}{r \Delta p_{max}} \quad (A.1)$$

Where r is the pitch radius representing the distance between the axis of rotation of the output shaft of the cylinder and its piston. However, since we are replacing the

appropriately sized steering gear with a cylinder of the same size, sizing of the new cylinder is not necessary.

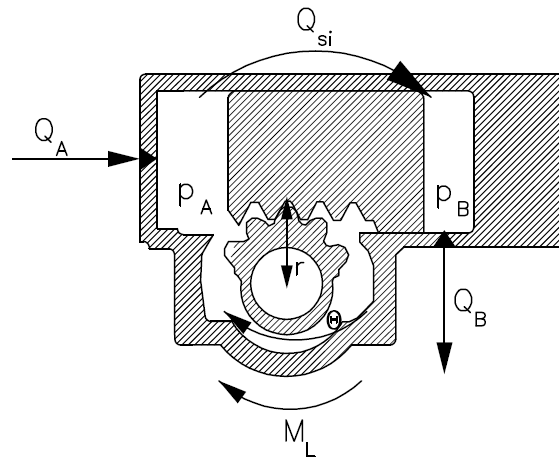


Figure A.1. Single Rack Cylinder used in Steer-by-Wire System

A.1.2 DC Pump Sizing

The required flow output of the pump depends on the required speed of the cylinder's piston which in turn depends on the maximum steering rate required from the system. Conventional steering systems are typically designed to withstand steering rates of about one and a half to two hand wheel turns per second. However, since we are designing a steer-by-wire system, the speed of the piston is no longer dictated by the motion of the steering wheel. As a result, the system designer can choose any reasonable steering rate of the road wheels that needs to be achieved and then compute the equivalent speed of the cylinder's output shaft, $\dot{\theta}_{piston}$. Subsequently, the required pump flow output can be computed:

$$Q = A_{piston} r \dot{\theta}_{piston} \quad (\text{A.2})$$

Finally, the pump displacement V_p can be determined using the minimum engine speed n_e , i.e. engine idle speed, and by taking into account the volumetric efficiency of the pump η_{vol} :

$$V_p = \frac{Q}{n_e \eta_{vol}} \quad (\text{A.3})$$

A.1.3 DC Swash Plate Control System Sizing

The displacement control system is sized such that it can support the desired dynamics of the steering system. From the main components of the DC system, namely, the swash plate, the control cylinder, the centering springs, and the proportional valve, it has been found by (Grabbel, 2003) that the dynamics of the control valve has the dominating bandwidth. As such, to insure the desired dynamic response of the steer-by-wire system, the proportional control valve should have the appropriate bandwidth. Moreover, in order to support the required fast changes in the swash plate angle, the control valve needs to be able to handle the necessary flow. This is calculated based on the change in volume of the control cylinder, V_{DC_Piston} , when going from -100% to $+100\%$ of swash plate angle in the desired amount of time, Δt_{min} :

$$Q_{DC} = \frac{V_{DC_Piston}}{\Delta t_{min}} \quad (\text{A.4})$$

A.2 Charge Pump Sizing

Once the flow, Q_{DC} , required to drive the pump displacement control has been determined, the necessary displacement of the charge can be computed at engine idle speed, n_{e_idle} while taking into account the volumetric efficiency of the pump:

$$V_{CP} = \frac{Q_{DC}}{n_{e_idle} \eta_{vol}} \quad (\text{A.5})$$

A.2.1 Sizing Exercise:

The system is sized such that it can respond as fast as the conventional steering system when needed such as in the case of emergency maneuvers. Starting at the hand wheel, a typical obstacle maneuver can require a steering rate up to $\dot{\theta}_{handwheel} = 2rev/sec$. Consequently, the corresponding piston velocity of a conventional steering system is:

$$\begin{aligned}\dot{x}_{piston} &= \dot{\theta}_{handwheel} r_{worm} \\ &= 2 \frac{rev}{sec} * .538 \frac{in}{rev} * .0254 \frac{m}{in} \\ &= .027 m/sec\end{aligned}$$

Where r_{worm} is the lead of the worm screw of the steering gear which represents the amount for linear motion of the piston for every hand wheel revolution. Subsequently, the computed piston velocity \dot{x}_{piston} is used to size the steer-by-wire system, and thus insuring the steering rate of the road wheels to be the same as the conventional system. As a result, the flow necessary to support the computed maximum steering rate is:

$$\begin{aligned}Q &= A_{piston} \dot{x}_{piston} \\ &= \pi r_{piston}^2 \dot{x}_{piston} = \pi (1.626 in)^2 * (.0254 \frac{m}{in})^2 * .027 \frac{m}{sec} * 10^{-3} \frac{L}{m^3} \\ &= 8.79 L/min\end{aligned}$$

Considering a minimum engine speed of $n_{e,idle} = 600rpm$ and a volumetric efficiency $\eta_{vol} = .98$, the desired displacement of the pump can be computed:

$$\begin{aligned}V_p &= \frac{Q}{n_e \eta_{vol}} \\ &= \frac{8.79 \frac{L}{min} * 10^3 \frac{cm^3}{L}}{600 rpm * .9} \\ &= 16.27 cm^3/rev\end{aligned}$$

As a result, a pump with the next available displacement of $18 cm^3/rev$ is selected.

The swash plate control system has a double acting cylinder with a diameter $D_{DC} = .022 \text{ m}$ and a stroke $H_{DC} = .054 \text{ m}$. Consequently, requiring the swash plate to to move from -100% to -100% in $\Delta t_{min} = .150 \text{ s}$ results in a flow requirement:

$$\begin{aligned}
 Q_{DC} &= \frac{V_{DC_Piston}}{\Delta t_{min}} \\
 &= \frac{\frac{\pi}{4} D_{DC}^2 H_{DC}}{\Delta t_{min}} \\
 &= \frac{\frac{\pi}{4} (.022 \text{ m})^2 * .054 \text{ m}}{.150 \text{ s}} * 10^{-3} \frac{\text{L}}{\text{m}^3} * \frac{1 \text{ sec}}{60 \text{ min}} \\
 &= 8.21 \text{ L/min}
 \end{aligned}$$

A proportional valve with a rated flow rate of 20 L/min at 35 bar per metering edge is selected.

Furthermore, for the planned prototype implementation, the charge pump is a gear pump with a fixed displacement $V_{CP} = 2 \text{ cm}^3/\text{rev}$, and is driven by an electric motor with variable speed. As such, the necessary speed, n_{CP} , at which to run the motor should be determined based on the computed necessary flow rate Q_{DC} and assuming a volumetric efficiency $\eta_{vol} = 90 \%$:

$$\begin{aligned}
 n_{CP} &= \frac{Q_{DC}}{V_{CP} \eta_{vol}} \\
 &= \frac{8.21 \frac{\text{L}}{\text{min}} * 10^3 \frac{\text{cm}^3}{\text{L}}}{2 \text{ cm}^3/\text{rev} * .9} \\
 &= 4562 \text{ rpm}
 \end{aligned}$$